Preparation, Structure and Vibrational Spectroscopy of Tetraperoxo Complexes of Cr^{V+}, V^{V+}, Nb^{V+} and Ta^{V+}

DISSERTATION

zur Erlangung des Grades eines Doktors

der Naturwissenschaften

vorgelegt von

General Chemist Gentiana Haxhillazi

Geb. am 16.01.1973 in Tirana

eingereicht beim Fachbereich 8

der Universität Siegen

Siegen 2003

Berichterstatter Prof. Dr. H. Haeuseler
Prof. Dr. H. J. Deiseroth

Tag der mündlichen Prüfung 04.11.2003

urn:nbn:de:hbz:467-523

Acknowledgements

This work was completed during the time form November 2000 to September 2003 in the Inorganic Chemistry branch, University of Siegen under the guidance of Professor Dr. H. Haeuseler.

I would like to express my heartfelt gratitude to my supervisor Professor Dr. H. Haeuseler for elaborate guidance and unlimited enthusiasm.

I would like to thank Mrs. Dr. Botova for many valuable discussions and Dipl. Chem. M. Schlosser for much help in the single crystal analysis.

I am especially pleased to acknowledge the assistance of Dipl. Ing. W. Büdenbender in the technique problems, Mrs. R. Stötzel and Mrs. J. Hermann for helping in the utilization of computers.

I am grateful to Mrs. Olm and Mrs. Kleinschmid, and the other members of the inorganic chemistry group of the University Siegen, with whom I had the pleasure of working, for their friendship, and helpful discussions.

Finally, I would like to thank my parents Pranvera and Pavli as well as my brothers Adrian and Dorian, and especially René, who cheered me on this endeavour.

Contents

1. Introduction

The chemistry of peroxo complexes of the transition elements has been an interesting subject since the 19th century. But only later on, starting in the 40th of the last century with the rapid development of modern structure determination methods, one was able to obtain detailed structural information on these compounds.

The isolation and characterisation of peroxo complexes and the variety of reactions that they themselves undergo are beginning to yield general information about bonding, structure, and reactivity of coordinated molecular oxygen. Biochemical interest in the interaction of molecular oxygen with the group of transition metal complexes is mainly the object of nowadays research [1, 2].

Coordination to a metal center activates peroxide toward the oxidation of a variety of substrates, rendering peroxometal complexes important as intermediates in biological and synthetic catalysis. The isolation and characterisation of stable dioxygen complexes and the variety of reactions that they themselves undergo are beginning to yield general information about bonding, structure, and reactivity of coordinated molecular oxygen.

Because of the importance of molecular oxygen as a reagent in biological and industrial processes and because dioxygen is an interesting ligand in its own right, current research in this area has been directed toward understanding the bonding of dioxygen to transition metal complexes and the effect of these bonding upon its reactivity toward other substrates.

The chemical interest in understanding metal – dioxygen interactions, has led to the creation of the host substances containing transition metals that bind to and/or react with dioxygen. While some of these substances may find use as materials or as industrial catalysts, they are also important to understand the active sites of biological dioxygen activators.

Earlier compilations on red perchromates by E. H. Riesenfeld [3] and later the work of R. Stomberg and C. Brosset [4] with the structure description of K_3CrO_8 provide a useful background and a good perspective of an extensive investigation of this group of compounds. Peroxo complexes of chromium, molybdenum, and tungsten are among the earliest known and best characterized. The vanadium peroxo compounds show to have biological as well as synthetic usefulness [5].

In this work a study of tetraperoxo complexes of chromium, vanadium, niobium and tantalum with the general formula $A_3[B(O_2)_4]$ is presented.

Group	1	2	3	4	5	6	7	8	9	10	11	12	13	14	15	16	17	18
Period	$A_3[B(O\text{-}O)_4]$																	
1	H		$A = (NH_4)^+, K^+, Rb^+$ or Cs^+															He
2	Li	Be	$B = Cr^{V+}, V^{V+}, Nb^{V+}$ or Ta^{V+}										B	C	N	O	F	Ne
3	Na	Mg											Al	Si	P	S	Cl	Ar
4	K	Ca	Sc	Ti	V	Cr	Mn	Fe	Co	Ni	Cu	Zn	Ga	Ge	As	Se	Br	Kr
5	Rb	Sr	Y	Zr	Nb	Mo	Tc	Ru	Rh	Pd	Ag	Cd	In	Sn	Sb	Te	I	Xe
6	Cs	Ba	*Lu	Hf	Ta	W	Re	Os	Ir	Pt	Au	Hg	Tl	Pb	Bi	Po	At	Rn
7	Fr	Ra	**Lr	Rf	Db	Sg	Bh	Hs	Mt									

lanthanoids	*La	Ce	Pr	Nd	Pm	Sm	Eu	Gd	Tb	Dy	Ho	Er	Tm	Yb
actinoids	**Ac	Th	Pa	U	Np	Pu	Am	Cm	Bk	Cf	Es	Fm	Md	No

Fig. 1.1: Periodic table indicating the different elements involved in the system of tetraperoxo complexes $A_3[B(O\text{-}O)_4]$ covered by this work.

With a very big interest the peroxo complexes of chromium have been studied, not only for the unusual oxidation state of a pentavalent chromium, but also for its ability to generate singlet oxygen in solutions [6].

The coordination of dioxygen to transition metals is a subject of extreme interest due to its utilisation by biological systems [7]. In biological processes, activation of molecular oxygen occurs by coordination in metalloproteins which catalyse oxygen insertion reactions and oxidation.

1.1. Literature survey and properties

The investigation of peroxo compounds has been an interesting subject since 1900 and later on new methods for preparing them have been developed.

The red peroxochromates were first discovered by E. H. Riesenfeld in 1905 [8] and have since then been the subject of many investigations, mainly concerning the unusual oxidation state +V of the chromium. Early the formula how the atoms are arranged in tetra peroxo chromates $A_3[Cr(O_2)_4]$ was shown as follows:

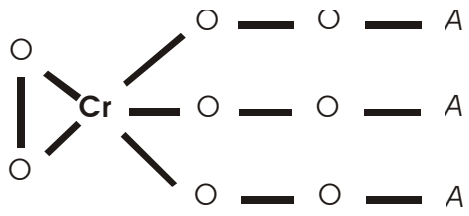

where *A*: $(NH_4)^+$, K^+, Rb^+ or Cs^+

But this formula is not correct, as it indicates that each ion A^+ should be connected only with one double oxygen ion. As the structural investigation of the potassium peroxo chromate by Wilson [3] and later by Stomberg and Brosset [4] revealed, each A^+ ion is in contact with not less than eight such ions and all peroxo – groups are side – on bonded to the chromium atom. So according to these investigations the following formula has been given as a correct notation of the compound.

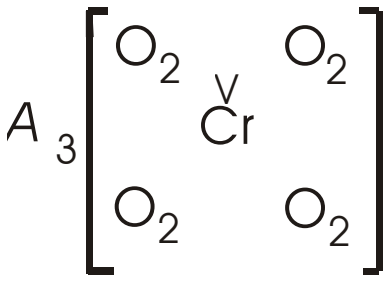

where *A*: $(NH_4)^+$, K^+, Rb^+ or Cs^+

This structure has also been found and determined by K. Gleu on the peroxo compound $K_3[Cr(O_2)_4]$ [9]. A study of corresponding peroxo compounds of vanadium, niobium and tantalum is also made [10, 11, 12], which concluded in the same structure for these peroxo complexes. According to these measurements $K_3[Cr(O_2)_4]$ crystallises in the tetragonal space group $I\bar{4}2m$. For the vanadium tetra peroxocompounds there is only one paper presenting only *d*-values [10] on the ammonium and potassium salts.

The investigation has shown that the $[Cr(O_2)_4]^{3-}$ ion has the symmetry $\bar{4}2m$ and that the geometrical arrangement of the oxygen atoms surrounding the central chromium atom is dodecahedral. It is rather remarkable that this configuration is given by an appropriate linear combination of *spd* – orbitals. It is highly probable that the bonds are d^4sp^3 – hybrids because the paramagnetism of the substance is in accordance with this orbital configuration [4]. Correlation between one – electron reduction and oxygen – oxygen bond strength in d^0 transition metal peroxo complexes of Cr (VI) and V (V) is done nowadays. The correlation holds for complexes of the same metal containing different ligands as well as for complexes of the various metals containing the same ligand. The nature of the ligands in affecting the one – electron – oxidizing ability of the peroxo complexes appears to play a more important role than the nature of the metal [13].

There is a series of peroxo compounds known in the literature crystallising in this structure type (see tabs. 1.1 and 1.4) though single crystal measurements have been performed only in the cases of $K_3[Cr(O_2)_4]$ [3, 4, 14 – 17], $K_3[Nb(O_2)_4]$ [3], $Rb_3[Nb(O_2)_4]$ [18] and $K_3[Ta(O_2)_4]$ [3, 19] (see tab. 1.4).

While Cr (V) compounds were initially described by Riesenfeld [8] in 1905, spectroscopic and magnetic investigations using crystals were first reported on $K_3[Cr(O_2)_4]$ in 1981 [20].

A new class of Cr (V) tetraperoxochromates, those containing water of hydration such as: $Li_3[Cr(O_2)_4]\cdot 10H_2O$, $Na_3[Cr(O_2)_4]\cdot 14H_2O$, and $Cs_3[Cr(O_2)_4]\cdot 3H_2O$, are also known nowadays. In that case, the Li salt crystallises in the orthorhombic (*Cmcm*) space group, whereas the Na and Cs salts exhibit triclinic ($P\bar{1}$) and monoclinic $P2(1)/n$ space groups, respectively [21]. Whereas, the Cr(V) based alkali-metal peroxochromates without water with the general formula $M_3[Cr(O_2)_4]$ ($M = Li^+, Na^+, K^+, Rb^+, Cs^+$) are found to exhibit a variety of interesting thermodynamic and magnetic properties [22].

Table 1.1: Known tetraperoxo complexes of Cr, Nb and Ta crystallising with the $K_3[Cr(O_2)_4]$ – type and their lattice constants.

Peroxo complexes	**a / Å**	**c / Å**	**Reference**
$K_3[Cr(O_2)_4]$	6.70	7.60	[3]
	6.703(3)	7.632(3)	[4, 15]
	7.632	6.705	[16]
	6.709(1)	7.627(1)	[14]
	6.6940(3)	7.5736(5)	[17, 23]
$(NH_4)_3[Cr(O_2)_4]$	Only *d*-values		[10]
$Rb_3[Cr(O_2)_4]$	6.9759	7.8176	[23]
$(NH_4)_3[V(O_2)_4]$	Only *d*-values		[10]
$K_3[V(O_2)_4]$	Only *d*-values		[10]
$(NH_4)_3[Nb(O_2)_4]$	7.00	8.56	[24, 25]
	7.00	8.57	[26]
$K_3[Nb(O_2)_4]$	6.78	7.86	[3]
	6.71	7.90	[26]
$Rb_3[Nb(O_2)_4]$	7.07	8.02	[26]
	7.061(1)	8.063(2)	[18]
$Cs_3[Nb(O_2)_4]$	7.42	8.18	[26]
$(NH_4)_3[Ta(O_2)_4]$	7.00	8.56	[25]
$K_3[Ta(O_2)_4]$	6.78	7.88	[3]
	6.7935(8)	7.9290(15)	[19]
$Rb_3[Ta(O_2)_4]$	7.05	8.05	[3]
$Cs_3[Ta(O_2)_4]$	7.37	8.34	[3]

As it can be seen from this table, there are some tetraperoxo compounds investigated, but at the same time some of them could not be refined, and are published only their *d* – values.

The thermal stabilities of the tetraperoxo salts of the group V elements in the periodic system has been discussed [27, 28]. The thermal stability of these compounds is increasing with increasing atomic radius of the group V element [10] as there is steric interference of the peroxo groups to be expected for the smaller central atom. So the peroxo compounds of Nb or Ta are more stable than the vanadium compounds and due to this fact there is more information about them found in the literature than for the vanadium complex. According to these authors the corresponding chromium compounds are an exception as the chromium is even smaller than the vanadium but their thermal stability is greater than for the vanadium compounds.

The bonds between the central atom and the peroxo groups are formed from an overlap of d^4sp^3 hybrid orbitals on the central atom with sp^3 hybrid orbitals of the oxygen atoms. The valence angels between the d^4sp^3 hybrid orbitals are sufficiently small to enable a sufficient overlap with σ – bonding electron pairs donated by each of the oxygen atoms of a peroxo-ligand [4, 10].

Most studies on peroxovanadates were done on oxo – diperoxo compounds such as that one of Ammonium μ – Oxo – bis (oxo – diperoxovanadate (V)), $(NH_4)_4[O(VO(O_2)_2)_2]$ [29], also on $Na_3[V(O-O)_4]\cdot H_2O_2\cdot 10.5H_2O$ and $Na_3[V(O-O)_4]\cdot 14H_2O$ [30].

There is only few information in the literature on the vibrational spectra of these tetra peroxo compounds. In most cases only one strong band in the infrared spectra is reported. So Fergusson et al. [10] and Griffith et al. [11, 31] report on an intense band at 875 cm^{-1} in the infrared spectrum of $K_3[Cr(O_2)_4]$. In the infrared spectra appears a strong absorption at 853, 814 and 813.5 cm^{-1} in the potassium salts of vanadium, niobium and tantalum, respectively [10]. Gili et al. [32] state that in the IR – spectra of the chromium peroxo complexes a strong band at 885 cm^{-1} is observed attributed to the O – O stretching vibration. Whereas, for $K_3[Nb(O_2)_4]$ [11] and $K_3[Ta(O_2)_4]$ [11, 31] the corresponding intense bands are found in the infrared spectra at 813 cm^{-1} and 807 cm^{-1}, respectively. Also, the O – O stretching vibration of the peroxo group produces an intense band in the Raman spectrum in the expected frequency region of 750 to 850 cm^{-1} [33].

1.2. The crystal and molecular structure of $K_3[Cr(O_2)_4]$

The crystal structure of $K_3[Cr(O_2)_4]$ has been determined first by Wilson [3] and later on different re-determinations were done [4, 14 – 17, 23]. The structure consists of a packing of K^+ and $[Cr(O_2)_4]^{3-}$ ion [34]. The $[Cr(O_2)_4]^{3-}$ ion has a central chromium ion bonded to four peroxide groups and has the symmetry $\bar{4}2m$ (see fig. 1.2). In fig. 1.2 also the interatomic distances in pm are given which have been found, according to the literature [23].

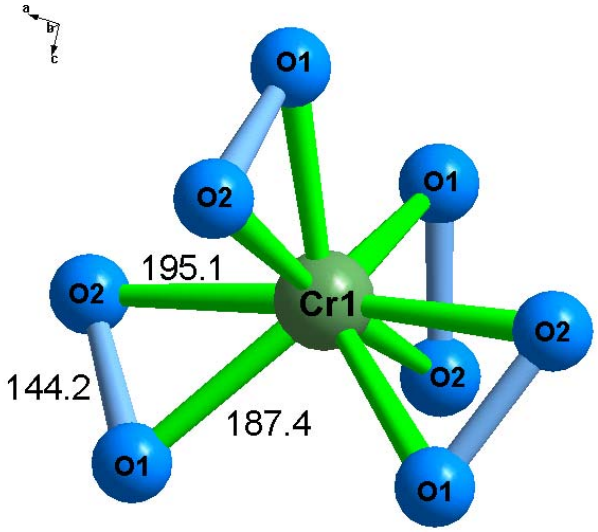

Figure 1.2: Structure of the (tetra)peroxochromate – anion $[Cr(O_2)_4]^{3-}$ in the structure of $K_3[Cr(O_2)_4]$.

The $[Cr(O_2)_4]^{3-}$ dodecahedral structure in fig. 1.2 may be thought of, as built from two interlocking distorted tetrahedra. One, a compressed tetrahedron essentially in the *xy* plane and the other extended along the *z* axis [23]. The Cr ion here is in its rather unusual, pentavalent, ($3d^1$) oxidation state.

The interatomic distance between two oxygen atoms in the peroxo groups is 144.2 pm [23]. Also from the investigation it has been shown that $[Cr(O_2)_4]^{3-}$ ion which has the geometrical arrangement of a distorted dodecahedron structure configurations is given by appropriate linear combination of *spd*-orbitals. It is highly probable that the bonds are d^4sp^3-hybrids, the arrangement is needed for the eight σ bonds with D_{2d} symmetry; as there are no available

f – orbitals in $[Cr(O_2)_4]^{3-}$ [4]. It can be mentioned that $[Cr(O_2)_4]^{4-}$ does not seem to exist. This may be explained by assuming that the configuration of this ion with a single electron in the 3*d* orbital has a stabilizing effect [4].

In this structure there are only two independent Cr – O bond lengths due to the crystallographically imposed $\bar{4}$ symmetry of the anion [35]. The chromium ion is nearer to one of the oxygen atoms of each peroxide group than to the other one and the oxygen – oxygen distance in the peroxide group is shorter than normal [16]. As opposed to the results of Stomberg and Brosset [4] it is found that the Cr – O(1) distance is significantly shorter (at the 0.5% level) than the Cr – O(2) distance [16]. Also it is found that the O(1) – O(2) (peroxide) distance is shorter than 1.49 Å usually found for the peroxide ion [16]. The difference in the Cr – O(1) and Cr – O(2) bond lengths has been ascribed to differences in metal *d* – O π orbital overlap [36] and to a difference in strength of interaction between the 2s atomic orbitals of the two different oxygen atoms with the metal p_z atomic orbital [37]. Since these effects are not mutually exclusive, both may be important [35].

Some results for the interatomic distances and bond angles from the literature are given in tab. 1.2 as follows:

Table 1.2: Comparison of some Bond Lengths (in Å) and angles (°) [a] in $K_3[Cr(O_2)_4]$.

Cr – O(1)	**Cr – O(2)**	**O(1) – O(2)**	**O(1) – Cr – O(1´**	**O(2) – Cr – O(2)´**	Reference
1.944	1.895	1.489	89.8	95.4	[4]
1.944	1.846	1.405	86.8 ± 1.4	173.7 ± 2.5	[16]
1.972	1.874	1.472	86.5 ± 1.2	90.1 ± 1.3	[15]
1.958	1.882	1.466			[14]
1.958	1.881	1.452			[17]
1.939	1.840	1.407			[32]
1.9584	1.8812	1.442	85.46	174.21	[23]

[a] With O at x, y, z then O´ is at x, $\bar{y}$, $\bar{z}$.

In fig. 1.3 the elementary cell of $K_3[Cr(O_2)_4]$ is shown in which the $[Cr(O_2)_4]^{3-}$ ion is presented in the centre and on the corners of the elementary cell.

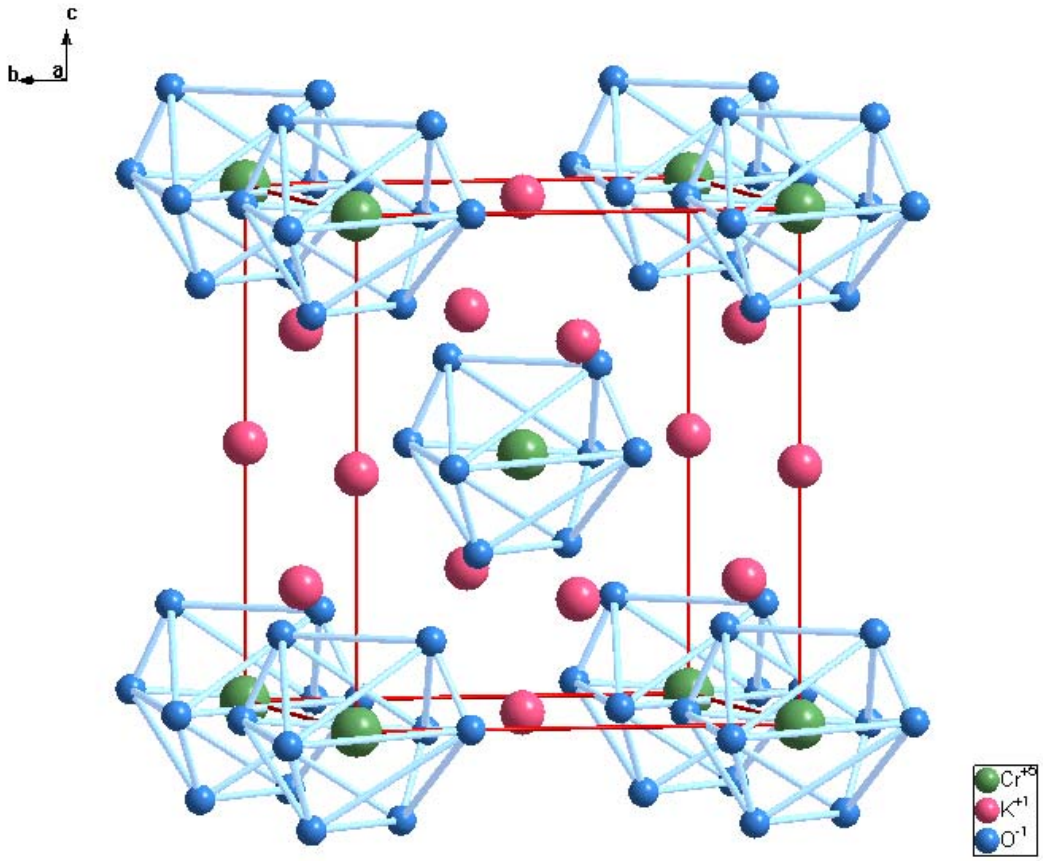

Figure 1.3: Structure of the elementary cell of potassium tetraperoxochromate $K_3[Cr(O_2)_4]$ projected down the *a* axis.

The atomic coordinates and the standard deviation on these positions in the structure of $K_3[Cr(O_2)_4]$ according to the literature [3] are given in tab. 1.3. Whereas, in tab. 1.4. the oxygen atom positions of all well known tetraperoxo compounds are presented. In that case there are presented only the oxygen atom position as the other atoms are standing at the same position parameters as in the structure of $K_3[Cr(O_2)_4]$ shown in tab. 1.3.

Table 1.3: Position parameter, relative atomic co – ordinates and standard deviation on these positions in the structure of $K_3[Cr(O_2)_4]$ [3].

Atom	Oxidation state	Site	x	y	z
Cr	+5	2a	0	0	0
K(1)	+1	2b	0	0	0.5
K(2)	+1	4d	0	0.5	0.25
O(1)	-1	8i	0.13483(14)	0.13483(14)	0.1825(2)
O(2)	-1	8i	0.20661(14)	0.20661(14)	0.0131(2)

Table 1.4: The oxygen position of tetraperoxo complexes of Cr, Nb and Ta crystallising with the $K_3[Cr(O_2)_4]$ – type.

Tetraperoxo complexes	**x[O(1)]**	**z[O(1)]**	**x[O(2)]**	**z[O(2)]**	**Reference**
$K_3[Cr(O_2)_4]$	0.142	0.183	0.211	0.031	[3]
	0.1355	0.1825	0.205	0	[4]
	0.1339(24)	0.1757(28)	0.2047(25)	0.0140(55)	[16]
	0.1355(23)	0.1788(21)	0.2079(20)	0.0082(22)	[15]
	0.1347(2)	0.1812(2)	0.2059(2)	0.0112(2)	[14]
	0.13483(14)	0.1825(2)	0.20661(14)	0.0131(2)	[17]
$K_3[Nb(O_2)_4]$	0.142	0.2	0.219	0.056	[3]
$Rb_3[Nb(O_2)_4]$	0.1342(8)	0.1827(8)	0.2054(8)	0.0182(11)	[18]
$K_3[Ta(O_2)_4]$	0.142	0.2	0.219	0.056	[3]
	0.1401(4)	0.1874(4)	0.2870(3)	0.018(1)	[19]
$Rb_3[Ta(O_2)_4]$	0.136	0.203	0.214	0.058	[3]
$Cs_3[Ta(O_2)_4]$	0.131	0.189	0.208	0.061	[3]

Another view of the unit cell of $K_3[Cr(O_2)_4]$ on the *ab* plane presenting more clearly the whole structure, is shown as follows:

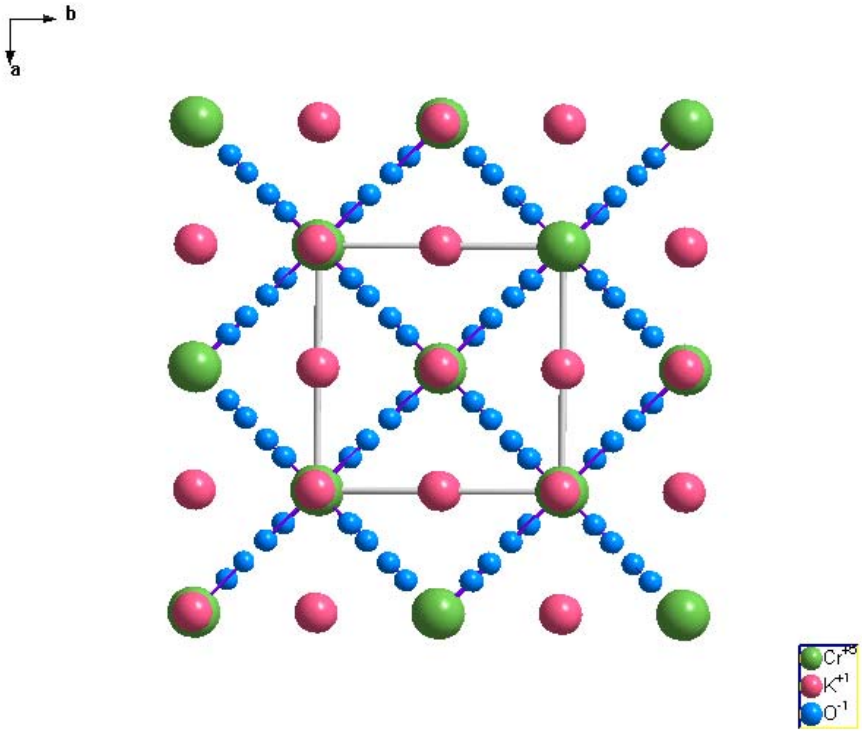

Figure 1.4: Unit cell in the structure of Tripotassium Tetraperoxochromate (V) $K_3[Cr(O_2)_4]$.

The way how the cations K^+ are coordinated in that structure is presented in fig. 1.5 and fig. 1.6. There are two types of K^+ atoms, showing them with symbols K(1) and K(2). In fig. 1.5 it is shown how the K atoms surround the peroxochromate ion of which only the Cr atom is visible in the structure. Eight atoms of K(2) type coordinate the peroxochromate ion in the form of a square column with a distance of 384.1 pm and six atoms of K(1) type form a distorted octahedron with Cr – K(1) distances of 378.1 pm and 472.9 pm.

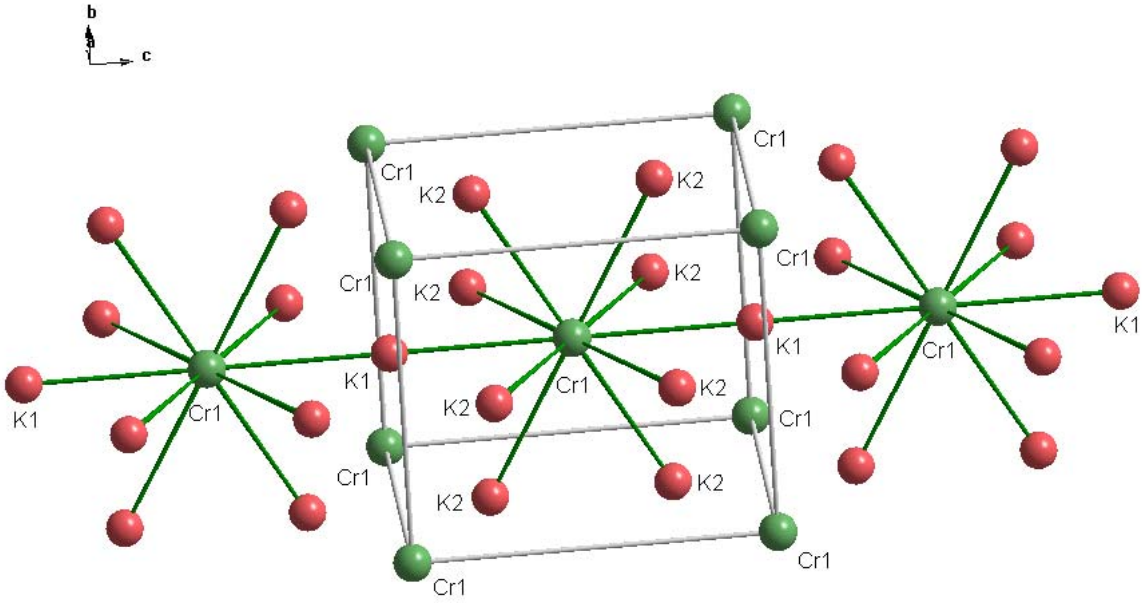

Figure 1.5: Coordinates Cr – K(1) in the structure of $K_3[Cr(O_2)_4]$.

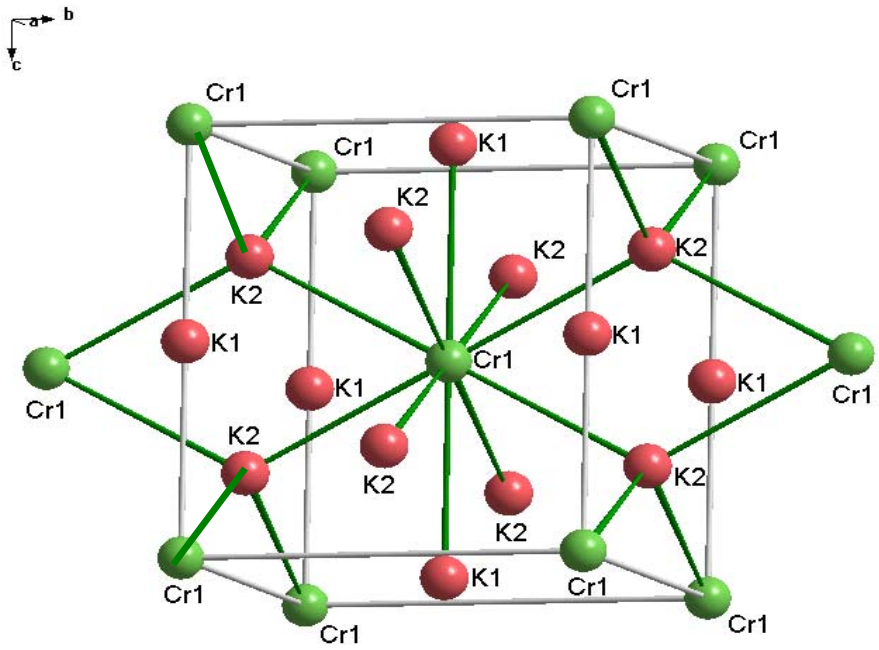

Figure 1.6: Coordinates Cr – K(2) in the structure of $K_3[Cr(O_2)_4]$.

In tab. 1.5. are given the reported interatomic distances (in pm) for chromium and both types of potassium.

Table 1.5: Reported interatomic distances (in pm) in the structure of Tripotassium (tetra)Peroxochromate (V) $K_3[Cr(O_2)_4]$.

Atom no.1	Atom no.2	Symmetry Code			Distance (pm)
Cr	K(1)	x	y	z	378.1
Cr	K(1)	0.5+x	0.5+y	-0.5+z	472.9
Cr	K(2)	x	y	z	384.1
Cr	Cr	0.5+x	0.5+y	0.5+z	605.5

It is necessary to add that the structure presented above is made according to the newest research that exist in literature [17].

1.3. The decomposition conditions of tetraperoxochromates

The decomposition of $[Cr(O_2)_4]^{3-}$ ion in alkaline aqueous solution has been studied. The mechanism appears to proceed through an oxotriperoxo intermediate species, and reversible exchange of peroxide groups between $[Cr(O_2)_4]^{3-}$ and H_2O_2 has been demonstrated [38, 39]. In aqueous medium, decomposition of the tetraperoxochromate ion occurs spontaneously. Above pH 8, this can be represented by a single, though complex, reaction according to the overall equation [39]:

$$4\,[Cr(O_2)_4]^{3-} + 2H_2O \longrightarrow 4\,CrO_4^{2-} + 4\,OH^- + 7O_2$$

This work confirmed a linear dependence of the reaction rate upon $[H^+]$ in the pH range 8.0-11.2. As the result the decomposition sequence is initiated by protonation of the tetraperoxochromate anion (see Scheme A) [39].

Scheme A:

$$[Cr(O_2)_4]^{3-} + H^+ \rightleftharpoons [HCr(O_2)_4]^{2-}$$

$$[HCr(O_2)_4]^{2-} + H_2O \rightleftharpoons [HCr(O_2)_3O]^{2-} + H_2O_2$$

$$[HCr(O_2)_3O]^{2-} \longrightarrow \text{products}$$

The protonated species appears to be able to lose a peroxide particle much more easily as the non – protonated ion. The resulting oxotriperoxointermediate may combine with H_2O_2 or may irreversibly decompose to give products. It seems possible that protonation followed by loss of a peroxide group may represent a more generalised mechanism for decomposition of the tetraperoxo complexes of transition metals in alkaline solution [39].

At neutral and lower pH the decomposition involves violet oxodiperoxochromate (VI) intermediates with the general formula $M^I[CrO(O_2)_2OH]$ (where M are the alkali metals) [40]. The overall equation at pH < 4 is:

$$2\,[Cr(O_2)_4]^{3-} + 12H^{+} \longrightarrow 2Cr^{3+} + 6H_2O + 5O_2$$

and at intermediate pH the final products are mixtures of Cr^{3+} and $(CrO_4)^{2-}$. It is possible that green peroxochromium (III) oligomers which have been reported [41] as intermediates in the reaction of acidic Cr(VI) with H_2O_2 (identified as $Cr_2O_2^{4+}$ and $Cr_3(O_2)_2^{5+}$) might also be formed during $[Cr(O_2)_4]^{3-}$ decomposition. Studies of the interaction of Cr(VI) with H_2O_2 in acid solution which also produces the blue and violet species are also relevant to the acid decomposition of $[Cr(O_2)_4]^{3-}$ [35]. Finally, during the decomposition of Tripotassium Tetraperoxochromate in neutral and lower pH singlet oxygen is generated, which makes the study more attractive despite the fact that chromium is in an untypical valence state (V).

The thermal decomposition of the potassium salt has been extensively investigated at [42 – 45].

$$K_3[Cr(O_2)_4] \xrightarrow{\Delta t} K_2CrO_4 + KO_2 + O_2$$

The products identified in the thermally decomposed sample of $K_3[Cr(O_2)_4]$ were K_2CrO_4, KO_2 and O_2.

The salt was rapidly heated under vacuum in the magnetic resonance spectrometer to a temperature of 150 – 170 °C in order to promote explosive decomposition [38]. The K_2CrO_4 salt was identified by its UV absorption spectrum (λ_{max} = 372 nm). UV measurements established that $K_3[Cr(O_2)_4]$ was quantitatively converted to K_2CrO_4 [38]. Another way of determination the decomposing species was made at [42], where the volume of oxygen generated was measured and the amount of chromate was determined iodometrically. The KO_2 and K_2CrO_4 species have been identified with the help of X-ray diffraction investigations [44]. It is performed a general idea of the fundamental physical and chemical processes in $K_3[Cr(O_2)_4]$ Self – propagating High – temperature Decomposition (SHD) [44, 45].

The kinetics of the isothermal decomposition of $K_3[Nb(O_2)_4]$ and $K_3[Ta(O_2)_4]$ were also investigated [27, 28].

1.4. Problems

As can be seen from table 1.1 which compiles the tetraperoxo complexes of chromium, vanadium, niobium and tantalum with the general formula $A_3[B(O_2)_4]$ where $A = K^+$, Rb^+, Cs^+, or $(NH_4)^+$ the knowledge on these compounds is limited. So there is only one paper on $(NH_4)_3[Cr(O_2)_4]$, $(NH_4)_3[V(O_2)_4]$ and $K_3[V(O_2)_4]$ giving some *d* – values [10] for these compounds but the powder X-ray data are not indexed and it is not yet known whether they are isotypic to the $K_3[Cr(O_2)_4]$ – type. Furthermore in some other cases the data given in the literature are not very precise due to the fact that they have been obtained in the 40^{th} of the last century with less accurate equipment as we have today. Therefore it seemed worthwhile to reinvestigate the whole group of compounds and in the same way to look for the possibility to prepare compounds like $Cs_3[Cr(O_2)_4]$ which have not been described in literature until now. As there are only three of the compounds fully characterised with the help of single crystal data another aim of this work was the preparation of single crystals and their structural investigation.

Totally missing is a systematic investigation of the vibrational properties of the peroxo compounds of Cr^{V+}, V^{V+}, Nb^{V+} and Ta^{V+} which are isostructural to the $K_3[Cr(O_2)_4]$ – type in the literature. Only in a few cases vibrational spectra have been recorded and only the frequencies of one strong band in the infrared spectra due to the O – O stretching vibration are reported. Therefore an investigation on the chromium peroxo complexes of ammonium, potassium and rubidium and the corresponding peroxo complexes of vanadium, niobium and tantalum with the main emphasis on their vibrational properties has been started.

2. Characterisation methods

2.1. Diffraction methods

X-rays for diffraction experiments are produced by bombarding a metal target with a beam of electrons emitted from a heated filament. X-rays are scattered by their interaction with atomic electrons, and interference takes place between X-rays scattered from different parts of a crystal. The diffraction method in which a detector is used to measure the scattered intensity of X-rays as a function of angle, yields both the 2Θ value and intensity of each reflection.

2.1.1. X-ray powder diffraction analysis

All the microcrystalline products have been characterized by X-ray diffraction methods using a Siemens powder diffractometer model D5000 equipped with a Germanium monochromator, using CuKα_1 (λ = 154.06 pm) radiation. The X-ray reflections (2Θ = 15 – 80°) are collected with a Braun GmbH, Garching, position sensitive detector PSD – 50M. The visualization of the diffraction data, their indexing and the refinement of the lattice parameters are done with the STOE program WinX^{Pow} [46].
This Program Package has also been used to calculate theoretical diffraction graphics according to the crystal data of a known substance in order to compare the theoretical and experimental diffraction graphics with the purpose to evaluate the purity of the prepared substance and their crystal structure.

2.1.2. Single crystal analysis (IPDS)

For the single crystal investigation an **I**maging **P**late **D**iffraction **S**ystem (IPDS) diffractometer of the company STOE, Darmstadt, was used which works with Mo – Kα

(λ = 71.073 pm) monochromatic radiation (Graphite monochromator). The crystal structure was solved using the program Shelxs [47] and refined with the program Shelxl [47]. The presentation of the structures and illustrations are done with the Diamond program [48].

2.2. Vibrational spectroscopy

2.2.1. Infrared spectroscopy analysis (MIR and FIR)

Infrared absorption spectra (KBr and Nujol mull as matrices) are recorded on an Bruker, Karlsruhe, IFS 113V Fourier transform interferometer, equipped with OPUS – Spectroscopy software of 2.2 version [49].

The potassium bromide disk method has been used for the recording of the spectra above 400 cm^{-1} (middle infrared region). A very small amount of finely ground solid sample is mixed with KBr and than pressed in an evacuated die under high pressure. The resulting transparent discs yielded good spectra in the region 4000 – 400 cm^{-1}.

The mineral oil (Nujol) mull method is used to record the spectra under 400 cm^{-1} wavelength (far infrared region). A small amount of solid sample is mulled in a mortar with a small amount of Nujol to yield a paste which is than transferred to polyethylene plates.

The MIR and FIR spectra are recorded at room and low temperature (liquid nitrogen temperature around 120 K). For the low temperature measurements the low temperature cell P\N 21.500 of Grasbey Specac, St. Mary Gray (GB) firm was employed. The temperature was controlled using the EU 808 temperature controller of the Eurotherm (Limburg) firm. The resolution of the infrared spectra was fixed to 2 cm^{-1}.

2.2.2. Raman spectroscopy

Raman spectra, with samples taken in sealed glass capillary tubes, are measured on a Bruker Raman – Fourier – Transform – Spectrometer Type RFS 100/S. For excitation the 1064 nm line of an Nd: YAG laser was employed. The measurements of ammonium compounds are made at low temperature (liquid nitrogen temperature around 120 K) and the other compounds are measured at room temperature. For measurements at low temperature the Bruker R 495 low-temperature cell with the 808 type of temperature controller was employed. The resolution of the Raman spectra was fixed to 2 cm^{-1}. The integration time is 1 ~ 30 sec and the number of accumulations is 30 ~ 50.

3. Preparation of tetraperoxo compounds with the general formula: $A_3[B(O_2)_4]$ where *A*: $(NH_4)^+$, K^+, Rb^+ or Cs^+ and *B*: Cr^{V+}, V^{V+}, Nb^{V+} or Ta^{V+}

3.1. General

The usual way of preparing the tetraperoxo compounds of chromium (V), vanadium (V), niobium (V) and tantalum (V) is by adding hydrogen peroxide (30 wt%) to cooled, slightly alkaline solutions of the corresponding chromates, vanadates, niobates and tantalates. It is necessary to add alcohol to the solutions in order to reduce the solubility of such compounds. A better procedure has been developed for getting pure compounds in the form of fine crystal powders or in the form of single crystals. The tetraperoxo compounds of Cr^{V+}, V^{V+}, Nb^{V+} and Ta^{V+} are not stable, therefore they have to be kept hold ($t° < 0°C$) during the preparations and stored in a refrigerator. For the same reason all measurements (X-ray diffraction, IR – spectra, Raman – spectra) are done immediately after preparation.

3.2. Experimental procedure

We can separate the whole experimental procedure into two main parts:

a) improving the preparation procedure of tetraperoxo compounds and
b) trying to improve the crystal growth procedure.

The way of preparation of the tetraperoxo compounds in microcrystalline form is based on the procedure described in the literature, making some slight changes. The first step is the preparation of the chromates, niobates and tantalates compounds. They are produced in solutions in the cases of $(NH_4)_2CrO_4$ and K_2CrO_4, and from the mixing of solid state substances reacting in the furnace at high temperature in the cases of Rb_2CrO_4, K_3NbO_4, Cs_3NbO_4, K_3TaO_4, Rb_3TaO_4 and Cs_3TaO_4. After that, the tetraperoxo compounds were produced by reaction with H_2O_2. A detailed description of the procedure for each compound is given in this chapter.

For getting single crystals of the compounds, there were tried different methods. The successful one was the slow crystallisation method. It was performed the slow crystal growth process where the temperature during crystal growth was hold constant. The solution with the product was let in an exsiccator under ethanol at a temperature around 4 °C where, as the result of an isotherm distillation the concentration of ethanol in the solution is slowly rising and so the crystals are formed. This method resulted in getting single crystals for the compound of $Rb_3[Ta(O_2)_4]$.

3.3. Chemical list

The substances, their origin and their purity used in the preparation of tetraperoxo compounds of chromium, vanadium, niobium and tantalum are presented in tab. 3.1.

Table 3.1: Origin and purity of the used educts.

Name	Formula	Producer	Purity
Chromium(VI) oxide	CrO_3	Merck	99 %
Ammonium hydroxide	NH_4OH	Riedel – Haën	Pure
Hydrogen peroxide	H_2O_2	Solvan HSL	30 %
Acetone	$H_3C–CO–CH_3$	Steiner	Technique
Diethyl ether	$H_5C_2–O–C_2H_5$	Biesterfeld	Technique
Potassium hydroxide	KOH	Solvan HSL	Technique
Ethanol	C_2H_5OH	Kisker	96 %
Rubidium carbonate	Rb_2CO_3	Chempur	99 %
Caesium carbonate	Cs_2CO_3	Chempur	99.9 %
Ammonium meta-vanadate	NH_4VO_3	Merck	99 %
Potassium meta-vanadate	KVO_3	Aldrich Chemical Co.	98 %
Niobium pentachloride	$NbCl_5$	Riedel – de Haën	99.99 %
Niobium pentaoxide	Nb_2O_5	Chempur	99.9 %
Potassium carbonate	K_2CO_3	Merck	99 %
Tantalum pentachloride	$TaCl_5$	Riedel – de Haën	99.99 %
Tantalum pentaoxide	Ta_2O_5	Chempur	99.9 %

3.4. Preparation of tetraperoxochromates $A_3[Cr(O_2)_4]$

The preparation of tetraperoxo compounds of Chromium with the general formula $A_3[Cr(O_2)_4]$ where *A*: $(NH_4)^+$, K^+, Rb^+ or Cs^+ is described in chapter 3.4.1, 3.4.2, 3.4.3 and 3.4.4, respectively.

3.4.1. $(NH_4)_3[Cr(O_2)_4]$

Ammonium Tetraperoxochromate was first produced by Hofmann and Hiendlmaier in 1905 [50].

The usual way of producing the peroxo compounds of chromium is by adding slowly hydrogen peroxide to cooled, slightly alkaline solutions of chromates.

$(NH_4)_3[Cr(O_2)_4]$ was prepared by the action of ammonium hydroxide on a solution of chromium oxide in the presence of an excess of hydrogen peroxide. The solution of 50 wt% CrO_3 (6.25 mL) was mixed with 25 mL NH_4OH 25 wt% and diluted with 37.5 mL H_2O. The resulting mixture was cooled with ice/sodium chloride mixture to – 5 °C. Than 12.5 mL 30 wt% H_2O_2 was added slowly to the reaction mixture under vigorous stirring. The resulting red brown precipitate was filtered off under vacuum and washed on the filter with acetone than dried with diethyl ether. In order to eliminate the oxidation to the chromate again, the product was stored in an exsiccator under – 4 °C in refrigerator.

Schema:

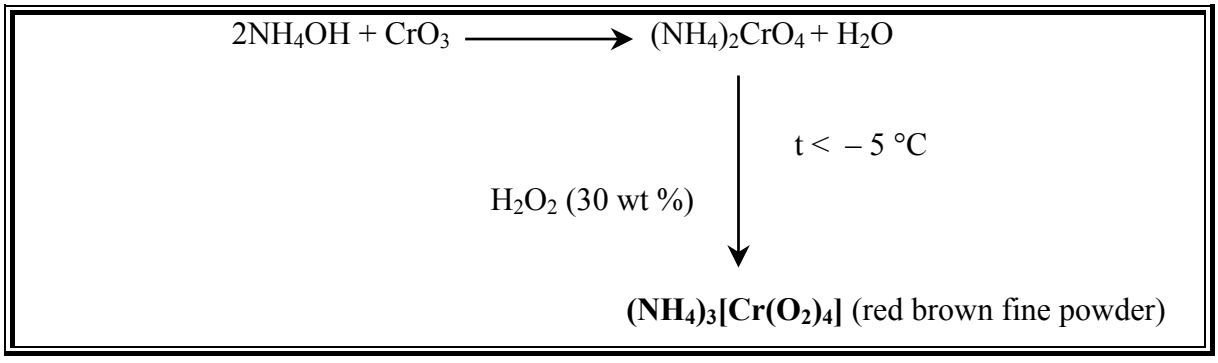

Chemical reactions for Ammonium, Potassium and Rubidium Tetraperoxo compound is based on these equations:

$$2\,(CrO_4)^{2-} + 8\,H_2O_2 \longrightarrow 2\,[Cr(O_2)_4]^{2-} + 8\,H_2O$$

$$2\,[Cr(O_2)_4]^{2-} + 2\,OH^- \longrightarrow 2\,[Cr(O_2)_4]^{3-} + H_2O_2$$

$$2\,(CrO_4)^{2-} + 7\,H_2O_2 + 2\,OH^- \longrightarrow 2\,[Cr(O_2)_4]^{3-} + 8\,H_2O$$

In general, the synthesis involves the reduction of Cr(VI) to Cr(V) by H_2O_2 in the appropriate base at a temperature under – 4 °C.

3.4.2. $K_3[Cr(O_2)_4]$

The synthesis of $K_3[Cr(O_2)_4]$ is accomplished by a slightly modified procedure published by Riesenfeld [8].

Schema:

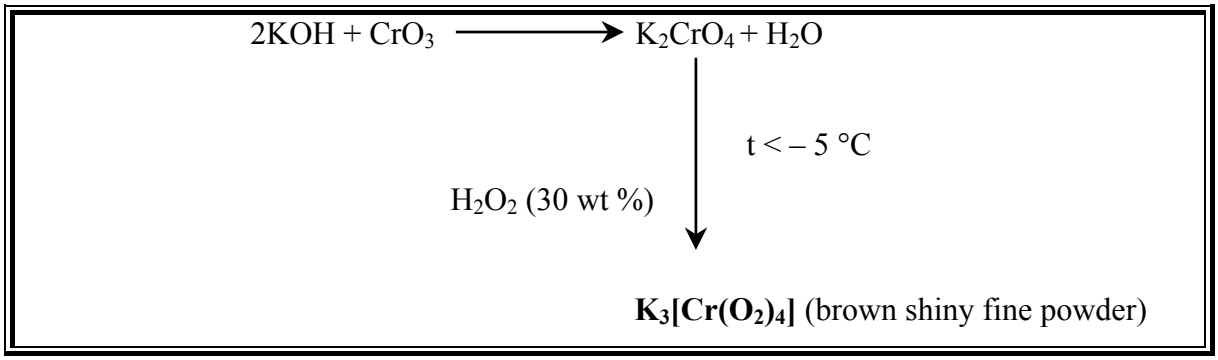

Specifically, 25 g of CrO_3 was dissolved in water from which 12.5 mL of 50 wt% solution was taken and mixed with 100 mL of an aqueous KOH 25 wt% solution (pH ~ 12). The mixture was cooled in an ice/sodium chloride bath to around – 5 °C then 15 mL of cold hydrogen peroxide (30 wt%) was added drop-wise slowly under vigorous stirring. The resulting precipitate in brown colour was filtered off under vacuum and washed with ethanol

than dried with diethyl ether. In order to avoid the possibility of oxidation to Cr(VI) it was stored in an exsiccator under – 4 °C in a refrigerator. So, as the result it is obtained a brown shiny very fine powder.

3.4.3. $Rb_3[Cr(O_2)_4]$

$Rb_3[Cr(O_2)_4]$ Rubidium Tetraperoxochromate was prepared nearly in the same way as Ammonium Tetraperoxochromate. It was also obtained from the reaction of water solutions of rubidium chromate and hydrogen peroxide under 0 °C. So, 0.5 g chromium oxide was mixed with 2.3 g rubidium carbonate (at a molar ratio $CrO_3 : Rb_2CO_3 = 1 : 2$). Rubidium chromate was prepared by melting the mixture of the above amount in an aluminia crucible in a furnace for two hours at 800 °C. The cooled melt was dissolved in water, cooled with ice/sodium chloride mixture under – 4 °C and to the alkaline solution of the chromate (pH ~ 11) 10 mL 30 wt% hydrogen peroxide was added slowly under vigorous stirring. The resulting solution was treated with 20 mL acetone to give a crystalline precipitate. The dark brown product was filtered off under vacuum and washed on the filter with acetone than dried with diethyl ether. In order to avoid the oxidation to chromate it was stored in an exsiccator under – 4 °C in a refrigerator. These compounds are very unstable as they decompose rapidly in room temperature. Rubidium chromate was prepared in different molar ratio of chromium oxide and rubidium carbonate and concluded the molar ratio of 1 : 2 the best one, which was also used to prepare the pure compound of Rubidium Tetraperoxochromate.

Schema:

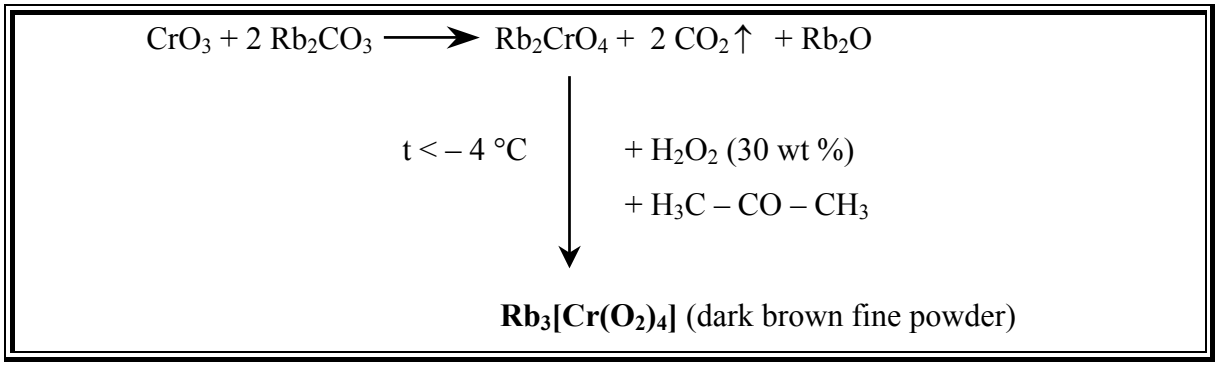

3.4.4. $Cs_3[Cr(O_2)_4]$

$Cs_3[Cr(O_2)_4]$ Caesium Tetraperoxochromate was prepared with the same procedure as described above for $Rb_3[Cr(O_2)_4]$, with the same molar ratio (CrO_3 : Cs_2CO_3 = 1 : 2). But in this case it was noted that a much darker almost black precipitate was obtained, which exploded violently when separated from the solution. The explanation in this case is given in chapter 3.4.4.1.

3.4.4.1. Discussion about $Cs_3[Cr(O_2)_4]$

The preparation of Caesium Tetraperoxochromate, as it is mentioned also in chapter 3.4.4 has not succeeded due to the unexpected explosion. This probably happened due to the fact that a peroxo – complex of the violet $[Cr^{VI}(O)(O_2)_2(OH)]^-$ or the blue $[Cr^{VI}(O)(O_2)_2(OH_2)]$ ion formed [32], which are very active and explode in the air rapidly.

The Cr (V) products is resulting from the interaction of Cr (VI) compounds with H_2O_2 [32]. During preparation of such compound (peroxo complex of Cr(V)) it is found the formation of Cr(VI) peroxo complexes "blue peroxochromic acid" in highly acid solution (pH < 4) $[Cr^{VI}(O)_5(H_2O)]$ or $[Cr^{VI}(O)(O_2)_2(OH_2)]$ and a violet deprotonated form of "peroxochromic acid" in weak acid solution ($4 \leq pH \geq 7$) $[Cr^{VI}(O)(O_2)_2(OH)]^-$, as well as, at least four Cr(V) – peroxo complexes (mono –, di –, tri – and tetra – peroxo) as a function of the pH and the relative concentration of the reactants [32].

The interaction in aqueous solution in the 4 – 7 pH range is complicated as it is mention in this range both species of $[Cr^{VI}(O)(O_2)_2(OH)]^-$ ion and Cr^V. The hydrogen peroxide is a strong oxidizing agent in either acid or basic solution but toward very strong oxidizing agents, such as Cr (VI) it will behave as a reducing agent. Both species Cr (VI) and Cr (V) peroxides coexist and are unstable.

The formation of the blue (pH < 4) $[Cr^{VI}(O)(O_2)_2(OH_2)]$ from violet ($4 \leq pH \leq 7$) $[Cr^{VI}(O)(O_2)_2(OH)]^-$ implies an electrophilic attack of the H^+ on the OH^- group of $[Cr^{VI}(O)(O_2)_2(OH)]^-$.

It has to be considered also the existence of the equilibrium:

$$[Cr^{VI}(O)(O_2)_2(OH_2)] \longleftrightarrow [Cr^{VI}(O)(O_2)_2(OH)]^- + H^+$$

In the following scheme the formation of the different species of Cr (VI) and Cr (V) is presented [32]:

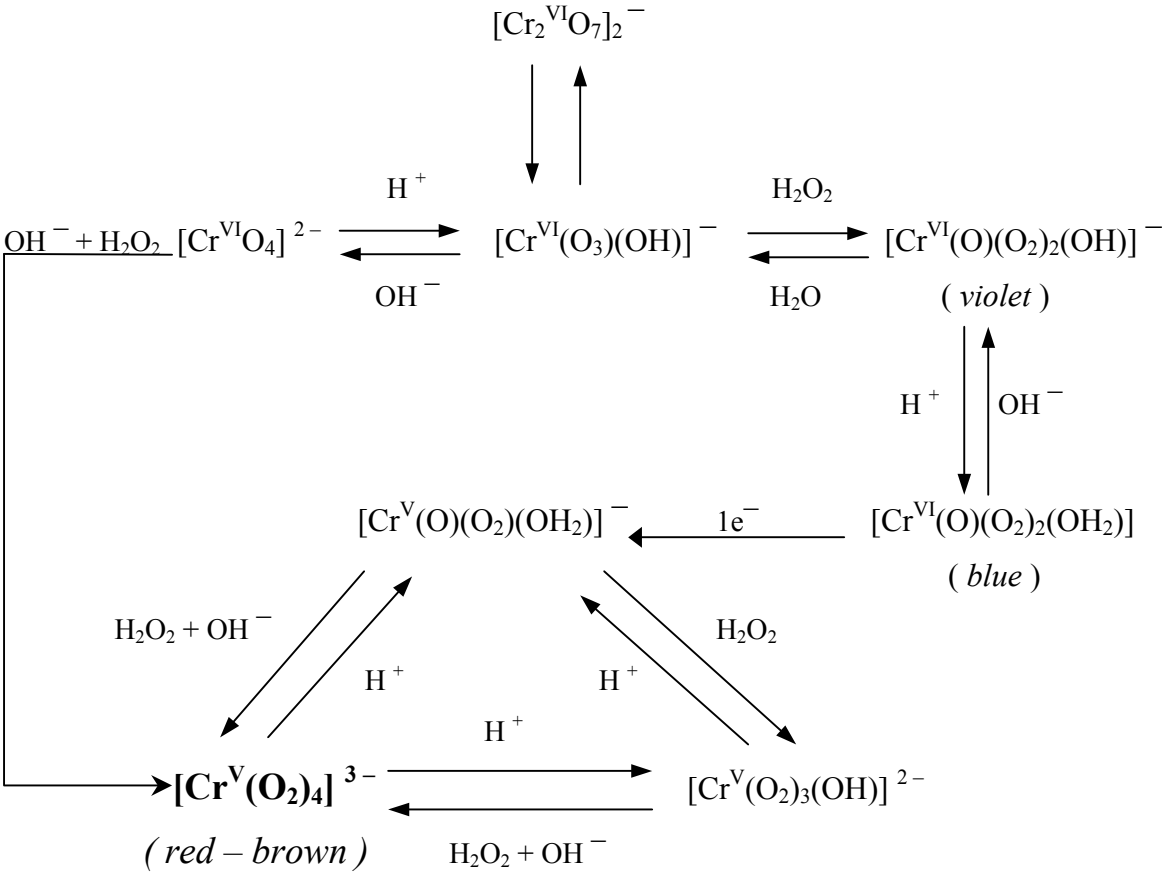

3.5. Preparation of tetraperoxovanadates $A_3[V(O_2)_4]$

Preparation of tetraperoxo compounds of Vanadium with the general formula $A_3[V(O_2)_4]$ where A: $(NH_4)^+$ or K^+ is done as follows:

3.5.1. $(NH_4)_3[V(O_2)_4]$

The way of preparation Ammonium Tetraperoxovanadate $(NH_4)_3[V(O_2)_4]$ was based on the method revealed by Martinez and Rodriguez]. Some modifications on the old method were done.

The chemical reaction is based on this equation:

$$NH_4VO_3 + 4\ H_2O_2 + 2\ NH_4OH \longrightarrow (NH_4)_3[V(O_2)_4] + 5\ H_2O$$

At first, it was dissolved 1.0 g Ammonium Vanadate in 10 mL 30 wt% hydrogen peroxide cooled before at temperature –5 °C. To the obtained yellow solution was added slowly and drop – wise the 25 wt% ammonia solution. At the beginning the yellow solution was becoming darker and then deep blue, finally the blue precipitate appeared. The solution with the precipitate was let for two hours in silence and after that it was filtered under a vacuum. The resulting precipitate was washed and dried with ethanol and diethyl ether. Finally, this product was a very fine blue powder which was stored in a refrigerator under –5 °C. Preparing single crystals from the solution was not successful, so all the measurements were done on powdered samples.

3.5.2. $K_3[V(O_2)_4]$

Preparation of Potassium Tetraperoxovanadate $K_3[V(O_2)_4]$ was also based on the literature [12]. Comparing to the procedure of preparing the vanadium peroxo salt of ammonium, this one was difficult. One could hardly prepare the clear peroxo vanadate salt of potassium.
The base chemical reaction of this procedure is:

$$KVO_3 + 4\ H_2O_2 + 2\ KOH \longrightarrow K_3[V(O_2)_4] + 5\ H_2O$$

Again one starts with dissolving the Potassium (meta)Vanadate KVO_3 (2.0 g) in 13 mL hydrogen peroxide 30 wt%. The solution was cooled under –5 °C with an ice/sodium chloride mixture. This temperature was hold constant during all the procedure. Then 6.0 g potassium hydroxide was dissolved with 8 mL of the 30 wt% hydrogen peroxide and cooled at –5 °C. After that, this solution was added under stirring slowly drop-wise to the mixture of potassium metavanadate and hydrogen peroxide. The colour of the solution changed

immediately from yellow to brown and at the end to the blue one. In order to help crystallisation of the salt, it was added at the end some drops of ethanol. The micro crystalline – precipitate was let in silence for an hour hoping to get fine crystals and after that, it was filtered off under a vacuum. The final product was washed on the filter with ethanol and then dried with diethyl ether. Storing of this compound was done as the others too, so placed them first into an exsiccator for further drying and let it in a refrigerator under –5 °C.

Finally, it was prepared the Tetraperoxovanadate salt of Potassium with the deep blue-violet colour which was a very fine powder.

3.6. Preparation of tetraperoxoniobates $A_3[Nb(O_2)_4]$

Preparation of tetraperoxo compounds of Niobium with the general formula $A_3[Nb(O_2)_4]$ where A: $(NH_4)^+$, K^+ or Cs^+ is presented as follows:

3.6.1. $(NH_4)_3[Nb(O_2)_4]$

There are two ways of preparing Ammonium Tetraperoxoniobate-salt known from literature [25, 51]. One is by adding 25 wt% ammonia solution to one of the niobic acid in a mixture of equal volumes of 50 wt% HNO_3 and 15 wt% H_2O_2 at pH 9 – 9.5 and cooled to 3 – 6 °C. The other one is by starting with niobium pentachloride and described in details as follows. In that case a few modifications have been made with respect to the literature [25].

The preparation of Tetraperoxoniobate – salt of Ammonium follows the equation:

$$NbCl_5 + 4\ H_2O_2 + 8\ NH_4OH \longrightarrow (NH_4)_3[Nb(O_2)_4] + 5\ NH_4Cl + 8\ H_2O$$

The method of preparing the Ammonium Tetraperoxoniobate $(NH_4)_3[Nb(O_2)_4]$ was starting from niobium pentachloride. The amount of 0.5 g of $NbCl_5$ was added to the hydrogen peroxide solution 5 wt% (12 mL), cooled before under –2 °C with an ice/sodium chloride mixture. The concentration of the aqueous hydrogen peroxide must not be greater than 5 wt% and it must be added in the stoichiometric ratio. The mixture was stirred until dissolution was

completed and it was getting a yellow solution. The ammonium peroxo–salt was precipitated by the gradual addition the 5 mL of 25 wt% aqueous ammonia and 5 mL ethanol. The resulting fine precipitate with white colour was filtered off under vacuum, washed with ethanol and dried with diethyl ether and at the end stored the precipitate in an exsiccator under 0 °C in a refrigerator. In order to obtain this tetraperoxo compound with high purity, it was added an equal volume of ethanol (the same volume as NH_4OH) to the reaction mixture. The preparation of this salt was done under some strictly conditions, such as:

a) the temperature during the procedure was strictly under 0 °C and

b) the storing of that product was done in a refrigerator under 0 °C too, in order to eliminate the decomposition of this compound to the niobate.

The Tetraperoxoniobate – salt of Ammonium was washed with alcohol and it was resulted more stable than the sample without washing with alcohol. Ethanol removed water from the sample, so the product was chemically more stable than the peroxoniobate – salt not washed with alcohol. So, washing the sample with ethanol and after that drying it with ether gave us a pure product. After three weeks, the stability of this tetraperoxo compound has been proved by the X-ray diffraction, which concluded positive without any foreign reflection as it means that the compound was not decomposed. When the Tetraperoxoniobate salt of Ammonium is kept in a refrigerator under 0 °C the decomposition is retarded.

So finally, the resulting precipitate was a white, very fine powder. In order to obtain single crystals it was tried also the slow re – crystallisation procedure, done in an exsiccator over ethanol, but with no success.

3.6.2. $K_3[Nb(O_2)_4]$

The Potassium Tetraperoxoniobate $K_3[Nb(O_2)_4]$ was prepared first by Balke and Smith [52] and later on with minor modifications all the procedures has been performed on the same way [53, 54].

In general, niobates of the alkali metals were obtained by fusing niobium oxide with the alkali carbonates. After that, the tetraperoxo compounds were produced by adding hydrogen peroxide in excess to solutions containing the corresponding niobates and an excess of the proper alkali carbonate or hydroxide. They were most easily obtained from such solutions by

the addition of an equal volume of alcohol. The Tetraperoxoniobate of Potassium was separating as a white powder, which was filtered by suction and finally washed with alcohol and diethyl ether [52].

This method follows these equations:

$$Nb_2O_5 + 3\ K_2CO_3 \longrightarrow 2\ K_3NbO_4 + 3\ CO_2\uparrow$$

$$(NbO_4)^{3-} + 4\ H_2O_2 \longrightarrow [Nb(O_2)_4]^{3-} + 4\ H_2O$$

Specifically, 0.6 g Nb_2O_5 was mixed with 2.0 g K_2CO_3 (in a molar ratio of 1 : 3) and was melted in an aluminia crucible in a furnace for one hour at 800 °C. After releasing the gas of CO_2, the resulting salt was dissolved in distilled water (25 mL) and cooled to –2 °C with an ice/sodium chloride mixture. To the alkaline solution of the niobium salt (pH ~ 11) and at a temperature under –2 °C was added slowly drop-wise 10 mL 30 wt% hydrogen peroxide under vigorous stirring. The resulting solution was treated with 10 mL ethanol to give a crystalline precipitate. After that, a white fine turbid appeared at once, which was let in silence for two hours. As the result, the white fine powder created was filtered off under vacuum and washed with ethanol than dried with diethyl ether. The final product of Tetraperoxoniobate was stored in an exsiccator under 0 °C in a refrigerator. During all the time of preparation the temperature was hold strictly under –2 °C in order to eliminate the possibility of decomposition. Under these conditions, it has been proved by X-ray diffraction the stability of this peroxo compound after three weeks, which concluded positive. The X-ray powder diffraction of the sample measured after three weeks was the same as the diffraction of the sample measured immediately after the preparation.

This compound was a white fine powder, which is perfectly stable in the air and very good dissolved in water.

3.6.3. $Cs_3[Nb(O_2)_4]$

Preparation of the Tetraperoxoniobate salt of Caesium $Cs_3[Nb(O_2)_4]$ was made in the same way as the rubidium salt described in literature [18]. First, was prepared caesium niobate

from melting niobium oxide with caesium carbonate. After that, adding hydrogen peroxide resulted in the desired tetra peroxo salt of caesium.

This method follows these equations:

$$Nb_2O_5 + 3\ Cs_2CO_3 \longrightarrow 2\ Cs_3NbO_4 + 3\ CO_2\uparrow$$
$$(NbO_4)^{3-} + 4\ H_2O_2 \longrightarrow [Nb(O_2)_4]^{3-} + 4\ H_2O$$

Specifically, 0.6 g Nb_2O_5 was mixed with 2.0 g Cs_2CO_3 (in a molar ratio 1 to 3) and the mixture was melted in an aluminia crucible in a furnace for one hour at 800 °C. The melt, after cooling was dissolved in 30 mL distilled water. The colourless solution was cooled under 0 °C with an ice/sodium chloride mixture. The temperature during the reactions was hold on constantly at 0 °C. Then, 5 mL of 30 wt% hydrogen peroxide was added slowly drop wise to the cooled solution under vigorous stirring. After adding ethanol to this solution, a white turbidity appeared and was let stand for one hour in silence for the possibility of taking fine crystals. It was observed that the precipitate was sticky and hardly to filter it under vacuum. However, after filtration, the precipitate was washed with ethanol and dried with diethyl ether. The resulting peroxo salt of caesium was dried in an exsiccator over calcium chloride and stored in a refrigerator under 0 °C.

Finally, the product was as Tetraperoxoniobate of Potassium, a fine powder in white colour which was stable at least for three weeks, if stored in a refrigerator under 0 °C. But, the stability of this compound under this condition may be even better as the sample tested by X-ray diffraction after two months did not show any sign of decomposition.

3.7. Preparation of tetraperoxotantalates $A_3[Ta(O_2)_4]$

Preparation of tetraperoxo compounds of Tantalum with the general formula $A_3[Ta(O_2)_4]$ where A: $(NH_4)^+$, K^+, Rb^+ or Cs^+ is presented as follows:

3.7.1. $(NH_4)_3[Ta(O_2)_4]$

The preparation of Ammonium Tetraperoxotantalate $(NH_4)_3[Ta(O_2)_4]$ was done similar to that procedure of preparing Ammonium Tetraperoxoniobate and based on the literature [25] with a few modifications.

The base chemical reaction of this procedure is:

$$TaCl_5 + 4\ H_2O_2 + 8\ NH_4OH \longrightarrow (NH_4)_3[Ta(O_2)_4] + 5\ NH_4Cl + 8\ H_2O$$

It was started again with tantalum pentachloride (0.5 g), which was dissolved in 10 mL 30 wt% hydrogen peroxide cooled before under –4 °C with an ice/sodium chloride mixture.

In difference to the procedure of preparing $(NH_4)_3[Nb(O_2)_4]$, it was used hydrogen peroxide solution of higher concentration, that one of 30 wt%. The mixture was stirred until dissolution was completed. After adding 3 mL of 25 wt% NH_4OH a turbidity appeared which was getting more after adding 5 mL ethanol. The reaction was accomplished by adding the solution slowly and holding on the constant temperature of –4 °C. The precipitate was filtered off under vacuum, washed and dried with ethanol and diethyl ether. The fine powder of white colour was placed in an exsiccator and stored in a refrigerator under –4 °C. In order to eliminate the possibility of decomposition of the peroxotantalate to ammonium tantalate, it was strictly needed to maintain the conditions mentioned above. Under these conditions, the range of stability of that compound was greater. After one month it was tested the decomposition of the tetraperoxo compound by the X-ray powder diffraction method and there were taken the same diffractions (measurements immediately after preparation and after one month), as it means that the compound was not decompose.

It was tried also the slow crystallisation procedure, letting the solution after adding NH_4OH and ethanol in an exsiccator over ethanol. It is concluded after one week in forming some very small shiny white crystals in the surface of the solution which were not grown up any more. After separating them from the solution, they were also dried in an exsiccator over calcium chloride and stored in a refrigerator under 0 °C. The crystals were so fine and small that they could not be used for a single crystal analysis.

As the result, all the measurements were done on the white fine powdered samples.

3.7.2. $K_3[Ta(O_2)_4]$

The preparation of Potassium Tetraperoxotantalate $K_3[Ta(O_2)_4]$ was performed in the same way as the procedure of preparing $K_3[Nb(O_2)_4]$. It is also known in literature [19] another way of preparation, but this was not successful.
The main equations for the procedure are shown as follows:

$$Ta_2O_5 + 3\ K_2CO_3 \longrightarrow 2\ K_3TaO_4 + 3\ CO_2\uparrow$$
$$(TaO_4)^{3-} + 4\ H_2O_2 \longrightarrow [Ta(O_2)_4]^{3-} + 4\ H_2O$$

Concretely, 0.6 g tantalum pentaoxide was mixed with 2.0 g potassium carbonate in a molar ratio of 1 to 3. This mixture was molten in a furnace for one hour at 800 °C resulting in producing potassium tantalate. After cooling, it was tried to dissolve the respective tantalate with 30 mL distilled water. It was observed that, this compound was hardly dissolvable in water, so it was filtered in order to proceed further on the clear solution. The condition of the reaction was also the same as in the other procedures of preparing peroxo compounds, such as the temperature under 0 °C realising with an ice/sodium chloride mixture.
The addition of 5 mL hydrogen peroxide (30 wt%) to the alkaline solution (pH ~ 11) was done slowly and drop – wise under vigorous stirring. As the result of adding 10 mL ethanol cooled before, it appeared the first white precipitate which was getting more after a pause of two hours.
The final white precipitate was filtered off under vacuum, washed on the filter with ethanol and later on dried with diethyl ether. The product was stored in the similar way as the other peroxo compounds. Keeping it continually in a refrigerator under 0 °C, the decomposition procedure was decelerated. The stability tested by X-ray diffraction method on this compound kept on the conditions described above resulted positive even after one month. It has not seen any different in the diffractions obtained in both cases.
The Potassium Tetraperoxotantalate is a white fine powder, stable in the air and at temperature under 0 °C.

3.7.3. $Rb_3[Ta(O_2)_4]$

The method of preparing Rubidium Tetraperoxotantalate $Rb_3[Ta(O_2)_4]$ [55] has been developed and performed also in getting single crystals. It was resulted successful the procedure of getting single crystals based on the same manner as it was described for getting single crystals in the case of Rubidium Tetraperoxoniobate [18]. At the beginning rubidium tantalate Rb_3TaO_4 was prepared from melting for one hour at 800 °C in the furnace tantalum oxide (0.6 g) with rubidium carbonate (2.0 g) in a molar ratio of 1 to 3. The CO_2 gas was released. After adding hydrogen peroxide and ethanol the tetra Peroxotantalate salt of Rubidium was obtained.

This method follows these equations:

$$Ta_2O_5 + 3\ Rb_2CO_3 \longrightarrow 2\ Rb_3TaO_4 + 3\ CO_2 \uparrow$$

$$(TaO_4)^{3-} + 4\ H_2O_2 \longrightarrow [Ta(O_2)_4]^{3-} + 4\ H_2O$$

The molten mixture of Ta_2O_5 and Rb_2CO_3, after cooling was dissolved in 25 mL distilled water and filtered, separating in that way the non-dissolved amount of the mixture. The clear solution obtained was cooled under –2 °C with an ice/sodium chloride mixture. It was added slowly and drop-wise under stirring 5 mL of 30 wt% hydrogen peroxide, holding on constantly the temperature of the alkaline solution (pH~11) under –2 °C. After adding 30 mL ethanol to the cooled solution, a turbidity was observed first which resulted after one hour in a white precipitate. This precipitate was filtered off under vacuum, washed and dried with ethanol and diethyl ether. The final product was a fine powder of white colour, which was stored in an exsiccator putting it in a refrigerator under 0 °C.

The way of getting single crystals was performed as follow: after adding the hydrogen peroxide, it was stopped stirring and slowly was added the half amount of ethanol. The solution was let in an exsiccator over ethanol in a refrigerator at 4 °C, hoping to grow up the seeds of single crystals during the slow process of crystallisation. Only after 10 days there appeared the first shiny crystals, which were separated carefully from the solution and

isolated for the further analysis. The resulting white-colour crystals were parallelepiped shape with prismatic ends and typical dimensions 0.42 x 0.37 x 0.20 mm^3.

Critical parameters for growth of good quality crystals were:

1) a slower growth process,
2) temperature homogeneity during crystal growth (concretely at 4 °C) and
3) absence of stirring during the mixing of compounds.

Purity of the samples was checked with X-ray diffraction powder patterns.

3.7.4. $Cs_3[Ta(O_2)_4]$

The way of preparation the Caesium Tetraperoxotantalate $Cs_3[Ta(O_2)_4]$ was similar to that one of rubidium with a few modifications.

The chemical reactions are as follows:

$$Ta_2O_5 + 3\ Cs_2CO_3 \longrightarrow 2\ Cs_3TaO_4 + 3\ CO_2\uparrow$$

$$(TaO_4)^{3-} + 4\ H_2O_2 \longrightarrow [Ta(O_2)_4]^{3-} + 4\ H_2O$$

Specifically, 0.6 g Ta_2O_5 was mixed with 2.0 g Cs_2CO_3 (in a molar ratio 1 to 3) and the mixture was molten in an aluminia crucible in a furnace for one hour at 800 °C. Similar to the procedure described above (see 3.7.3.) the mixture was dissolved, filtered and cooled at –1 °C. After adding 5 mL of 30 wt% hydrogen peroxide, no precipitate was observed. Only after adding 20 mL ethanol a white precipitate was obtained, which was filtered off as usual under vacuum, washed and dried with ethanol and diethyl ether. The white fine powder was stored also in a refrigerator under –4 °C. It was also tried the same procedure of slow crystallisation, but in this case it was not successful. The precipitate, appearing immediately after adding the ethanol was sticky and no growth of crystals could be observed. Further analysis were done on the powder samples.

4. Structural characterisation of the tetraperoxo compounds

4.1. X-ray powder diffraction of tetraperoxochromates $A_3[Cr(O_2)_4]$

The X-ray diffraction patterns of the tetra peroxochromates of Ammonium, Potassium and Rubidium prove them to be isomorphous. The lattice dimensions obtained from the powder patterns are presented in the respective tables (see tab. 4.13). For comparison the intensities of the diffraction peaks are calculated on the basis of the fractional coordinates from single crystal structure of $K_3[Cr(O_2)_4]$ known from the literature [14]. It can be seen from the good matches of the experimental and the calculated powder diffraction patterns that in all cases the preparations resulted in single – phase products. The lattice constants are refined for each compound using the $WinX^{Pow}$ STOE program.

The powder diffraction data of $(NH_4)_3[Cr(O_2)_4]$, $K_3[Cr(O_2)_4]$ and $Rb_3[Cr(O_2)_4]$ are shown in fig. 4.1, fig. 4.2 and fig. 4.3, respectively in comparison to diffraction patterns calculated on the basis of the fractional co – ordinates of $K_3[Cr(O_2)_4]$ [14].

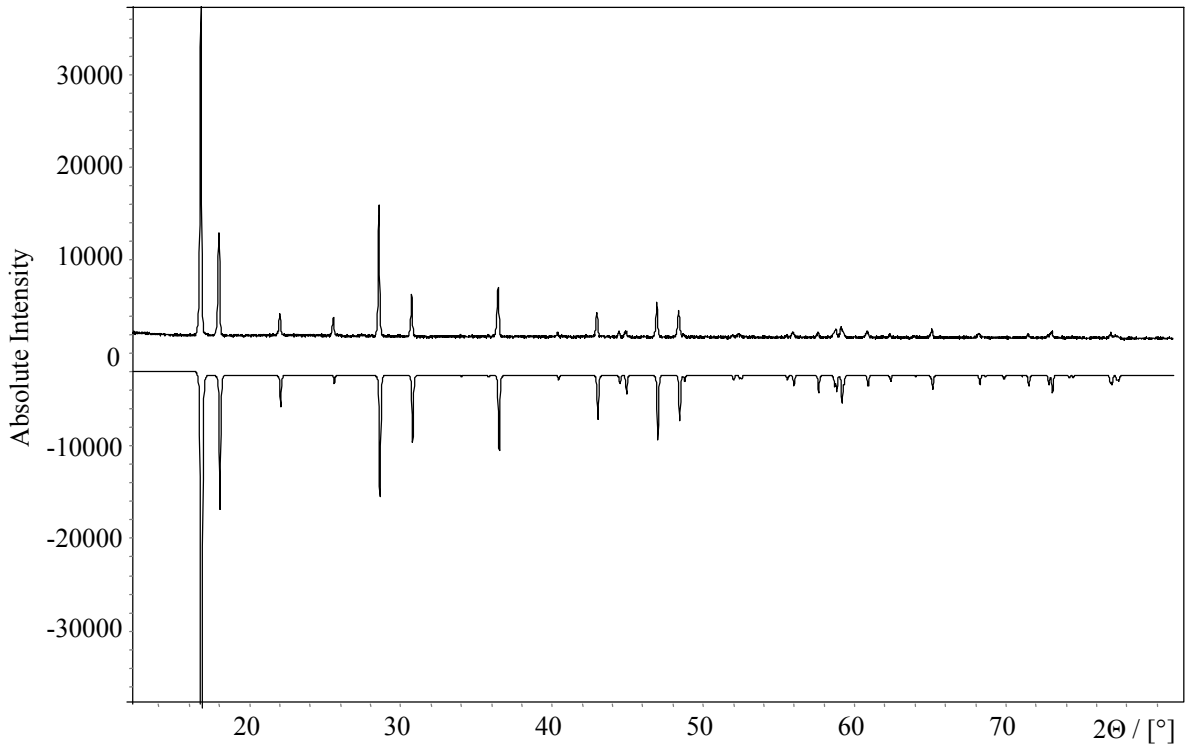

Figure 4.1: X-ray powder diffraction pattern of $(NH_4)_3[Cr(O_2)_4]$ (top) in comparison to a pattern calculated on the basis of the fractional co – ordinates of $K_3[Cr(O_2)_4]$ [14] (bottom).

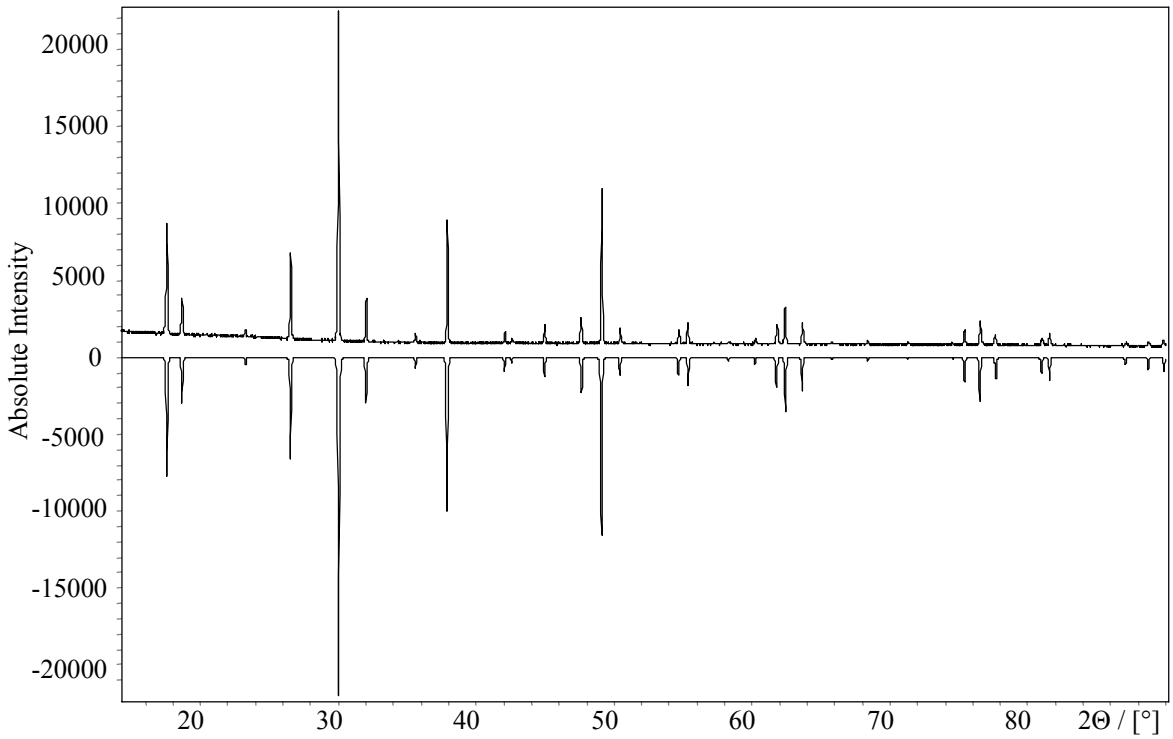

Figure 4.2: X-ray powder diffraction pattern of $K_3[Cr(O_2)_4]$ (top) in comparison to a pattern calculated on the basis of the fractional co – ordinates of $K_3[Cr(O_2)_4]$ [14] (bottom).

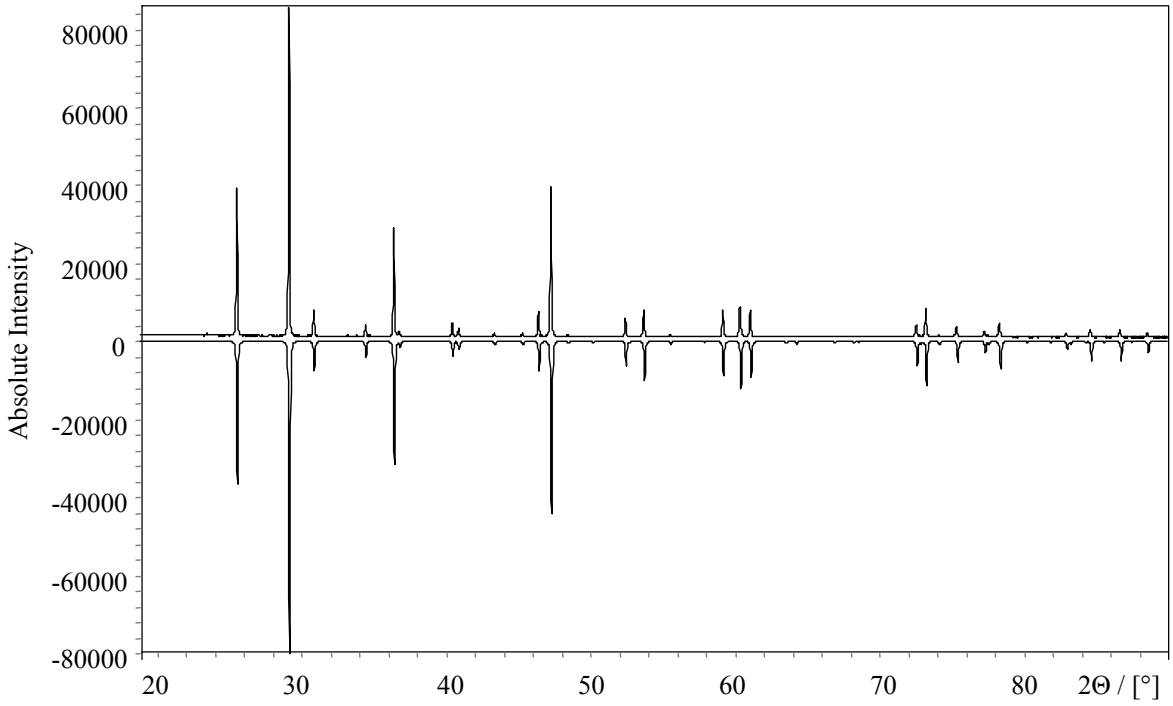

Figure 4.3: X-ray powder diffraction pattern of $Rb_3[Cr(O_2)_4]$ (top) in comparison to a pattern calculated on the basis of the fractional co – ordinates of $K_3[Cr(O_2)_4]$ [14] (bottom).

Using Louër´s algorithm on the 22 X-ray reflections of $(NH_4)_3[Cr(O_2)_4]$ a tetragonal crystal system, space group $I\bar{4}2m$ (No. 121) is found with the lattice parameters a = 697.01(4) and c = 807.44(11) pm. In this case the X-ray powder data can be fully indexed on the basis of the tetragonal cell (see tab. 4.1) and as can be seen from the good match of the experimental and the calculated powder diffraction patterns, there is no doubt that this peroxo compound crystallises in the $K_3[Cr(O_2)_4]$ – type.

At the same way, using again Louër´s algorithm on the 26 X-ray reflections of $K_3[Cr(O_2)_4]$ a tetragonal crystal system, space group $I\bar{4}2m$ (No. 121) is found with the lattice parameters a = 670.49(3) and c = 763.14(7) pm. These refined cell parameters are nearly the same as in literature [14] coming from the single crystal analysis. Again in this case the X-ray powder data can be fully indexed on the basis of the tetragonal cell (see table 4.2) and as can be seen

from the good match of the experimental and the well – known powder diffraction pattern of $K_3[Cr(O_2)_4]$ [14] there is no doubt that this peroxo compound crystallises also in the tetragonal crystal system.

The same for the 26 X-ray reflections of $Rb_3[Cr(O_2)_4]$, a tetragonal crystal system, space group $I\bar{4}2m$ (No. 121) is found with the lattice parameters a = 698.24(1) and c = 782.73(2) pm. Again in this case the X-ray powder data can be fully indexed on the basis of the tetragonal cell (see tab. 4.2) and as can be seen from the good match of the experimental and the calculated powder diffraction patterns there is no doubt again that this peroxo compound crystallises in the $K_3[Cr(O_2)_4]$ – type.

Table 4.1: X-ray powder diffraction data of $(NH_4)_3[Cr(O_2)_4]$ (tetragonal, a = 697.01(4) and c = 807.44(11) pm).

$(NH_4)_3[Cr(O_2)_4]$						
No.	$\mathbf{d_{obs}}$	$\mathbf{d_{cal}}$	**h**	**k**	**l**	$\mathbf{I_{obs}}$
1	5.2731	5.2762	1	0	1	100.0
2	4.9283	4.9286	1	1	0	37.3
3	4.0364	4.0372	0	0	2	15.4
4	3.4845	3.4851	2	0	0	14.2
5	3.1221	3.1232	1	1	2	44.3
6	2.9074	2.9080	2	1	1	20.9
7	2.4639	2.4643	2	2	0	22.6
8	2.2327	2.2328	3	0	1	10.3
9	2.1032	2.1034	2	2	2	15.9
10	2.0372	2.0372	2	1	3	10.5
11	2.0184	2.0186	0	0	4	10.6
12	1.9343	1.9346	3	1	2	18.5
13	1.8797	1.8800	3	2	1	16.4
14	1.6427	1.6429	3	3	0	10.6
15	1.5997	1.5999	4	0	2	10.4
16	1.5705	1.5701	3	2	3	11.3
17	1.5216	1.5217	3	3	2	10.8
18	1.4886	1.4887	3	1	4	10.1
19	1.4317	1.4315	4	1	3	11.0
20	1.3737	1.3737	5	0	1	10.3
21	1.2947	1.2948	5	1	2	10.6
22	1.2383	1.2378	5	0	3	10.1

Table 4.2: X-ray powder diffraction data of $K_3[Cr(O_2)_4]$ (tetragonal, a = 670.49(3) and c = 763.14(7) pm) and $Rb_3[Cr(O_2)_4]$ (tetragonal a = 698.24(1) and c = 782.73(2) pm).

	$K_3[Cr(O_2)_4]$						$Rb_3[Cr(O_2)_4]$					
No.	d_{obs}	d_{cal}	**h**	**k**	**l**	I_{obs}	d_{obs}	d_{cal}	**h**	**k**	**l**	I_{obs}
1	5.0350	5.0370	1	0	1	38.7	5.2121	5.2105	1	0	1	3.0
2	4.7399	4.7411	1	1	0	16.7	3.4913	3.4912	2	0	0	45.7
3	3.8162	3.8157	0	0	2	7.8	3.0672	3.0670	1	1	2	100.0
4	3.3514	3.3524	2	0	0	30.3	2.9007	2.9003	2	1	1	9.0
5	2.9720	2.9726	1	1	2	100.0	2.6053	2.6052	2	0	2	5.2
6	2.7902	2.7908	2	1	1	17.1	2.4686	2.4686	2	2	0	33.8
7	2.5181	2.5185	2	0	2	6.8	2.4449	2.4440	1	0	3	3.2
8	2.3699	2.3705	2	2	0	39.5	2.2309	2.2309	3	0	1	5.6
9	2.1443	2.1449	3	0	1	7.2	2.2081	2.2080	3	1	0	3.9
10	2.1198	2.1203	3	1	0	5.2	2.0022	2.0022	2	1	3	2.5
11	2.0132	2.0136	2	2	2	9.0	1.9566	1.9568	0	0	4	8.8
12	1.9078	1.9078	0	0	4	11.3	1.9231	1.9231	3	1	2	46.7
13	1.8531	1.8534	3	1	2	48.9	1.7456	1.7456	4	0	0	6.8
14	1.8065	1.8067	3	2	1	7.9	1.7070	1.7070	2	0	4	9.4
15	1.6761	1.6762	4	0	0	7.6	1.5613	1.5613	4	2	0	9.3
16	1.6582	1.6581	2	0	4	9.8	1.5335	1.5335	2	2	4	10.4
17	1.5344	1.5347	4	0	2	5.1	1.5171	1.5171	3	3	2	9.4
18	1.4993	1.4993	4	2	0	9.5	1.3026	1.3026	4	0	4	5.0
19	1.4864	1.4863	2	2	4	14.5	1.2925	1.2925	5	1	2	9.4
20	1.4600	1.4601	3	3	2	9.9	1.2612	1.2613	1	1	6	4.4
21	1.2593	1.2592	4	0	4	7.5	1.2343	1.2343	4	4	0	3.1
22	1.2433	1.2432	5	1	2	10.5	1.2204	1.2204	4	2	4	5.6
23	1.2287	1.2288	5	2	1	6.4	1.1637	1.1637	6	0	0	2.7
24	1.1856	1.1853	4	4	0	5.1	1.1451	1.1451	5	3	2	3.7
25	1.1789	1.1788	4	2	4	6.9	1.1232	1.1232	3	1	6	3.3
26	1.1010	1.1010	5	3	2	4.5	1.1040	1.1041	1	0	7	2.7

4.2. X-ray powder diffraction of tetraperoxovanadates $A_3[V(O_2)_4]$

The X-ray diffraction patterns of the tetra peroxovanadates of Ammonium and Potassium prove them to be isomorphous. The lattice constants are refined for each compound using the $WinX^{Pow}$ STOE program. The diffraction patterns are calculated on the basis of the fractional coordinates for $K_3[Nb(O_2)_4]$ known from the literature [3]. The lattice constants obtained from the powder patterns are presented in the respective tables. It can be seen from the good matches of the experimental and the calculated powder diffraction patterns that in both cases there are produced single – phase products.

The powder diffraction data of $(NH_4)_3[V(O_2)_4]$ and $K_3[V(O_2)_4]$ are shown in fig. 4.4 and in fig. 4.5, respectively in comparison to diffraction patterns calculated on the basis of the fractional co – ordinates of $K_3[Nb(O_2)_4]$ [3].

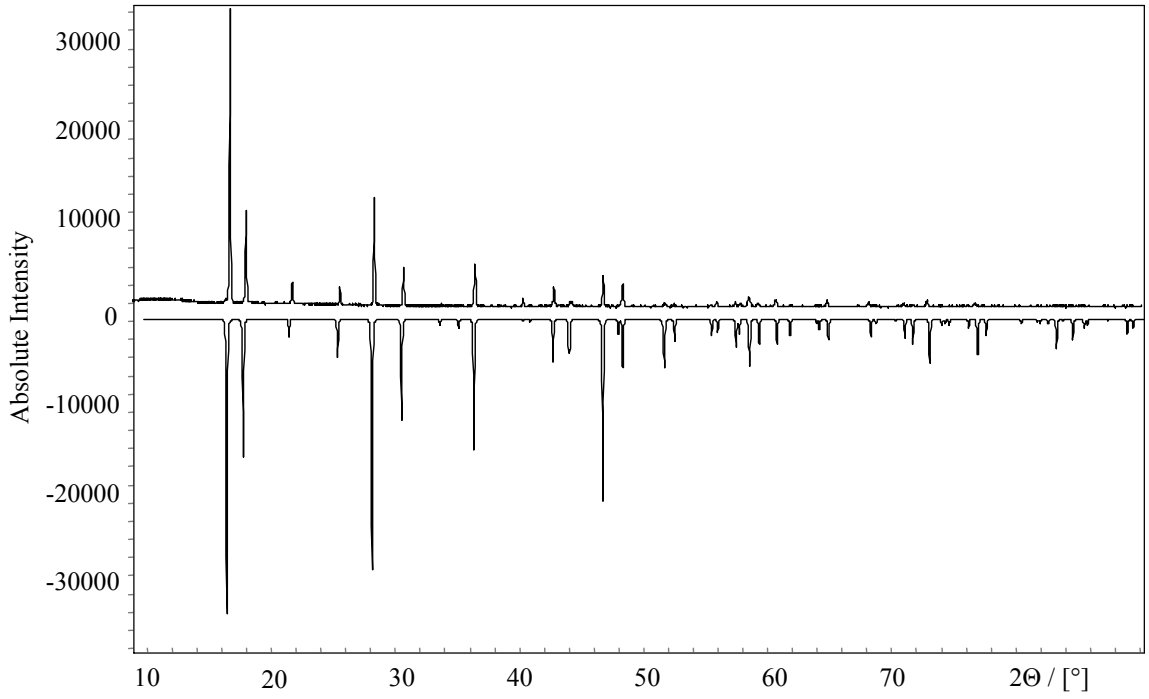

Figure 4.4: X-ray powder diffraction pattern of $(NH_4)_3[V(O_2)_4]$ (top) in comparison to a pattern calculated on the basis of the fractional co – ordinates of $K_3[Nb(O_2)_4]$ [3] (bottom).

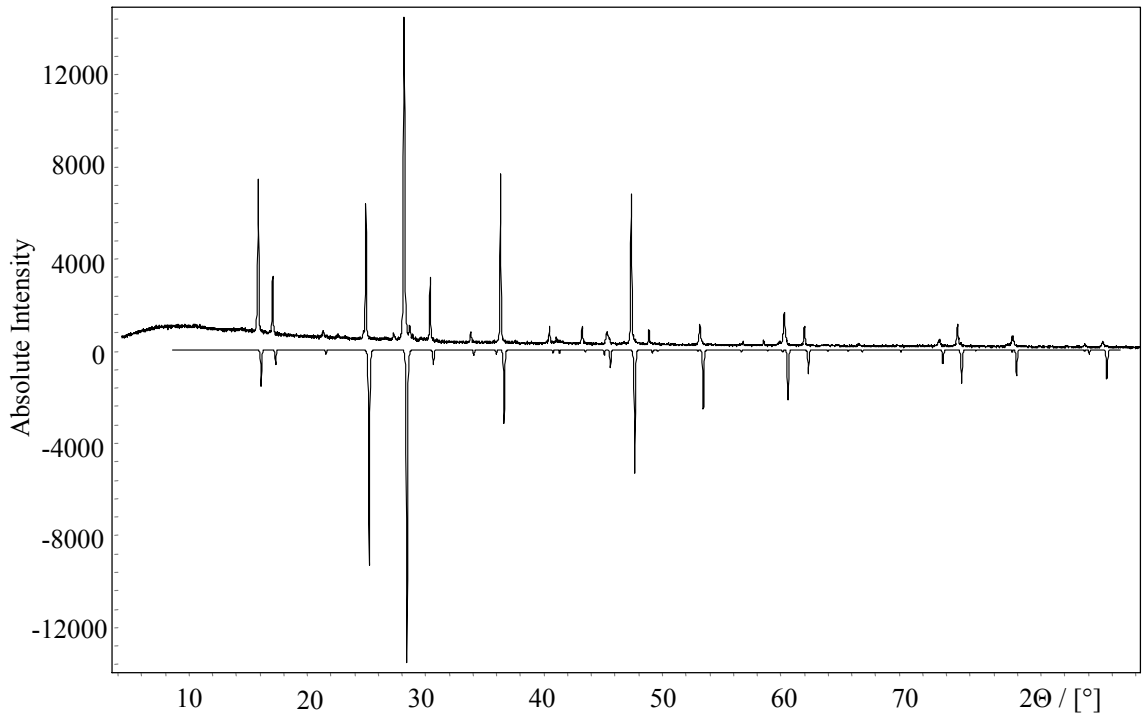

Figure 4.5: X-ray powder diffraction pattern of $K_3[V(O_2)_4]$ (top) in comparison to a pattern calculated on the basis of the fractional co – ordinates of $K_3[Nb(O_2)_4]$ [3] (bottom).

If the sample is stored at room temperature, a decomposition of the compound occurred, which can be seen clearly also from the X-ray analysis. As an example, a sample of $(NH_4)_3[V(O_2)_4]$ was let at room temperature for one week. After four days the sample was investigated once again by X-ray diffraction. The result is shown in fig. 4.6 and compared to a theoretical pattern of the tetraperoxovanadate. This shows very clearly the total decomposition of the compound. Thus, the Ammonium tetraperoxovanadate is a compound which is stable at temperature under 0 °C but at room temperature is decomposing. It is coming in the same conclusion also for the other tetraperoxo compounds.

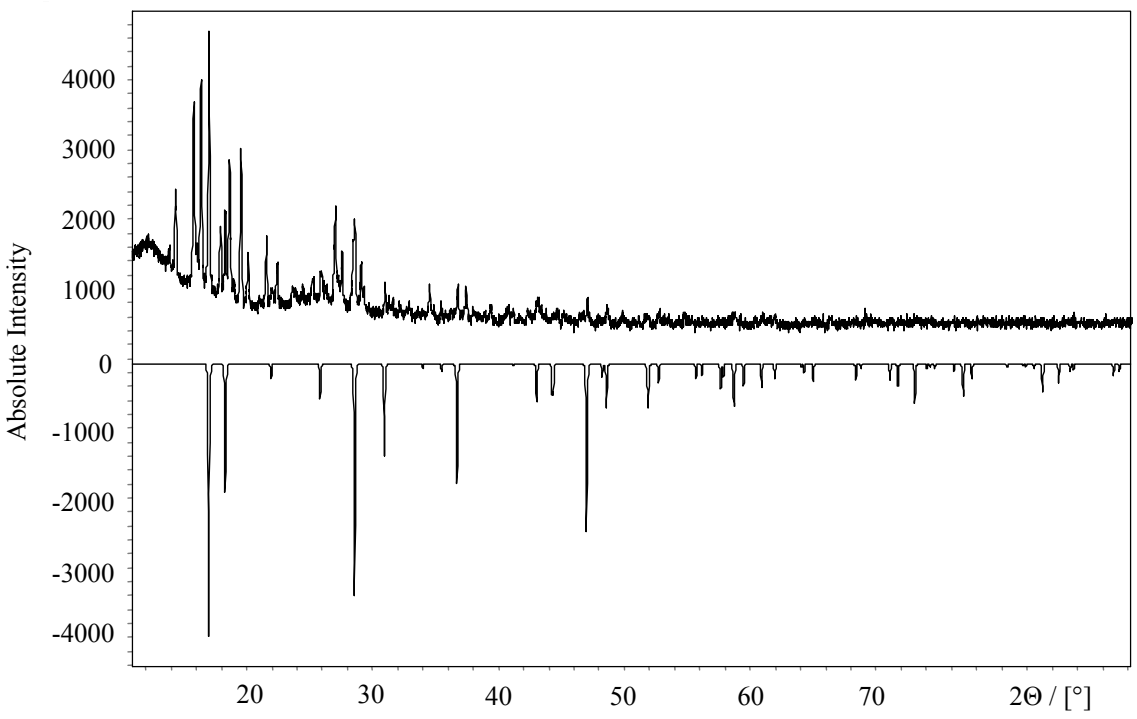

Figure 4.6: X-ray powder diffraction pattern of $(NH_4)_3[V(O_2)_4]$ in room temperature (top) in comparison to a pattern calculated on the basis of the fractional co – ordinates of $K_3[Nb(O_2)_4]$ [3] (bottom).

Using Louër´s algorithm on the 21 X-ray reflections of $(NH_4)_3[V(O_2)_4]$ a tetragonal crystal system, space group $I\bar{4}2m$ (No. 121) is found with the lattice parameters a = 697.25(5) and c = 819.42(14) pm. In this case the X-ray powder data can be fully indexed on the basis of the tetragonal cell (see tab. 4.3).

For the 21 X-ray reflections of $K_3[V(O_2)_4]$, also a tetragonal crystal system, space group $I\bar{4}2m$ (No. 121) is found with the lattice parameters a = 669.43(6) and c = 773.03(11) pm with the exception of two reflections. The X-ray powder data can be fully indexed on the basis of the tetragonal cell (see tab. 4.4).

As can be seen from the good match of the experimental and the calculated powder diffraction patterns, there is no doubt that these peroxo compounds crystallise in the

$K_3[Cr(O_2)_4]$ – type. In the Potassium tetraperoxovanadate there are only two reflections not indexed, but still it does not change the result of crystallising in tetragonal crystal system.

Table 4.3: X-ray powder diffraction data of $(NH_4)_3[V(O_2)_4]$ (tetragonal, a = 697.25(5) and c = 819.42(14) pm).

$(NH_4)_3[V(O_2)_4]$						
No.	$\mathbf{d_{obs}}$	$\mathbf{d_{cal}}$	**h**	**k**	**l**	$\mathbf{I_{obs}}$
1	5.3061	5.3102	1	0	1	100.0
2	4.9287	4.9303	1	1	0	36.1
3	4.0933	4.0971	0	0	2	12.5
4	3.4853	3.4862	2	0	0	11.2
5	3.1496	3.1511	1	1	2	40.9
6	2.9139	2.9143	2	1	1	17.0
7	2.4650	2.4651	2	2	0	18.1
8	2.2360	2.2360	3	0	1	7.0
9	2.1120	2.1123	2	2	2	11.0
10	1.9413	1.9416	3	1	2	14.3
11	1.8821	1.8821	3	2	1	11.9
12	1.7663	1.7662	2	0	4	5.8
13	1.6435	1.6434	3	3	0	6.0
14	1.6038	1.6040	4	0	2	6.2
15	1.5764	1.5755	2	2	4	7.7
16	1.5592	1.5591	4	2	0	5.8
17	1.5252	1.5253	3	3	2	6.5
18	1.4378	1.4378	4	1	3	6.6
19	1.3748	1.3747	5	0	1	6.1
20	1.3274	1.3276	4	0	4	5.7
21	1.2972	1.2971	5	1	2	6.8

Table 4.4: X-ray powder diffraction data of $K_3[V(O_2)_4]$ (tetragonal, a = 669.43(6) and c = 773.03(11) pm).

$K_3[V(O_2)_4]$						
No.	**d_{obs}**	**d_{cal}**	**h**	**k**	**l**	**I_{obs}**
1	5.0626	5.0605	1	0	1	51.5
2	4.7359	4.7336	1	1	0	23.4
3	3.8674	3.8651	0	0	2	7.3
4	3.3478	3.3471	2	0	0	45.2
5	3.0811	------- not indexed -------				6.4
6	2.9944	2.9939	1	1	2	100.0
7	2.9472	------- not indexed -------				9.0
8	2.7921	2.7917	2	1	1	22.8
9	2.5308	2.5302	2	0	2	7.0
10	2.3670	2.3668	2	2	0	54.0
11	2.1442	2.1439	3	0	1	8.3
12	2.0183	2.0184	2	2	2	8.4
13	1.9328	1.9326	0	0	4	6.8
14	1.8566	1.8567	3	1	2	47.8
15	1.8055	1.8053	3	2	1	7.8
16	1.6735	1.6736	2	0	4	9.4
17	1.4968	1.4969	2	2	4	12.9
18	1.4608	1.4608	3	3	2	8.5
19	1.2648	1.2651	4	0	4	4.5
20	1.2430	1.2432	1	1	6	8.8
21	1.1831	1.1834	4	2	4	5.6

4.3. X-ray powder diffraction of tetraperoxoniobates $A_3[Nb(O_2)_4]$

The X-ray diffraction patterns of the tetra peroxoniobates of Ammonium, Potassium and Caesium prove them also to be isomorphous. The lattice dimensions obtained from the powder patterns are presented. The diffraction patterns are calculated on the basis of the fractional coordinates for $Rb_3[Nb(O_2)_4]$ from to the literature [18]. It can be seen from the good matches of the experimental and the theoretical powder diffraction patterns that in all cases the products of the preparation are single – phase. The lattice constants are refined for each compound using the $WinX^{Pow}$ STOE program.

The powder diffraction data of $(NH_4)_3[Nb(O_2)_4]$, $K_3[Nb(O_2)_4]$ and $Cs_3[Nb(O_2)_4]$ are shown in fig. 4.7, fig. 4.8 and fig. 4.9, respectively in comparison to diffraction patterns calculated on the basis of the fractional co – ordinates from single crystal structure of $Rb_3[Nb(O_2)_4]$ known from the literature [18].

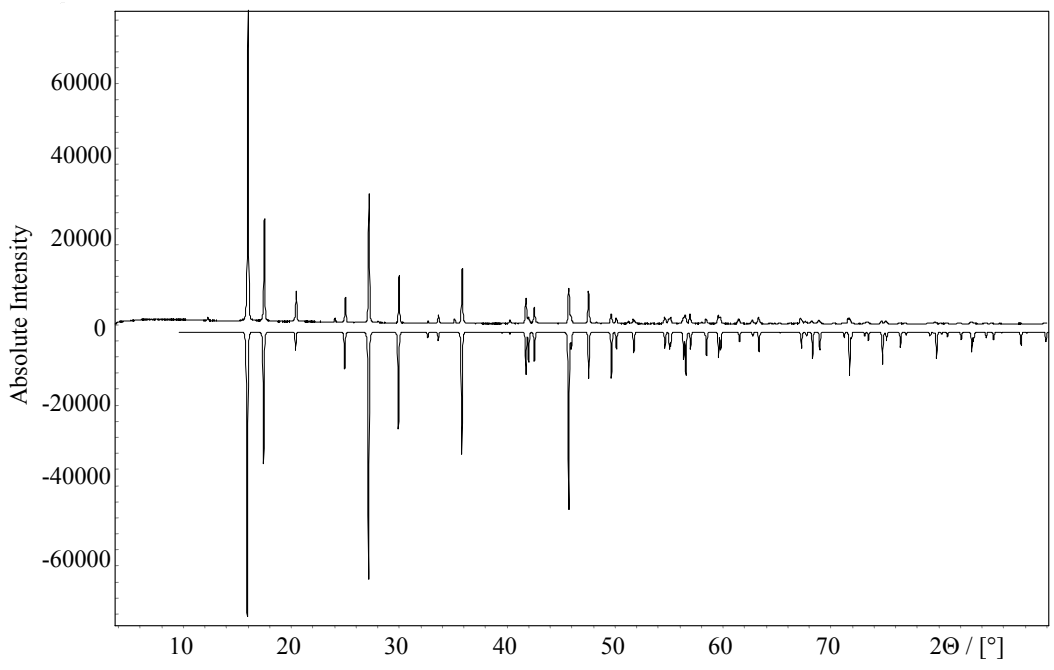

Figure 4.7: X-ray powder diffraction pattern of $(NH_4)_3[Nb(O_2)_4]$ (top) in comparison to a pattern calculated on the basis of the fractional co – ordinates of $Rb_3[Nb(O_2)_4]$ [18] (bottom).

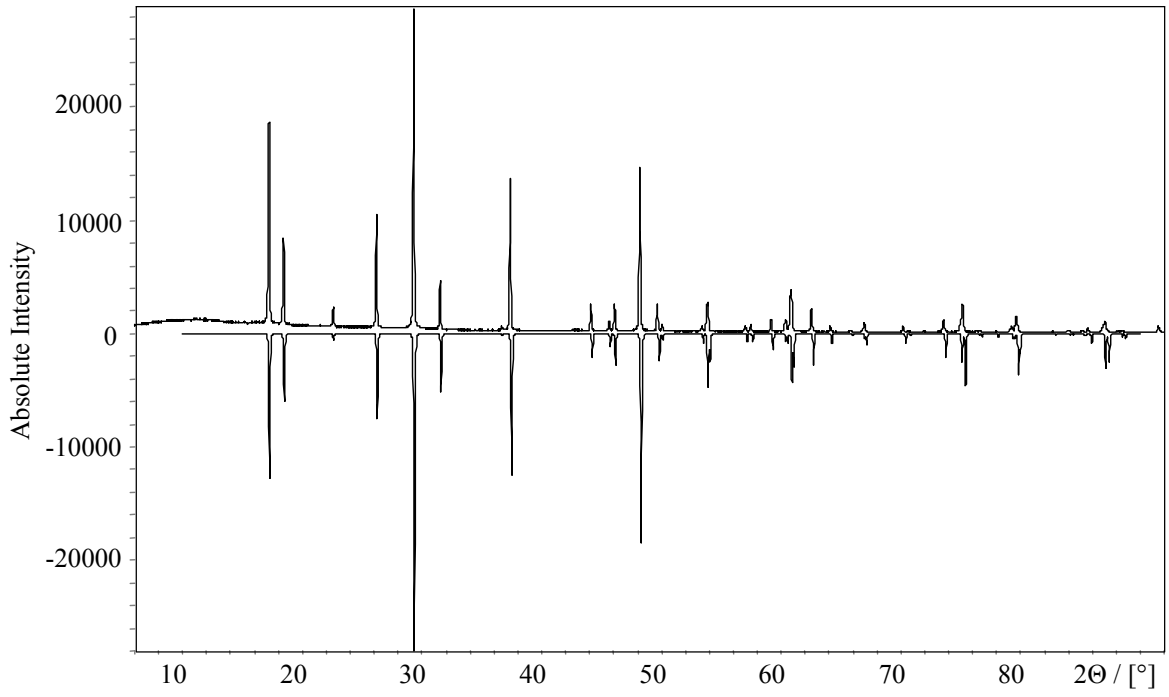

Figure 4.8: X-ray powder diffraction pattern of $K_3[Nb(O_2)_4]$ (top) in comparison to a pattern calculated on the basis of the fractional co – ordinates of $Rb_3[Nb(O_2)_4]$ [18] (bottom).

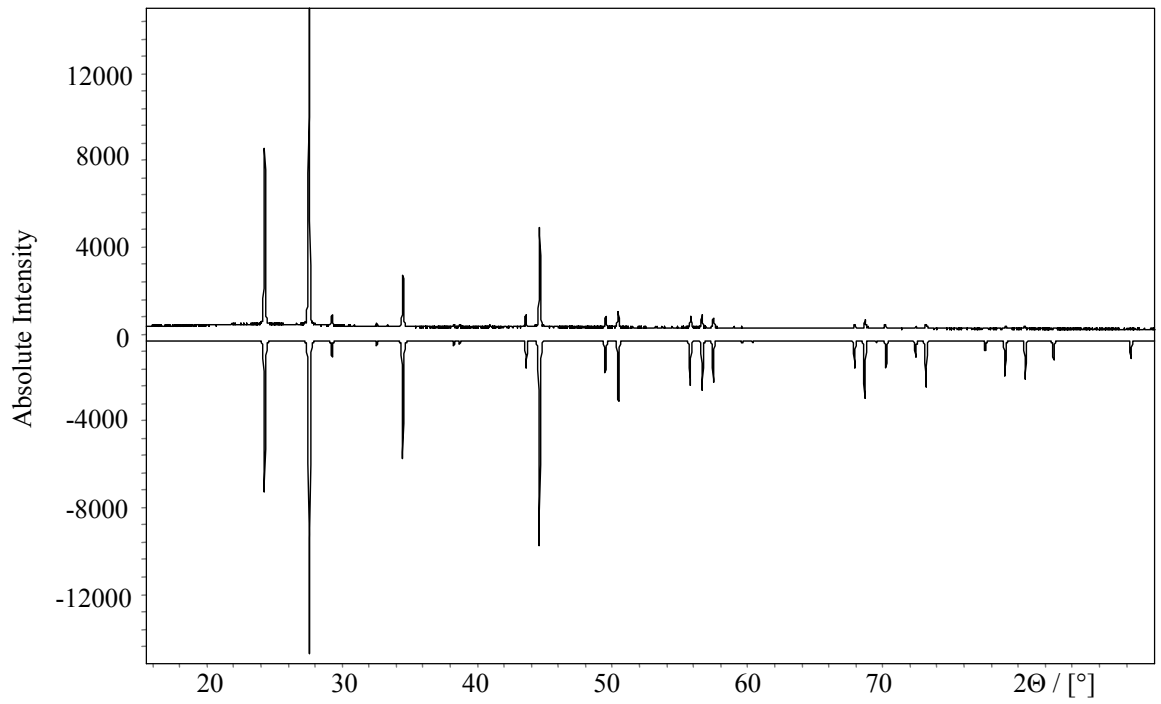

Figure 4.9: X-ray powder diffraction pattern of $Cs_3[Nb(O_2)_4]$ (top) in comparison to a pattern calculated on the basis of the fractional co – ordinates of $Rb_3[Nb(O_2)_4]$ [18] (bottom).

Using Louër´s algorithm on the 23 X-ray reflections of $(NH_4)_3[Nb(O_2)_4]$ a tetragonal crystal system, space group $I\bar{4}2m$ (No. 121) is found with the lattice parameters a = 704.65(4) and c = 856.81(12) pm. In this case the X-ray powder data can be fully indexed on the basis of the tetragonal cell (see tab. 4.5) where only one d-value was not indexed. However as can be seen from the good match of the experimental and the calculated powder diffraction patterns, there is no doubt that this peroxo compound crystallises in the $K_3[Cr(O_2)_4]$ – type.

Similarly, using Louër´s algorithm on the 22 X-ray reflections of $K_3[Nb(O_2)_4]$ for this compound also the tetragonal crystal system, space group $I\bar{4}2m$ (No. 121) with the lattice parameters a = 680.26(5) and c = 787.18(12) pm is found. The X-ray powder data can be fully indexed on the basis of the tetragonal cell (see tab. 4.6) and as can be seen from the

good match of the experimental and the calculated powder diffraction patterns, there is no doubt that this peroxo compound crystallises also in the $K_3[Cr(O_2)_4]$ – type.

On the 21 X-ray reflections of $Cs_3[Nb(O_2)_4]$ using Louër´s algorithm, too a tetragonal crystal system, space group $I\bar{4}2m$ (No. 121) is found with the lattice parameters a = 739.47(4) and c = 834.54(4) pm. In this case the X-ray powder data can be fully indexed on the basis of the tetragonal cell (see tab. 4.6) and as can be seen from the good match of the experimental and the calculated powder diffraction patterns, there is no doubt that this peroxo compound crystallises in the $K_3[Cr(O_2)_4]$ – type.

Table 4.5: X-ray powder diffraction data of $(NH_4)_3[Nb(O_2)_4]$ (tetragonal, a = 704.65(4) and c = 856.81(12) pm).

$(NH_4)_3[Nb(O_2)_4]$						
No.	**d_{obs}**	**d_{cal}**	**h**	**k**	**l**	**I_{obs}**
1	5.4417	5.4424	1	0	1	100.0
2	4.9826	4.9827	1	1	0	33.4
3	4.2843	4.2841	0	0	2	10.3
4	3.5226	3.5233	2	0	0	8.8
5	3.2481	3.2484	1	1	2	41.4
6	2.9569	2.9576	2	1	1	15.4
7	2.6469	2.6469	1	0	3	3.0
8	2.5375	------- not indexed -------				1.9
9	2.4906	2.4913	2	2	0	17.8
10	2.1533	2.1536	2	2	2	8.3
11	2.1162	2.1162	2	1	3	5.6
12	1.9765	1.9769	3	1	2	11.7
13	1.9051	1.9054	3	2	1	10.6
14	1.8304	1.8303	2	0	4	3.4
15	1.8140	1.8141	3	0	3	2.1
16	1.6763	1.6760	4	1	2	2.3
17	1.6611	1.6609	3	3	0	2.3
18	1.6246	1.6242	2	2	4	3.1
19	1.6128	1.6129	3	2	3	3.2
20	1.5755	1.5755	4	2	0	1.8
21	1.5483	1.5486	3	3	2	3.0
22	1.4664	1.4665	4	1	3	2.4
23	1.3911	1.3906	5	0	1	2.0

Table 4.6: X-ray powder diffraction data of $K_3[Nb(O_2)_4]$ (tetragonal, a = 680.26(5) and c = 787.18(12) pm) and $Cs_3[Nb(O_2)_4]$ (tetragonal, a = 739.47(4) and c = 834.54(4) pm).

$K_3[Nb(O_2)_4]$							$Cs_3[Nb(O_2)_4]$					
No.	d_{obs}	d_{cal}	**h**	**k**	**L**	I_{obs}	d_{obs}	d_{cal}	**h**	**k**	**l**	I_{obs}
1	5.1478	5.1470	1	0	1	65.6	3.6973	3.6973	2	0	0	55.4
2	4.8112	4.8101	1	1	0	29.6	3.2616	3.2615	1	1	2	100.0
3	3.9366	3.9359	0	0	2	8.0	3.0744	3.0744	2	1	1	5.0
4	3.4013	3.4013	2	0	0	36.5	2.7677	2.7673	2	0	2	2.3
5	3.0464	3.0461	1	1	2	100.0	2.6145	2.6144	2	2	0	17.1
6	2.8378	2.8377	2	1	1	16.1	2.3640	2.3639	3	0	1	1.8
7	2.4049	2.4051	2	2	0	47.9	2.3384	2.3384	3	1	0	1.6
8	2.0521	2.0522	2	2	2	9.1	2.0862	2.0863	0	0	4	4.9
9	1.9868	1.9870	2	1	3	3.7	2.0398	2.0399	3	1	2	31.7
10	1.9680	1.9679	0	0	4	9.0	1.8488	1.8487	4	0	0	4.1
11	1.8875	1.8876	3	1	2	50.9	1.8169	1.8170	2	0	4	5.9
12	1.8345	1.8347	3	2	1	9.4	1.6533	1.6535	4	2	0	4.1
13	1.7019	1.7034	2	0	4	9.3	1.6308	1.6307	2	2	4	4.7
14	1.5609	1.5611	4	0	2	4.2	1.6083	1.6083	3	3	2	4.0
15	1.5323	1.5318	3	2	3	4.3	1.3836	1.3836	4	0	4	1.9
16	1.5220	1.5231	2	2	4	13.5	1.3700	1.3698	5	1	2	3.2
17	1.4848	1.4849	3	3	2	7.5	1.3443	1.3442	1	1	6	1.8
18	1.3967	1.3967	4	1	3	3.0	1.3073	1.3072	4	4	0	1.1
19	1.2866	1.2867	4	0	4	4.3	1.2957	1.2959	4	2	4	2.0
20	1.2634	1.2635	5	1	2	9.2	1.2134	1.2134	5	3	2	1.3
21	1.2030	1.2035	4	2	4	5.2	1.1954	1.1954	3	1	6	1.2
22	1.1187	1.1185	5	3	2	3.7						

4.4. X-ray powder diffraction of tetraperoxotantalates $A_3[Ta(O_2)_4]$

The X-ray diffraction patterns of the tetra peroxotantalates of Ammonium, Potassium, Rubidium and Caesium prove them also to be isomorphous. The lattice dimensions obtained from the powder patterns are presented. The diffraction patterns are calculated on the basis of the fractional coordinates from the single crystal analysis of $K_3[Ta(O_2)_4]$ according to the literature [19]. It can be seen from the good matches of the experimental and the calculated powder diffraction patterns that in all cases there are single – phase products. The lattice constants are refined for each compound using the $WinX^{Pow}$ STOE program.

The powder diffraction data of $(NH_4)_3[Ta(O_2)_4]$, $K_3[Ta(O_2)_4]$, $Rb_3[Ta(O_2)_4]$ and $Cs_3[Ta(O_2)_4]$ are shown in fig. 4.10, fig. 4.11, fig. 4.12 and fig. 4.13, respectively in comparison to diffraction patterns calculated on the basis of the fractional co – ordinates from single crystal structure of $K_3[Ta(O_2)_4]$ known from the literature [19].

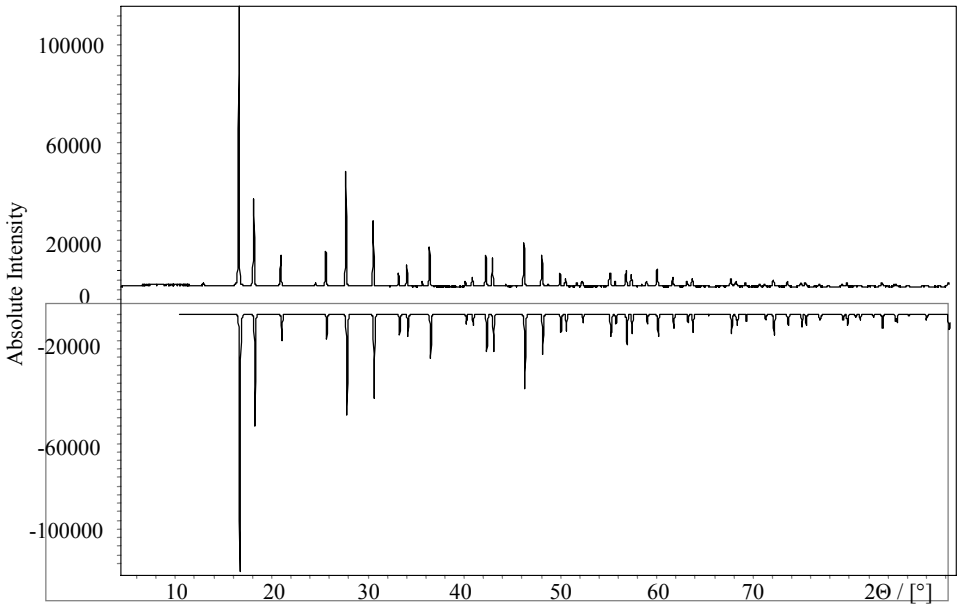

Figure 4.10: X-ray powder diffraction pattern of $(NH_4)_3[Ta(O_2)_4]$ (top) in comparison to a pattern calculated on the basis of the fractional co – ordinates $K_3[Ta(O_2)_4]$ [19] (bottom).

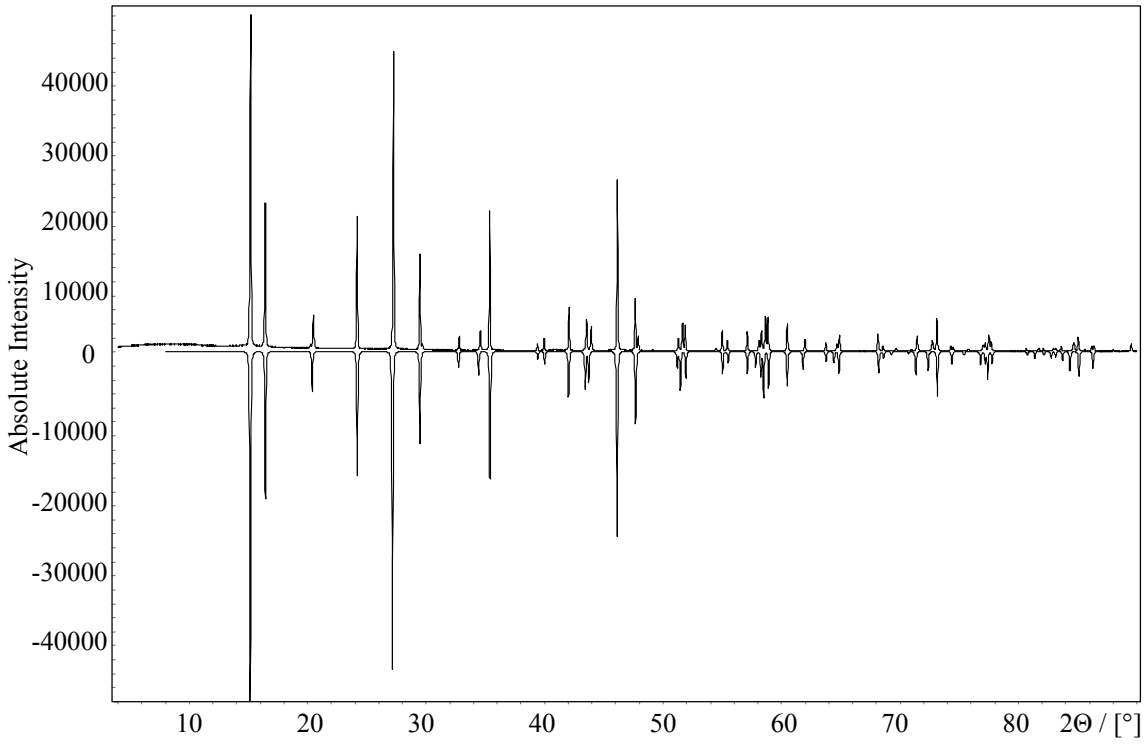

Figure 4.11: X-ray powder diffraction pattern of $K_3[Ta(O_2)_4]$ (top) in comparison to a pattern calculated on the basis of the fractional co – ordinates of $K_3[Ta(O_2)_4]$ [19] (bottom).

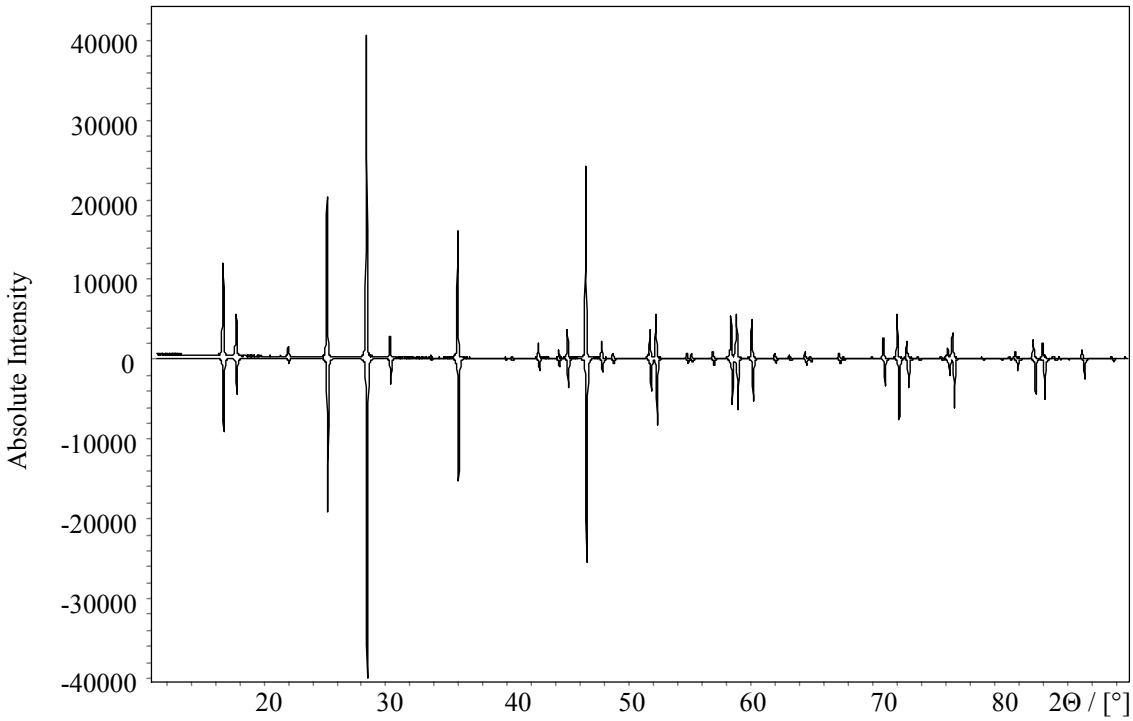

Figure 4.12: X-ray powder diffraction pattern of $Rb_3[Ta(O_2)_4]$ (top) in comparison to a pattern calculated on the basis of the fractional co – ordinates of $K_3[Ta(O_2)_4]$ [19] (bottom).

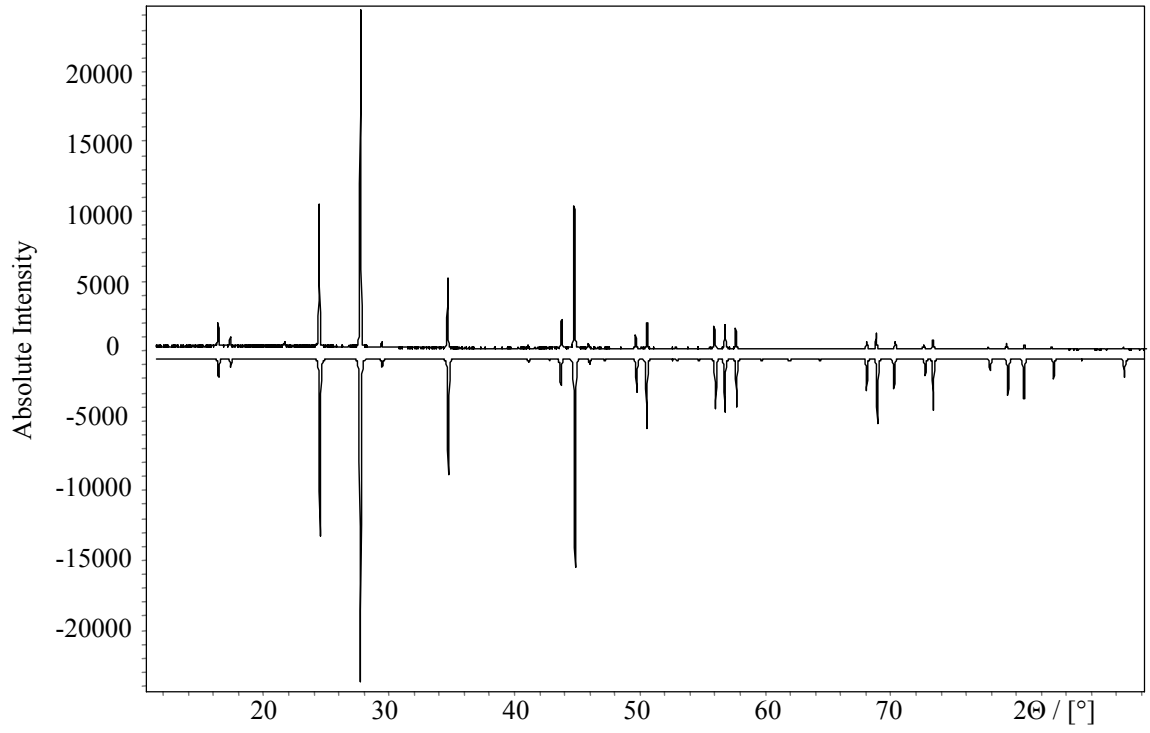

Figure 4.13: X-ray powder diffraction pattern of $Cs_3[Ta(O_2)_4]$ (top) in comparison to a pattern calculated on the basis of the fractional co – ordinates of $K_3[Ta(O_2)_4]$ [19] (bottom).

Using Louër´s algorithm on the 23 X-ray reflections of $(NH_4)_3[Ta(O_2)_4]$ a tetragonal crystal system, space group $I\bar{4}2m$ (No. 121) is found with the lattice parameters a = 703.97(3) and c = 861.21(6) pm. In this case the X-ray powder data can be fully indexed on the basis of the tetragonal cell (see tab. 4.7) and as can be seen from the good match of the experimental and the calculated powder diffraction patterns, there is no doubt that this peroxo compound crystallises in the $K_3[Cr(O_2)_4]$ – type.

Similarly for the 23 X-ray reflections of $K_3[Ta(O_2)_4]$ using Louër´s algorithm a tetragonal crystal system, space group $I\bar{4}2m$ (No. 121) is found with the lattice parameters a = 680.00(2) and c = 789.30(4) pm. As it can be seen, the X-ray powder data can be fully indexed on the basis of the tetragonal cell (see tab. 4.7) and as the result of the good match of

the experimental and the calculated powder diffraction patterns, there is no doubt that this peroxo compound crystallises also in the $K_3[Cr(O_2)_4]$ – type.

Table 4.7: X-ray powder diffraction data of $(NH_4)_3[Ta(O_2)_4]$ (tetragonal, a = 703.97(3) and c = 861.21(6) pm) and $K_3[Ta(O_2)_4]$ (tetragonal, a = 680.00(2) and c = 789.30(4) pm).

	$(NH_4)_3[Ta(O_2)_4]$						$K_3[Ta(O_2)_4]$					
No.	$\mathbf{d_{obs}}$	$\mathbf{d_{cal}}$	**h**	**k**	**l**	$\mathbf{I_{obs}}$	$\mathbf{d_{obs}}$	$\mathbf{d_{cal}}$	**h**	**k**	**l**	$\mathbf{I_{obs}}$
1	5.4497	5.4505	1	0	1	100.0	5.1488	5.1518	1	0	1	100.0
2	4.9793	4.9778	1	1	0	32.2	4.8068	4.8083	1	1	0	44.9
3	4.3053	4.3061	0	0	2	11.5	3.9455	3.9465	0	0	2	11.2
4	3.5202	3.5198	2	0	0	13.1	3.3990	3.4000	2	0	0	40.2
5	3.2561	3.2567	1	1	2	41.9	3.0502	3.0505	1	1	2	89.5
6	2.9570	2.9569	2	1	1	23.9	2.8374	2.8377	2	1	1	28.8
7	2.7250	2.7252	2	0	2	4.9	2.5757	2.5759	2	0	2	4.8
8	2.6577	2.6582	1	0	3	7.7	2.4535	2.4537	1	0	3	6.4
9	2.4889	2.4889	2	2	0	14.7	2.4039	2.4042	2	2	0	42.2
10	2.2268	2.2261	3	1	2	3.4	2.0531	2.0532	2	2	2	13.0
11	2.1543	2.1549	2	2	2	11.3	1.9897	1.9897	2	1	3	9.7
12	2.1212	2.1212	2	1	3	10.8	1.9732	1.9732	0	0	4	7.4
13	1.9771	1.9775	3	1	2	16.3	1.8882	1.8882	3	1	2	51.6
14	1.9042	1.9041	3	2	1	11.3	1.8343	1.8343	3	2	1	15.8
15	1.8366	1.8367	2	0	4	5.0	1.7066	1.7066	2	0	4	8.5
16	1.8168	1.8168	3	0	3	3.0	1.6143	1.6144	4	1	1	6.2
17	1.6734	1.6731	1	0	5	5.2	1.5613	1.5613	4	0	2	5.9
18	1.6284	1.6283	2	2	4	5.9	1.5329	1.5328	3	2	3	6.3
19	1.6145	1.6144	3	2	3	4.6	1.5254	1.5253	2	2	4	10.5
20	1.5481	1.5483	3	3	2	6.7	1.4850	1.4850	3	3	2	8.4
21	1.5110	1.5111	2	1	5	3.3	1.3403	1.3403	5	0	1	5.2
22	1.4676	1.4674	4	1	3	2.8	1.2880	1.2879	4	0	4	4.5
23	1.3894	1.3895	5	0	1	3.0	1.2635	1.2634	5	1	2	9.8

Using Louër´s algorithm on the 22 X-ray reflections of $Rb_3[Ta(O_2)_4]$ results in a tetragonal crystal system, space group $I\bar{4}2m$ (No. 121) with the lattice parameters a = 706.28(2) and c = 806.28(3) pm. In this case the X-ray powder data can be also fully indexed on the basis of the tetragonal cell (see tab. 4.8) and as can be seen from the good match of the experimental and the calculated powder diffraction patterns, there is no doubt that this peroxo compound crystallises too in the $K_3[Cr(O_2)_4]$ – type.

In the same way, using Louër´s algorithm on the 22 X-ray reflections of $Cs_3[Ta(O_2)_4]$ a tetragonal crystal system, space group $I\bar{4}2m$ (No. 121) is found with the lattice parameters a = 739.41(2) and c = 834.30(2) pm. As in the other cases, the X-ray powder data can be fully indexed on the basis of the tetragonal cell (see tab. 4.8) and from the good match of the experimental and the theoretic powder diffraction patterns, there is no doubt that this peroxo compound crystallises like the other compounds, in the $K_3[Cr(O_2)_4]$ – type.

Table 4.8: X-ray powder diffraction data of $Rb_3[Ta(O_2)_4]$ (tetragonal, a = 706.28(2) and c = 806.28(3) pm) and $Cs_3[Ta(O_2)_4]$ (tetragonal, a = 739.41(2) and c = 834.30(2) pm).

	$Rb_3[Ta(O_2)_4]$						$Cs_3[Ta(O_2)_4]$					
No.	d_{obs}	d_{cal}	**h**	**k**	**l**	I_{obs}	d_{obs}	d_{cal}	**h**	**k**	**l**	I_{obs}
1	5.3154	5.3127	1	0	1	29.2	5.5338	5.5336	1	0	1	8.1
2	4.9974	4.9942	1	1	0	13.6	5.2292	5.2284	1	1	0	3.9
3	4.0322	4.0314	0	0	2	3.9	4.1718	4.1715	0	0	2	2.4
4	3.5322	3.5314	2	0	0	50.1	3.6972	3.6971	2	0	0	43.0
5	3.1374	3.1369	1	1	2	100.0	3.2607	3.2608	1	1	2	100.0
6	2.9415	2.9410	2	1	1	7.1	3.0741	3.0741	2	1	1	2.5
7	2.4971	2.4971	2	2	0	39.3	2.6142	2.6142	2	2	0	21.3
8	2.1228	2.1228	2	2	2	4.8	2.0855	2.0857	0	0	4	9.2
9	2.0156	2.0157	0	0	4	9.2	2.0396	2.0397	3	1	2	42.3
10	1.9536	1.9537	3	1	2	59.4	1.9915	1.9915	3	2	1	1.9
11	1.9035	1.9035	3	2	1	5.5	1.8485	1.8485	4	0	0	4.8
12	1.7656	1.7657	4	0	0	9.0	1.8166	1.8166	2	0	4	8.3
13	1.7506	1.7506	2	0	4	14.0	1.6534	1.6534	4	2	0	6.9
14	1.5793	1.5793	4	2	0	13.5	1.6304	1.6304	2	2	4	7.7
15	1.5685	1.5685	2	2	4	13.8	1.6081	1.6081	3	3	2	6.7
16	1.5387	1.5387	3	3	2	12.1	1.3835	1.3834	4	0	4	2.7
17	1.3281	1.3282	4	0	4	6.6	1.3697	1.3697	5	1	2	5.0
18	1.3099	1.3100	5	1	2	13.6	1.3438	1.3438	1	1	6	2.7
19	1.2977	1.2976	1	1	6	5.6	1.3070	1.3071	4	4	0	1.5
20	1.2432	1.2432	4	2	4	8.0	1.2957	1.2957	4	2	4	3.3
21	1.1600	1.1600	5	3	2	5.9	1.2132	1.2133	5	3	2	1.9
22	1.1514	1.1514	3	1	6	4.6	1.1952	1.1951	3	1	6	1.8

4.5. Single crystal analysis of Trirubidium Tetraperoxotantalate $Rb_3[Ta(O_2)_4]$

For the single crystal measurement an Imaging Plate Diffraction System diffractometer at room temperature was employed, which works with Mo – Kα (λ = 71.073 pm) monochromatic radiation (graphite monochromator). The white crystal with 0.42 x 0.37 x 0.20 mm^3 dimension, putting on the top of a glass capillary was turned from φ = -1° to φ = 360° with an angle of φ = 1°. All the individual picture were taken by Imaging Plate Diffraction. The crystal structure of $Rb_3[Ta(O_2)_4]$ was solved using the program Shelxs [47] and refined with the program Shelxl [47]. The structure of $Rb_3[Ta(O_2)_4]$ could be refined with the value of wR_2 = 5.35% (see tab. 4.9).

$Rb_3[Ta(O_2)_4]$ crystallises in the tetragonal crystal system in the space group $I\bar{4}2m$ (No. 121) and with the lattice constants a = 706.20(10) and c = 815.6(2) pm, Z = 2. The determinate crystal structure proves that $Rb_3[Ta(O_2)_4]$ is isotypic with Tripotassium Tetraperoxochromate. Similar to the crystal structure of $K_3[Cr(O_2)_4]$, each tantalum atom is surrounded by four peroxo groups. So the oxygen atoms assume a distorted dodecahedral arrangement around the central tantalum atom (fig. 4.14):

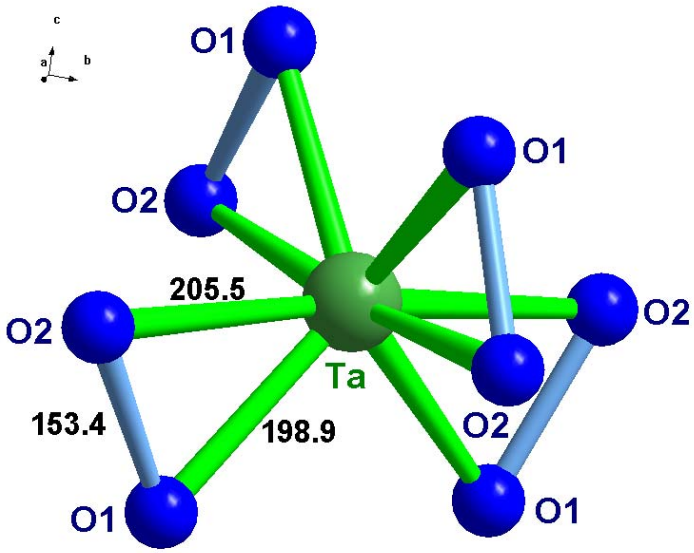

Figure 4.14: Structure of the tetraperoxotantalate – anion $[Ta(O_2)_4]^{3-}$ in the structure of $Rb_3[Ta(O_2)_4]$.

In this structure there are only two independent Ta – O bond lengths due to the crystallographically imposed $\bar{4}$ symmetry of the anion. The "equatorial" Ta – O bonds [Ta – O(2)] are about 6.6 pm longer than the "axial" bonds [Ta – O(1)]. The calculated bond lengths are Ta – O(1) = 198.9 pm and Ta – O(2) = 205.5 pm. The O(1) – O(2) bond length is 153.4 pm, slightly longer than that of the free peroxide ion (149 pm) [56]. Normally, that was expected that the distance between O – O in the $[Ta(O_2)_4]^{3-}$ ion increase with increasing ionic radius of the cation. In fact, that is evident if we compare the value 151.2(8) pm for the O – O distance in the structure of $K_3[Ta(O_2)_4]$ [19] with that one of 153.4 pm found in the case of $Rb_3[Ta(O_2)_4]$.

The tantalum atoms occupy the position 2*a* and the rubidium atoms 2*b* and 4*d* (see tab. 4.10).

In tab. 4. 9 are presented some experimental details and information of refinement parameters for Trirubidium Tetraperoxotantalate.

Table 4.9: Experimental details and information of refinement parameters for $Rb_3[Ta(O_2)_4]$.

Space group	$I\bar{4}2m - D_{2d}^{11}$ (No. 121)
Crystal system	tetragonal
Unit cell dimension (pm)	a = 706.20(10)
	c = 815.6(2)
Volume (10^6 pm^3)	406.75(13)
Z (no. of the molecule presented in the unit cell)	2
F(000)	496
Calculated density (Mg/m^3)	4.616
Linear absorption coefficient (mm^{-1})	31.351
Crystal size (mm)	0.42 × 0.37 × 0.20
Crystal form, – colour	parallelepiped with prismatic ends, white
Temperature (K)	293
Theta range θ (°)	3.82 – 31.49
h k l ranges	$-10 \le h, \le 10, -10 \le k \le 8, -11 \le l, \le 11$
No. of measured reflections	2089
No. of independent reflections ($I \ge 2\sigma_i$)	381
No. of parameters / restraints	20 / 0
R_1, wR_2[a)] (%) ($I > 2\sigma_I$)	5.35; 12.84
R_1, wR_2[a)] (%) (all dates)	6.07; 13.02
GooF	1.049
Extinction coefficient	0.0028(13)
Absolute structure parameter	0.10(12)
Residual electron density (e/10^6 pm^3)	4.674, -6.122

[a)] $w = [\sigma^2(F_0^2) + (0.0633 \cdot P)^2 + 11.13 \cdot P]$ with $P = (F_0^2 + 2F_c^2)/3$

The atomic coordinates of $Rb_3[Ta(O_2)_4]$ are presented in tab. 4.10 and in tab 4.11 the anisotropic displacement parameters of $Rb_3[Ta(O_2)_4]$ are given:

Table 4.10: Final atomic coordinates and equivalent isotropic displacement parameters (10^4 pm^2) of $Rb_3[Ta(O_2)_4]$ according to $U_{eq} = (1/3) \sum_i \sum_j U_{ij} a_i a_j \mathbf{a}_i^* \mathbf{a}_j^*$.

Atom	Site	x	y	z	U_{eq}
Ta	2a	0	0	0	0.013(1)
Rb(2)	4d	0.5	0	0.75	0.028(1)
Rb(1)	2b	0	0	0.5	0.020(1)
O(1)	8i	0.1335(11)	0.1335(11)	0.1809(14)	0.023(2)
O(2)	8i	0.2054(10)	0.2054(10)	0.0150(50)	0.026(4)

Table 4.11: Anisotropic displacement parameters U_{ij} (10^2 pm^2) of $Rb_3[Ta(O_2)_4]$ according to $T = \exp[-2\pi^2(h^2a^{*2}U_{11}+...+2hka^*b^*U_{12}+...)]$.

	U_{11}	U_{22}	U_{33}	U_{23}	U_{13}	U_{12}
Ta	0.8(1)	0.8(1)	2.2(1)	0	0	0
Rb(2)	1.6(1)	1.6(1)	5.1(1)	0	0	0
Rb(1)	1.4(1)	1.4(1)	3.3(1)	0	0	0
O(1)	2.4(3)	2.4(3)	1.9(5)	-0.4(3)	0.4(3)	0.9(4)
O(2)	1.8(2)	1.8(2)	4.3(13)	-0.1(5)	0.1(5)	1.0(3)

The elementary cell of $Rb_3[Ta(O_2)_4]$ is presented in fig. 4.15. The tetraperoxotantalate ion is shown in the centre and on the corners of the elementary cell. These are presented with polyhedra and each polyhedron is a distorted dodecahedron.

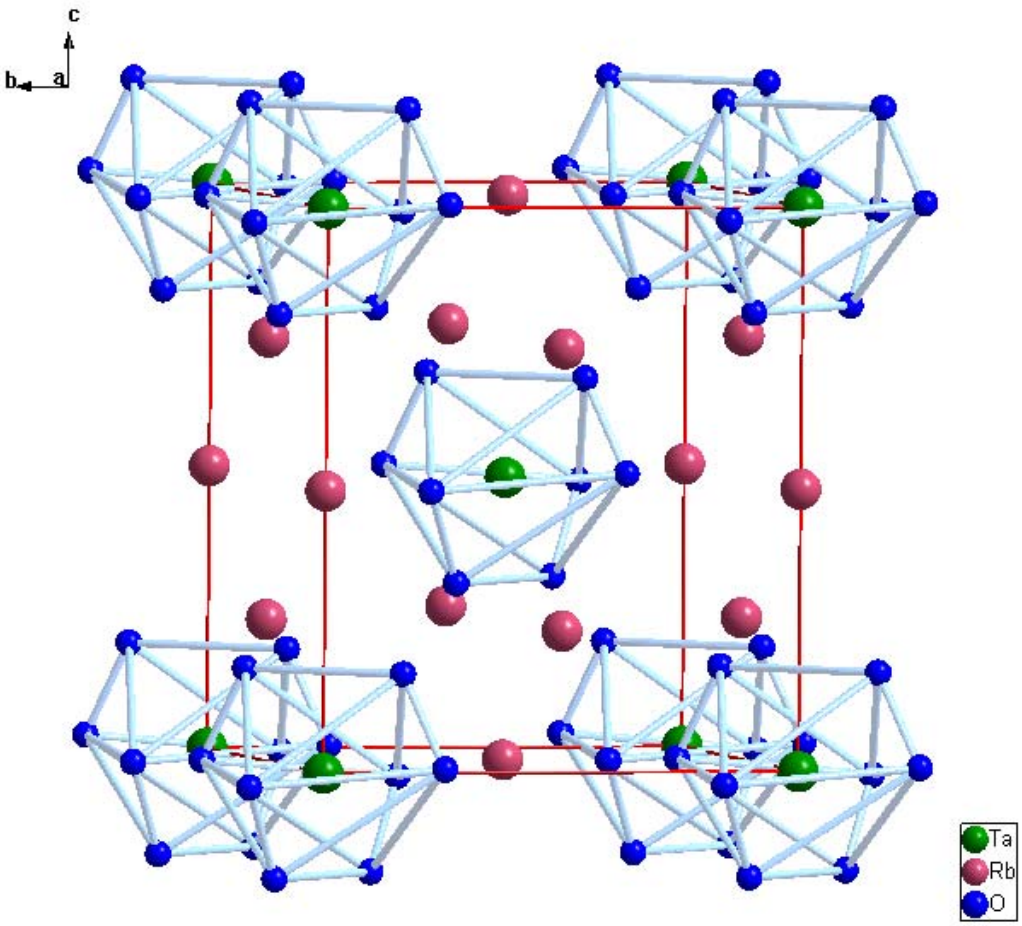

Figure 4.15: The elementary cell of Trirubidium Tetraperoxotantalate(V) $Rb_3[Ta(O_2)_4]$.

Another view of this unit cell, parallel to the *c* axis is given in the fig. 4.16, giving in that way clearly the whole structure. Here are presented the Ta – O bonds, as well as the O – O and Rb – O bonds. In order to clarify the whole structure in figs 5.17 and 5.18 only the coordination of the Ta atoms by Rb and of the Rb atoms by Ta, making the oxygen atoms invisible is presented.

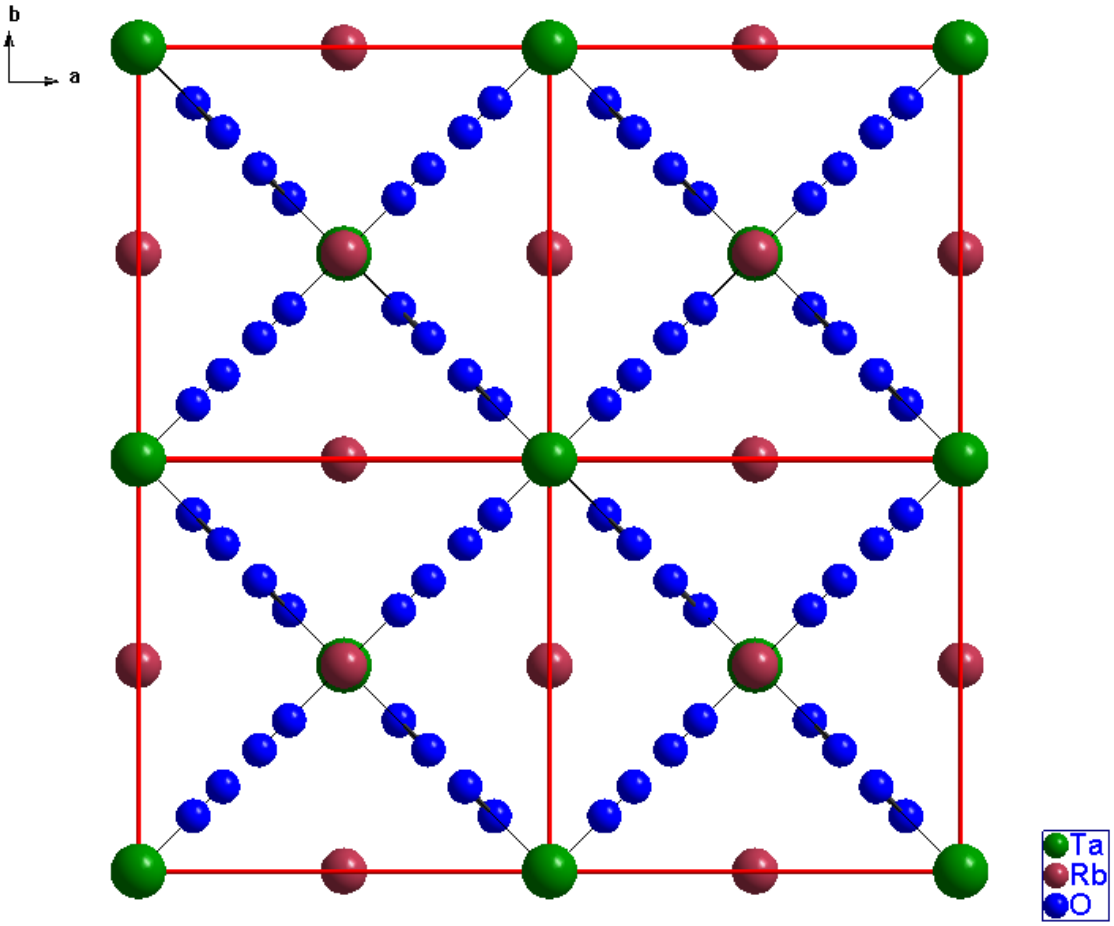

Figure 4.16: Four unit cells of the structure of Trirubidium Tetraperoxotantalate(V) $Rb_3[Ta(O_2)_4]$ in a projection on the *ab* plane.

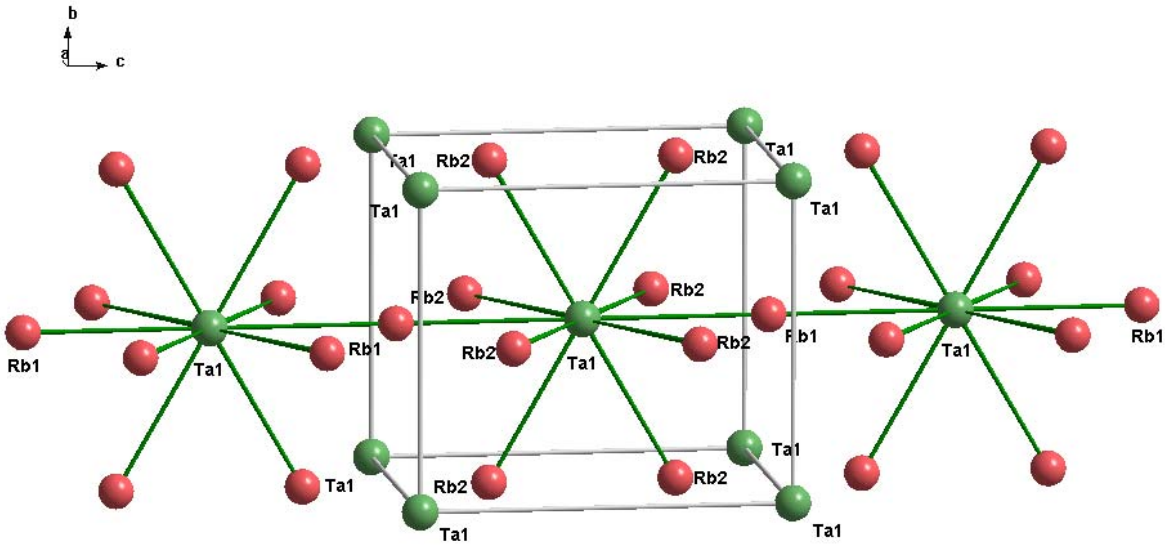

Figure 4.17: Ta – Rb(1) coordination in the structure of $Rb_3[Ta(O_2)_4]$.

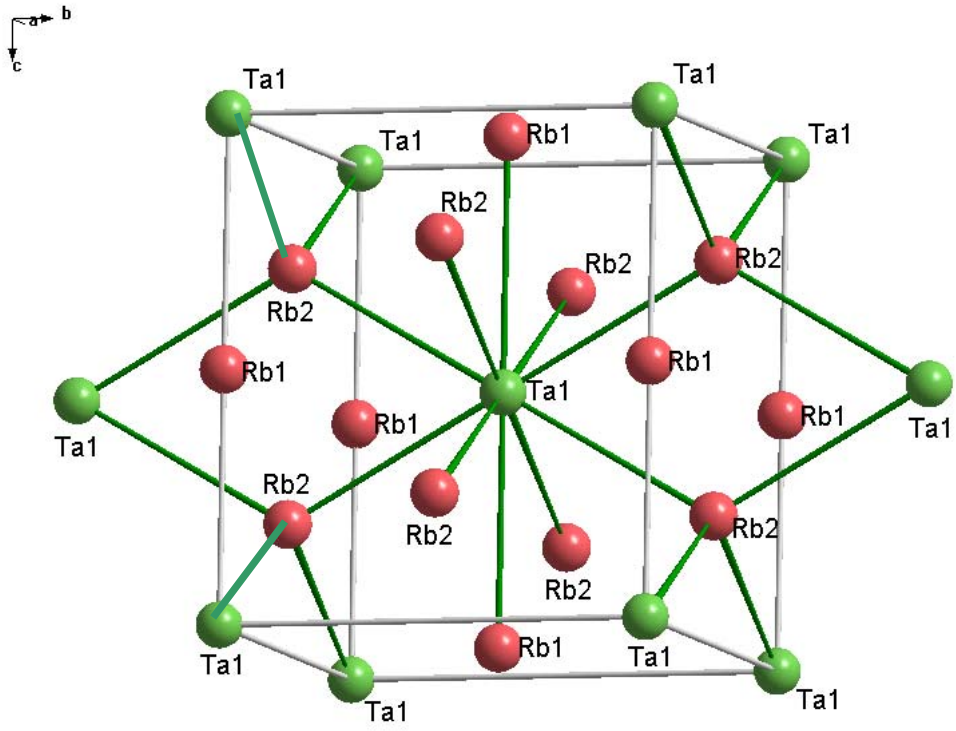

Figure 4.18: Ta – Rb(2) coordination in the structure of $Rb_3[Ta(O_2)_4]$.

As it can be seen, there are two different types of rubidium atoms, showing them with symbols Rb(1) and Rb(2). In fig. 4.17 it is shown how the rubidium atoms surround the tetraperoxotantalate ion of which only the tantalum atom is visible in the picture. Eight atoms of Rb(2) type coordinate the tetraperoxotantalate ion in the form of a square column with a distance of 407.7(1) pm and six atoms of Rb(1) type form a distorted octahedron with Ta – Rb(1) distances of 407.8(1) pm and 499.4(1) pm. In the tab. 4.12 the interatomic distances in pm in the structure of $Rb_3[Ta(O_2)_4]$ are given.

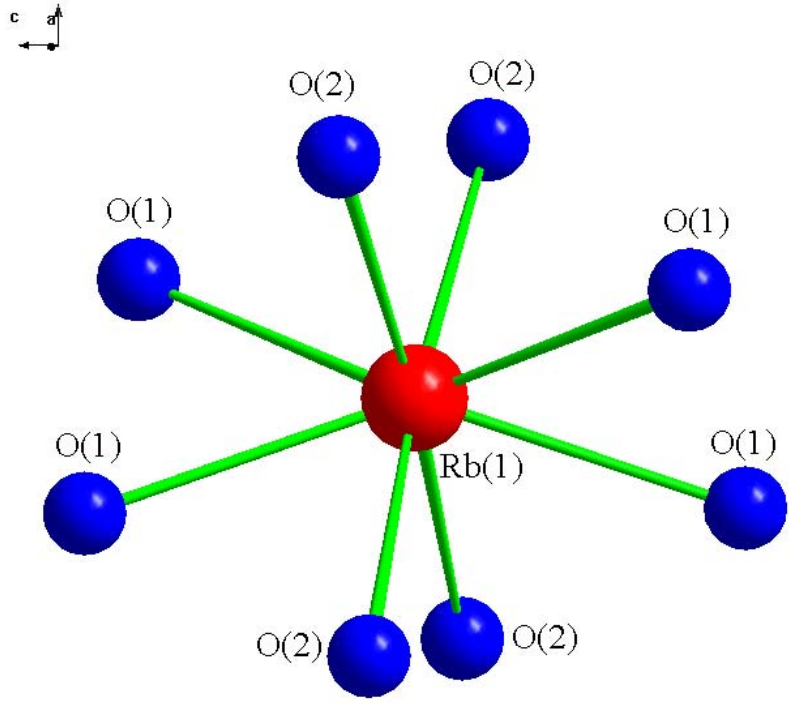

Figure 4.19: Coordination of Rb(1) with eight oxygen atoms in the structure of $Rb_3[Ta(O_2)_4]$.

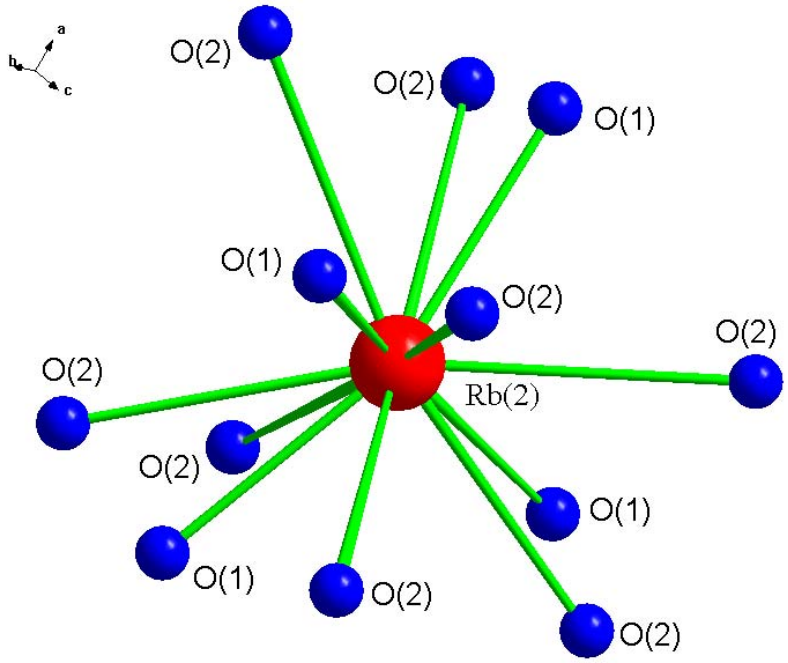

Figure 4.20: Coordination of Rb(2) with 12 oxygen atoms in the structure of $Rb_3[Ta(O_2)_4]$.

As it can be seen in the figs. 4.19 and 4.20 are presented the coordination of the rubidium atoms with oxygens. In the picture only Rb and O atoms are visible. The two different types of rubidium atoms Rb(1) and Rb(2) are surrounded from oxygen atoms, forming polyhedron. The Rb(1) atom is surrounded from eight oxygens, four are found of the type one (1) and the other four are of the type two (2), see fig. 4.19. The distances between them are shown in the tab. 4.12.

From the other hand, the Rb(2) is surrounded from 12 oxygen atoms, where only four oxygen atoms are found of the type one (1) and the other eight oxygen atoms are of the type two (2), see fig. 4.20. Also, the distances between them are shown in the tab. 4.12.

Table 4.12: **S**elected atomic distances (pm) of $Rb_3[Ta(O_2)_4]$.

$[Ta(O_2)_4]$ – polyhedron		$Rb(2)O_{12}$ – polyhedron	
4 x Ta – O(1)	198.9(11)	4 x Rb(2) – O(1)	281.2(5)
4 x Ta – O(2)	205.5(10)	4 x Rb(2) – O(2)	318(3)
		4 x Rb(2) – O(2)	333(3)
$Rb(1)O_8$ – polyhedron			
4 x Rb(1) – O(1)	292.4(12)		
4 x Rb(1) – O(2)	294.5(10)		
Peroxo group			
O(1) – O(2)	153.4(0)		

4.6. Discussion and conclusions

X-ray analyses of all 12 tetraperoxo-compounds (described in chapter 4.1 – 4.4) have proven these compounds to be isomorphous. From the powder X-ray diffraction data it can be shown that all these compounds belong to the same space group (SG $I\bar{4}2m$, No. 121) and so it comes to the conclusion that they are isotypic to the $K_3[Cr(O_2)_4]$ – structure. As it can be seen from the results (see tab. 4.13) these tetraperoxo compounds are indexed on the basis of the tetragonal cell with Z = 2. All these compounds are very unstable as they decompose very rapidly at room temperature.

Table 4.13: The refined cell parameters of tetraperoxocompounds crystallising in the $K_3[Cr(O_2)_4]$ – type [tetragonal, space group $I\bar{4}2m$ (No. 121)].

Tetraperoxo compounds	a / pm	c / pm
$K_3[Cr(O_2)_4]$	670.49(3)	763.14(7)
$Rb_3[Cr(O_2)_4]$	698.24(1)	782.73(2)
$(NH_4)_3[Cr(O_2)_4]$	697.01(4)	807.44(11)
$K_3[V(O_2)_4]$	669.43(6)	773.03(11)
$(NH_4)_3[V(O_2)_4]$	697.25(5)	819.42(14)
$K_3[Nb(O_2)_4]$	680.26(5)	787.18(12)
$Cs_3[Nb(O_2)_4]$	739.47(4)	834.54(4)
$(NH_4)_3[Nb(O_2)_4]$	704.65(4)	856.81(12)
$K_3[Ta(O_2)_4]$	680.00(2)	789.30(4)
$Rb_3[Ta(O_2)_4]$	706.28(2)	806.28(3)
$Cs_3[Ta(O_2)_4]$	739.41(2)	834.30(2)
$(NH_4)_3[Ta(O_2)_4]$	703.97(3)	861.21(6)

Like in the structure of $K_3[Cr(O_2)_4]$, the tetraperoxometallate $[M(O_2)_4]^{3-}$ ion where *M*: Cr^{V+}, V^{V+}, Nb^{V+} or Ta^{V+}, is of the form of a distorted dodecahedron built up from four peroxo groups (see fig. 5.14). In all the cases of peroxo – chromate, – niobate and – tantalate, the distances between the metal atom (centre atom) and the two oxygen atoms of the peroxo group are not equal, one being slightly, i.e. 4 – 7 pm, longer than the other. The O − O distances are dependent on the central metal ion (see tab. 4.14) and the cations with which they are binding.

Table 4.14: The O – O distances in potassium tetraperoxo – chromate, – niobate and – tantalate .

Compounds	d_{O-O} / pm	Reference
$K_3[Cr(O_2)_4]$	144.2(2)	[17]
$K_3[Nb(O_2)_4]$	145.8(10)	[3]
$K_3[Ta(O_2)_4]$	151.2(8)	[18]

As it can be seen from tab. 4.14 the O – O bong length increases with increasing ionic radius of the central atom from 144.2(2) pm for $K_3[Cr(O_2)_4]$ to 145.8(10) pm for $K_3[Nb(O_2)_4]$ and 151.2(8) pm for $K_3[Ta(O_2)_4]$. Also, for the tetraperoxocompunds with the same central atom (– chromate , – niobate and – tantalate) it is expected that the O – O distance in the peroxo groups is different for the different alkali and ammonium cations with which they are binding and is increasing with increasing ionic radius of the cation. So, it can be shown that the O – O distance is increasing from 151.2(8) pm for $K_3[Ta(O_2)_4]$ [57] to 153.4(0) pm in the case of $Rb_3[Ta(O_2)_4]$.

These distances can be estimated assuming the same fractional coordinates for the oxygen atoms as it has been found in the structure of the single crystal of $K_3[Cr(O_2)_4]$ [17] in the case of tetraperoxochromate, $Rb_3[Nb(O_2)_4]$ [18] for tetraperoxoniobate and $Rb_3[Ta(O_2)_4]$ in the case of tetraperoxotantalate and the lattice constants obtained (see tab. 4.13) for the different compounds. By that way it can be shown that the oxygen – oxygen distance is increasing from for K^+, Rb^+, Cs^+ and $(NH_4)^+$ in the tetraperoxocompounds of chromium, niobium and tantalum, respectively (see tab. 4.15). This is also shown by the diagrams in fig. 4.21.

Table 4.15: Calculated O – O distances of tetraperoxo – chromates, – niobates and – tantalates assuming constant fractional coordinates of the oxygen atoms for constant central atoms.

Compound	d_{O-O} / pm	Reference
$K_3[Cr(O_2)_4]$	144.2(2)	[17]
$Rb_3[Cr(O_2)_4]$	149.6(2)	
$(NH_4)_3[Cr(O_2)_4]$	153.2(2)	
$K_3[Nb(O_2)_4]$	145.8(10)	[3]
$Rb_3[Nb(O_2)_4]$	150.5(11)	[18]
$Cs_3[Nb(O_2)_4]$	156.2(11)	
$(NH_4)_3[Nb(O_2)_4]$	157.8(11)	
$K_3[Ta(O_2)_4]$	151.2(8)	[19]
$Rb_3[Ta(O_2)_4]$	153.4(0)	this work
$Cs_3[Ta(O_2)_4]$	157.3(0)	
$(NH_4)_3[Ta(O_2)_4]$	159.6(0)	

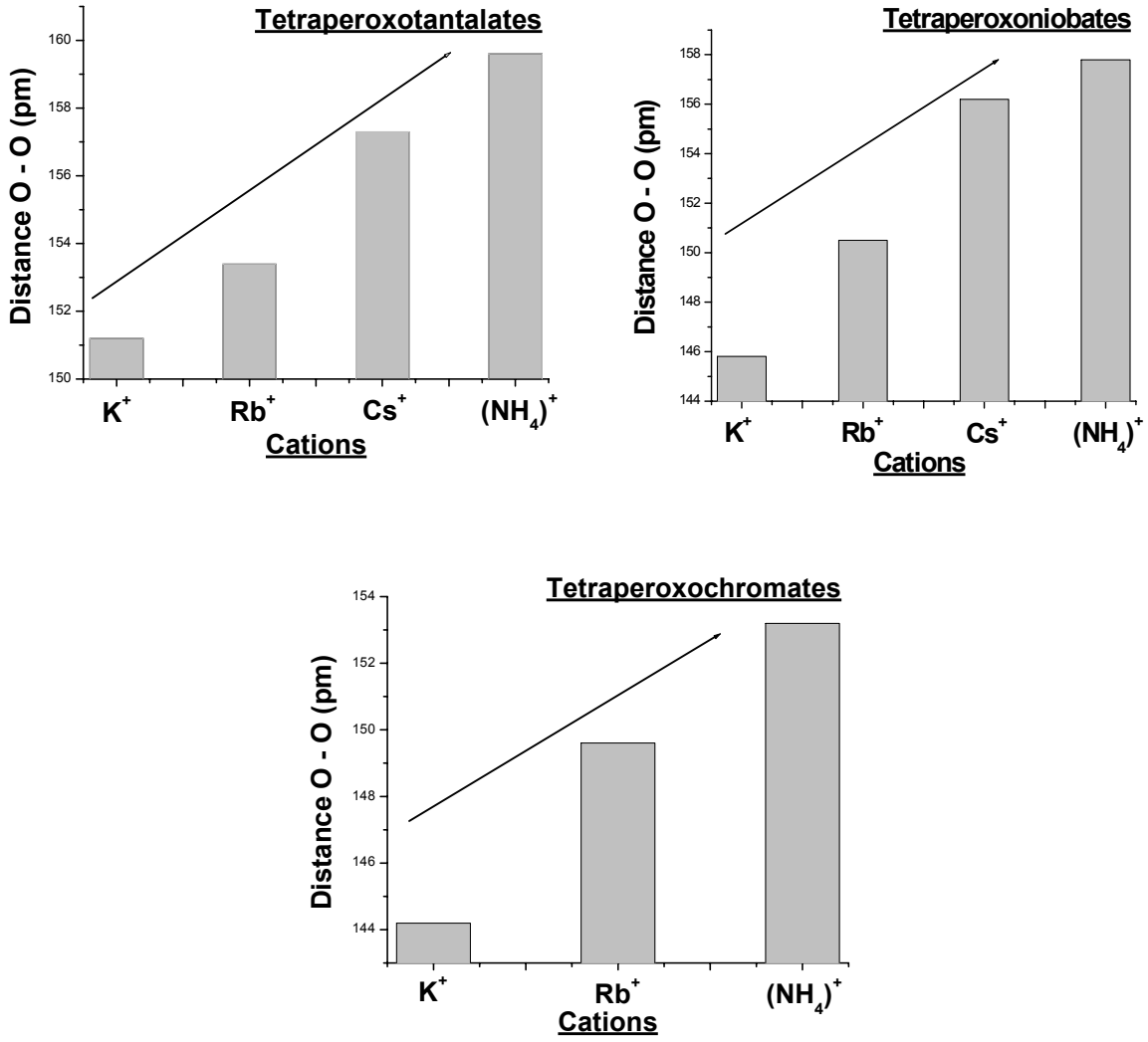

Figure 4.21: Diagrams of tetraperoxo – chromates, – niobates and tantalates.

In general, we conclude that there is a correlation between the bond length of the O – O atoms in the peroxo – groups with the radius of the central atom of the tetraperoxometallate ion. It is increasing with increasing radius of the central atom with which the four peroxo groups are binding. In the case of the tetraperoxo vanadates we could not determine the O – O distances, as there are no single crystal data for any compound of this group.

5. Vibrational spectroscopic investigation of the tetraperoxo compounds

In this chapter it will discuss in details how molecular vibrations and rotations interact with radiation to create the infrared and Raman spectra. The infrared– and Raman spectra (recorded on powdered samples) are discussed with respect to the internal vibrations of the peroxo – group and the dodecahedral $[B(O_2)_4]^{3-}$ ion (where $B = Cr^{V+}$, V^{V+}, Nb^{V+} or Ta^{V+}).

5.1. IR and Raman spectra of tetraperoxochromates $A_3[Cr(O_2)_4]$

The infrared and Raman spectra of the Tetraperoxochromates of Ammonium, Potassium and Rubidium are presented in the fig. 5.1, 5.2 and 5.3, respectively.

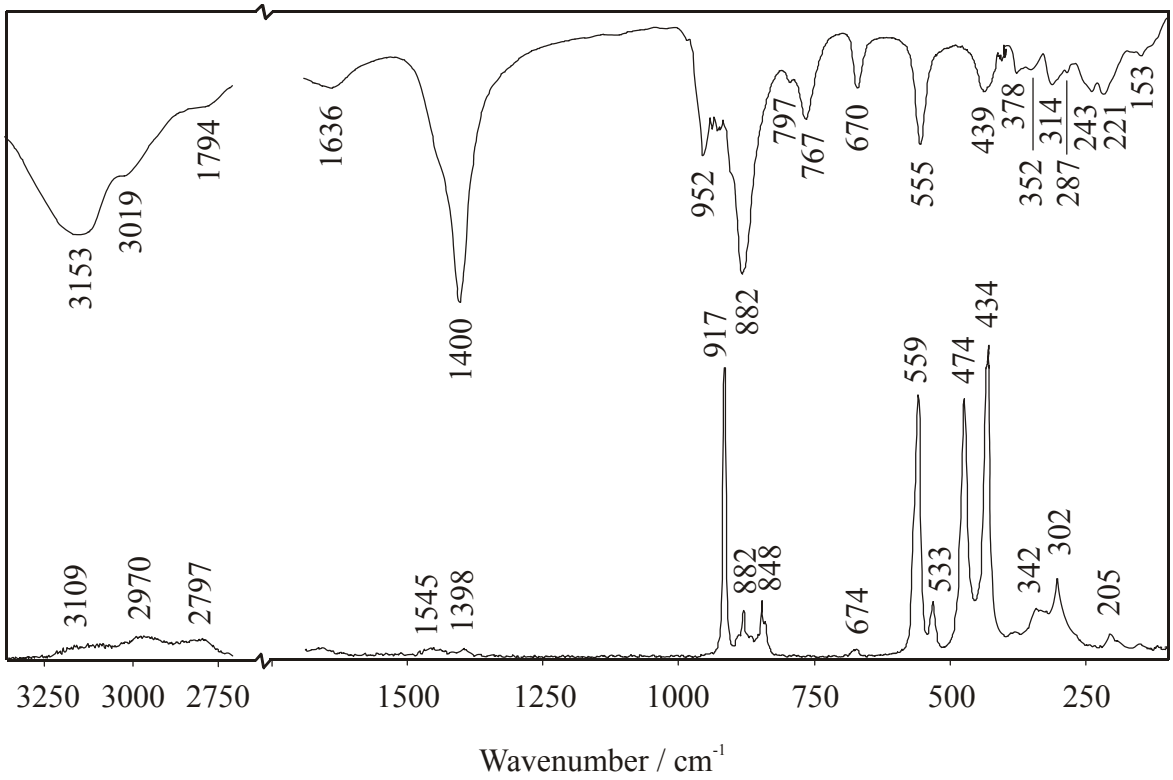

Figure 5.1: Infrared and Raman spectra of $(NH_4)_3[Cr(O_2)_4]$.

The infrared and Raman spectra of Ammonium Tetraperoxochromate are recorded at low temperature (around 120 K). On cooling the samples, the spectrum became better resolved as

the several bands are split into other different components. In general, the peaks were found to shift a little bit to higher frequency on cooling, a behaviour consistent with the expected increase in force constant as the substance contracted.

The 120 K Raman spectrum contains 16 bands, viz. at 205, 302, 342, 434, 474, 533, 559, 674, 848, 882, 917, ~1398, ~1545, ~2797, ~2970, and ~3109 cm^{-1}.

While the 120 K middle infrared spectrum contains 12 bands, viz. at 439, 555, 670, 767, 797, 882, 952, 1400, 1636, ~1794, ~3019, and ~3153 cm^{-1}, the 120 K far infrared spectrum contains seven bands, viz. at 153, 221, 243, 287, 314, 352, and 378 cm^{-1} (see fig. 5.1).

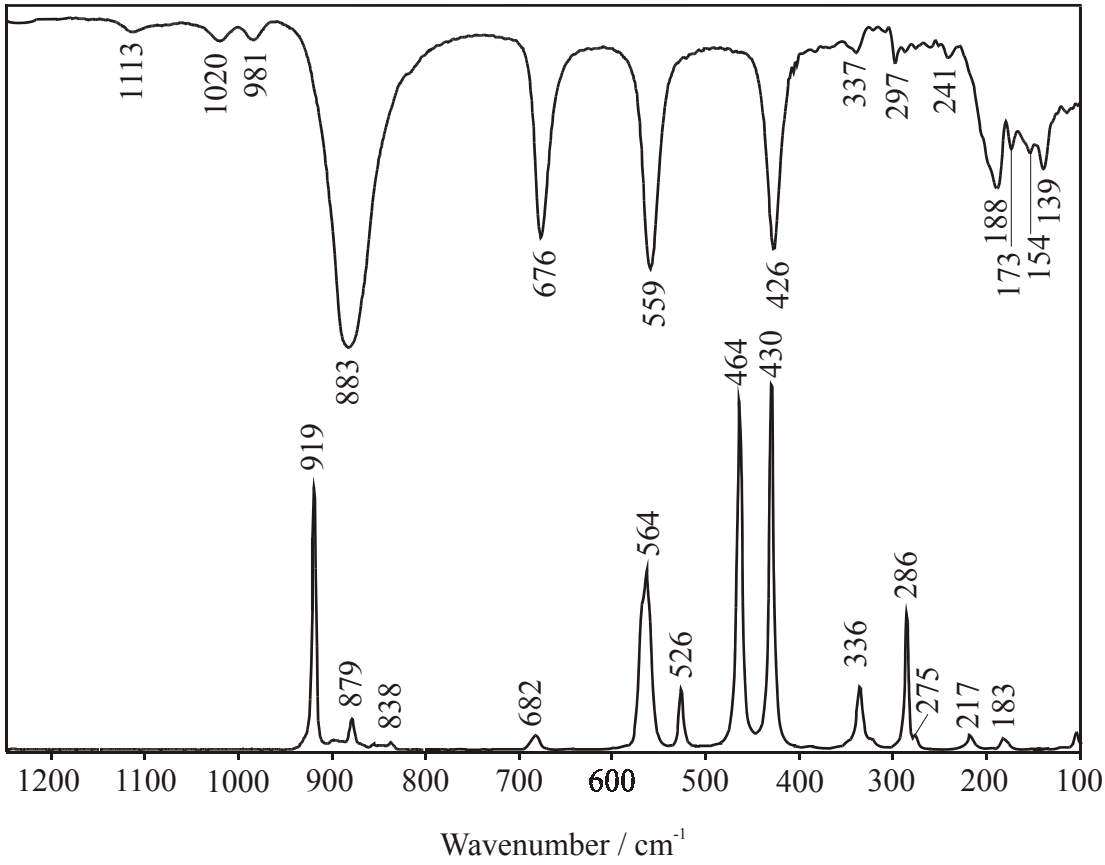

Figure 5.2: Infrared and Raman spectra of $K_3[Cr(O_2)_4]$.

In the case of other Tetraperoxochromates of Potassium or Rubidium, the infrared and Raman spectra are recorded at ambient temperature, as there has been seen not such a big difference, when the measurements were done at low temperature (liquid nitrogen temperature), they were nearly identical. In the case of Tetraperoxochromate of Potassium

and Rubidium all the infrared and Raman bands are located in the 100 ~ 1150 cm^{-1} spectral region.

As the result, the Raman spectrum of $K_3[Cr(O_2)_4]$ contains 13 bands, viz. at 183, 217, 275, 286, 336, 430, 464, 526, 564, 682, 838, 879, and 919 cm^{-1}.

The middle infrared spectrum contains seven bands, viz. at 426, 559, 676, 883, 981, 1020, and 1113 cm^{-1}, whereas the far infrared spectrum contains seven bands, viz. at 139, 154, 173, 188, 241, 297, and 337 cm^{-1} (see fig. 5.2).

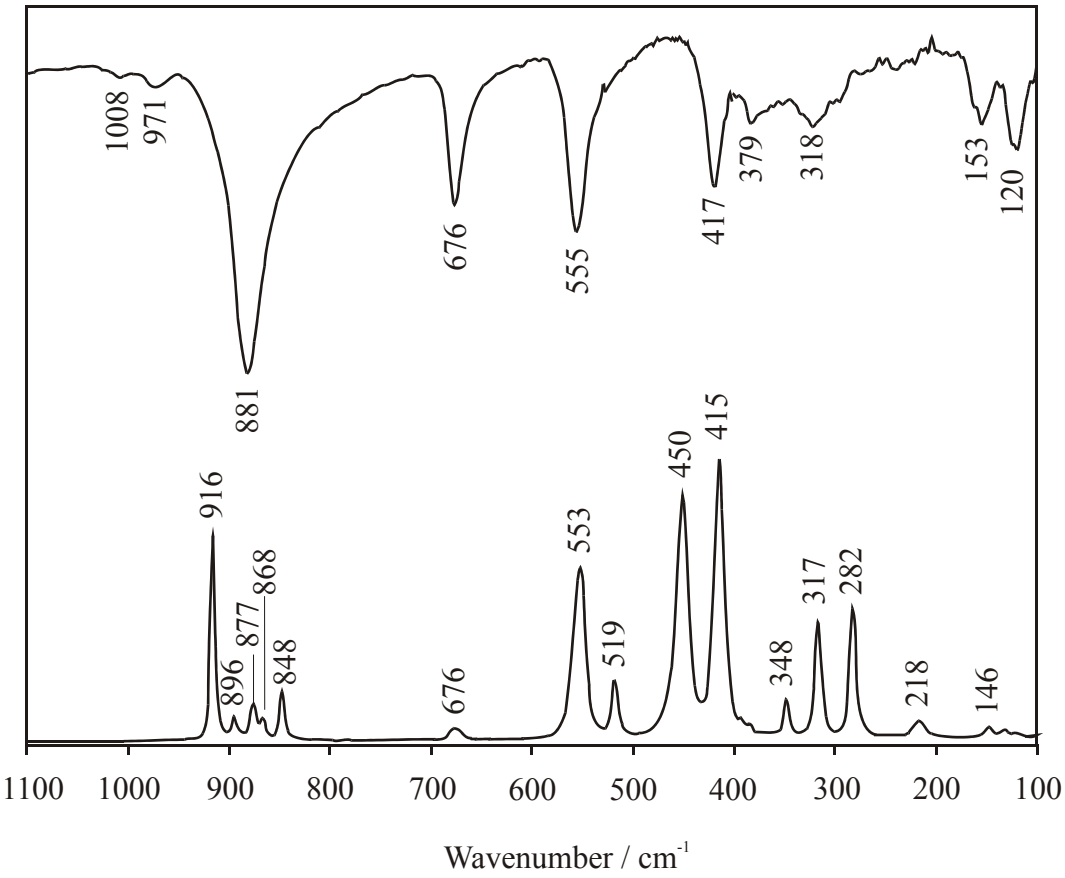

Figure 5.3: Infrared and Raman spectra of $Rb_3[Cr(O_2)_4]$.

As it is shown in fig. 5.3, the Raman spectrum of $Rb_3[Cr(O_2)_4]$ reveals up to 15 bands, viz. at 146, 218, 282, 317, 348, 415, 450, 519, 553, 676, 848, 868, 877, 896, and 916 cm^{-1}.

While the middle infrared spectrum contains six bands, viz. at 417, 555, 676, 881, 971, and 1008 cm^{-1}, the far infrared spectrum contains four mainly bands, viz. at 120, 153, 318, and 379 cm^{-1}.

The stretching vibrations of the O_2^{2-} groups in these three compounds are found at 916 – 919 cm^{-1} (Raman) and 881 – 883 cm^{-1} (IR). For discussion in details see chapter 5.5.

5.2. IR and Raman spectra of tetraperoxovanadates $A_3[V(O_2)_4]$

The infrared and Raman spectra of the Tetraperoxovanadates of Ammonium and Potassium are presented in the fig. 5.4 and 5.5, respectively.

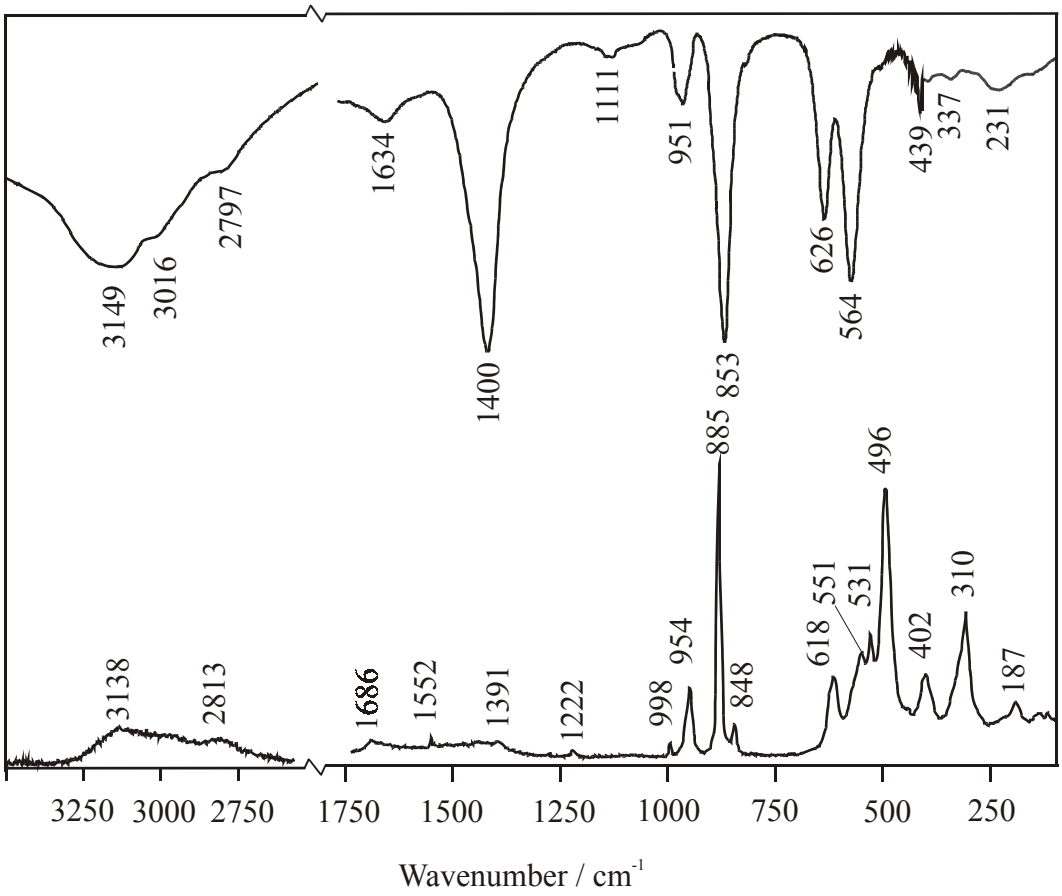

Figure 5.4: Infrared and Raman spectra of $(NH_4)_3[V(O_2)_4]$.

The infrared and Raman spectra of Ammonium Tetraperoxovanadate are recorded also at low temperature (sample cooled with liquid nitrogen).

The 120 K Raman spectrum of $(NH_4)_3[V(O_2)_4]$ contains 17 bands, viz. at 187, 310, 402, 496, 531, 551, 618, 848, 885, 954, 998, 1222, 1391, 1552, 1686, ~2813, and ~3138 cm^{-1}.

Whereas, the 120 K middle infrared spectrum reveals up to 11 bands, viz. at 439, 564, 626, 853, 951, 1111, 1400, 1634, ~2797, ~3016, and ~3149 cm^{-1}, the 120 K far infrared spectrum consists mainly in two bands, viz. at 231 and 337 cm^{-1} (see fig. 5.4).

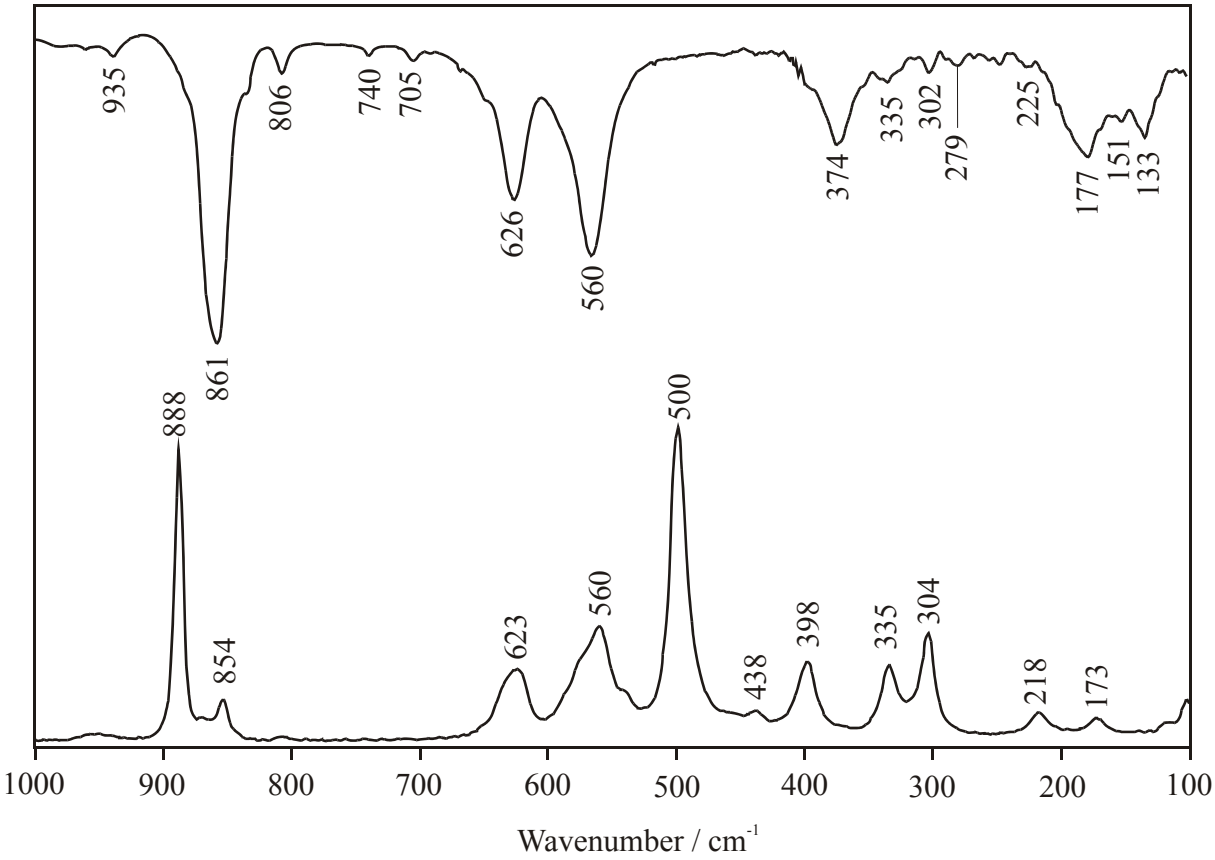

Figure 5.5: Infrared and Raman spectra of $K_3[V(O_2)_4]$.

All the infrared and Raman bands of $K_3[V(O_2)_4]$ are located in 100 – 1000 cm^{-1} spectral region. The results are taken from the measurement of powdered samples at ambient temperature.

As the result, from the Raman spectrum of $K_3[V(O_2)_4]$ are recorded 11 bands, viz. at 173, 218, 304, 335, 398, 438, 500, 560, 623, 854, and 888 cm^{-1}.

The middle infrared spectrum of this compound contains seven bands, viz. at 560, 626, 705, 740, 806, 861, and 935 cm^{-1}, while the far infrared spectrum reveals up to other seven bands, viz. at 133, 151, 177, 225, 279, 302, 335, and 374 cm^{-1} (see fig. 5.5).

The stretching vibrations of the O_2^{2-} groups in these two compounds are found at 885 and 888 cm^{-1} (Raman) for $(NH_4)_3[V(O_2)_4]$ and $K_3[V(O_2)_4]$, respectively. In the infrared, the

stretching vibrations of the peroxo groups are found at 853 and 861 cm^{-1} for $(NH_4)_3[V(O_2)_4]$ and $K_3[V(O_2)_4]$, respectively. As it can be seen, the values of the wavelength are getting bigger, so they are shifted on the right with increasing the radius of the cation. Normally the influence of the cation is very small and mainly is related to the radius of the central atom and the force constant. See chapter 5.5 for a more detailed discussion of this correlation.

5.3. IR and Raman spectra of tetraperoxoniobates $A_3[Nb(O_2)_4]$

The infrared and Raman spectra of the Tetraperoxoniobates of Ammonium, Potassium and Caesium are presented in the fig. 5.6, 5.7 and 5.8, respectively.

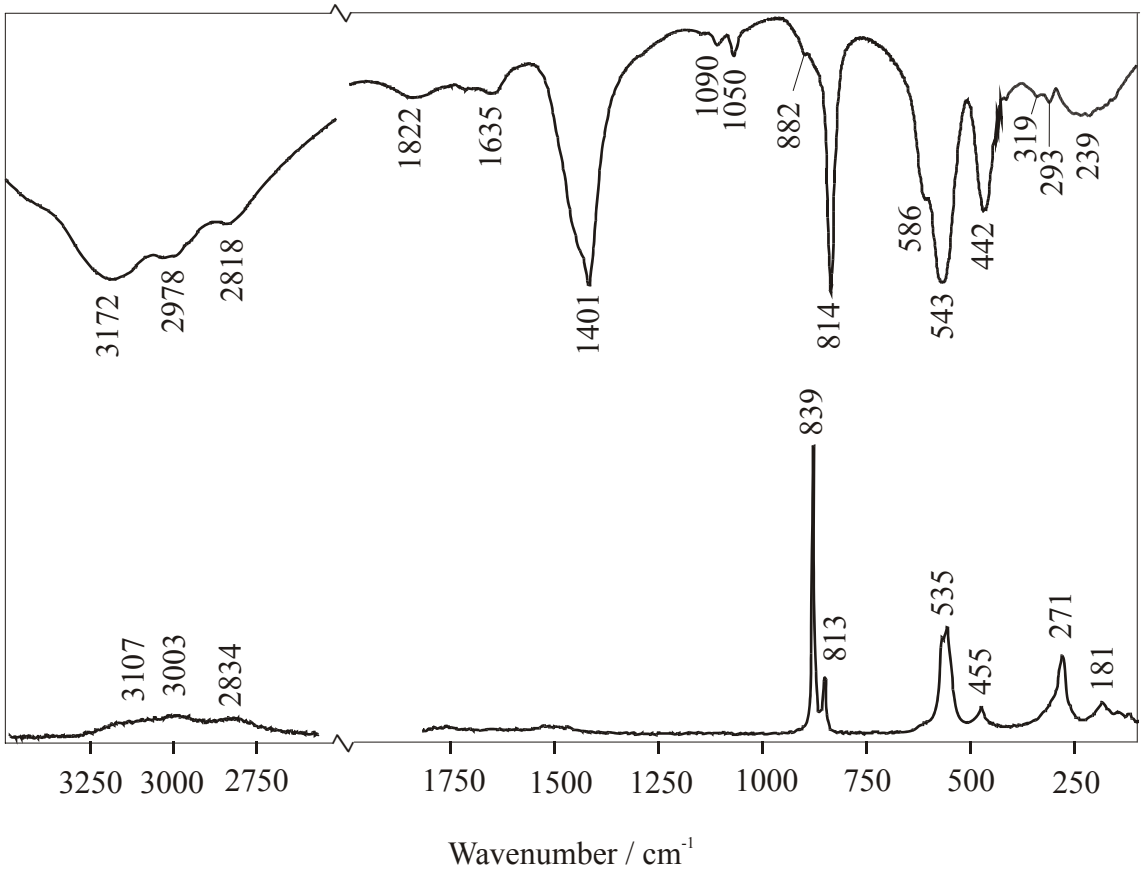

Figure 5.6: Infrared and Raman spectra of $(NH_4)_3[Nb(O_2)_4]$.

The infrared and Raman spectra of Ammonium Tetraperoxoniobate are recorded at low temperature (liquid nitrogen temperature). All the infrared and Raman bands are located in the 100 ~ 3500 cm^{-1} spectral region.

The 120 K Raman spectrum of $(NH_4)_3[Nb(O_2)_4]$ shows us nine bands, viz. at 181, 271, 455, 535, 813, 839, ~2834, ~3003, and ~3107 cm^{-1}.

According to the 120 K middle infrared measurement, we find a spectrum with 12 bands, viz. at 442, 543, 586, 814, 1050, 1090, 1401, 1635, ~1822, ~2818, ~2978, and ~3172 cm^{-1}. On the same conditions, at 120 K results the far infrared spectrum, which contains three main bands, viz. at ~239, 293, and 319 cm^{-1} (see fig. 5.6).

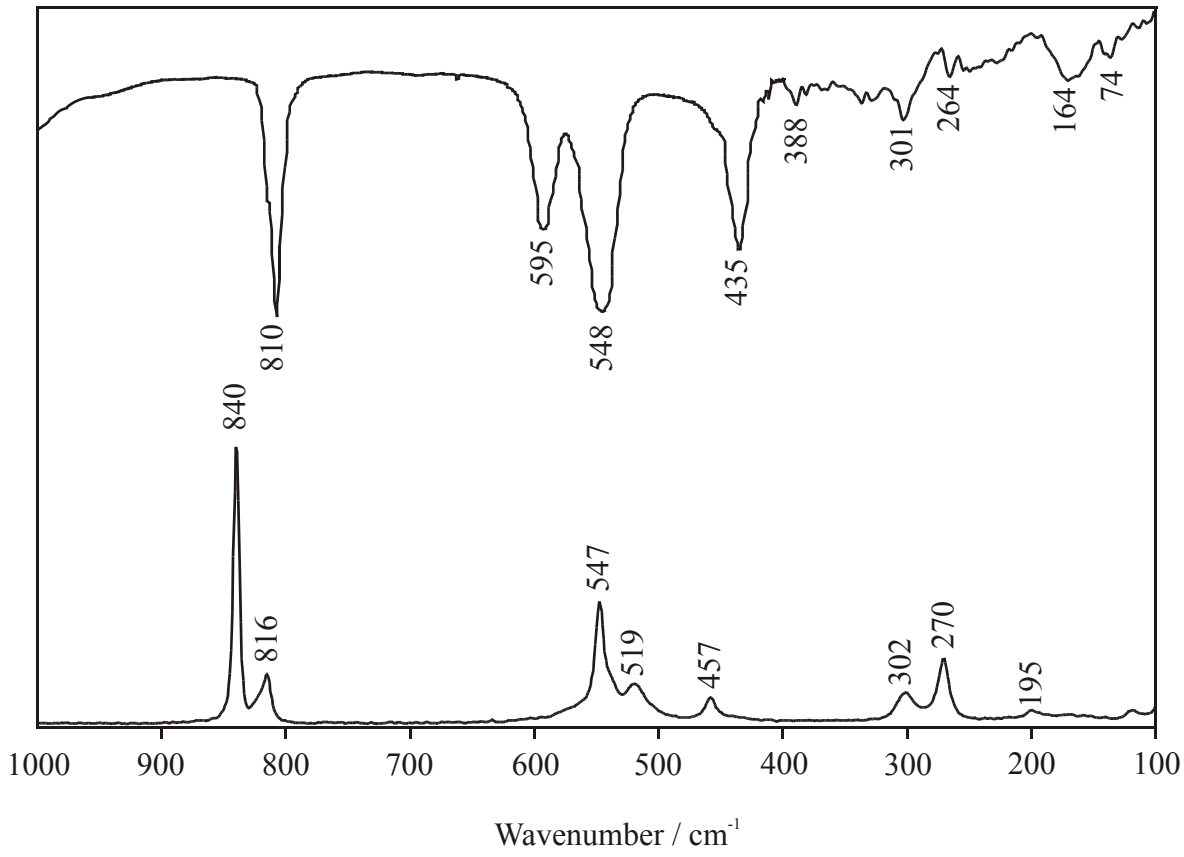

Figure 5.7: Infrared and Raman spectra of $K_3[Nb(O_2)_4]$.

The infrared and Raman spectra of Tripotassium Tetraperoxoniobate are taken as the result of measurement at ambient temperature. At the same condition were done the measurements for the other peroxoniobate compound of Caesium. The spectral region, where the different bands are located, is 100 – 1000 cm^{-1}.

The Raman spectrum of $K_3[Nb(O_2)_4]$ reveals up to eight bands, viz. at 195, 270, 302, 457, 519, 547, 816, and 840 cm^{-1}.

Whereas, the middle infrared spectrum contains four bands, viz. at 435, 548, 595, and 810 cm^{-1}; the far infrared spectrum reveals up to five bands, viz. at 135, 164, 264, 301, and 388 cm^{-1} (see fig. 5.7).

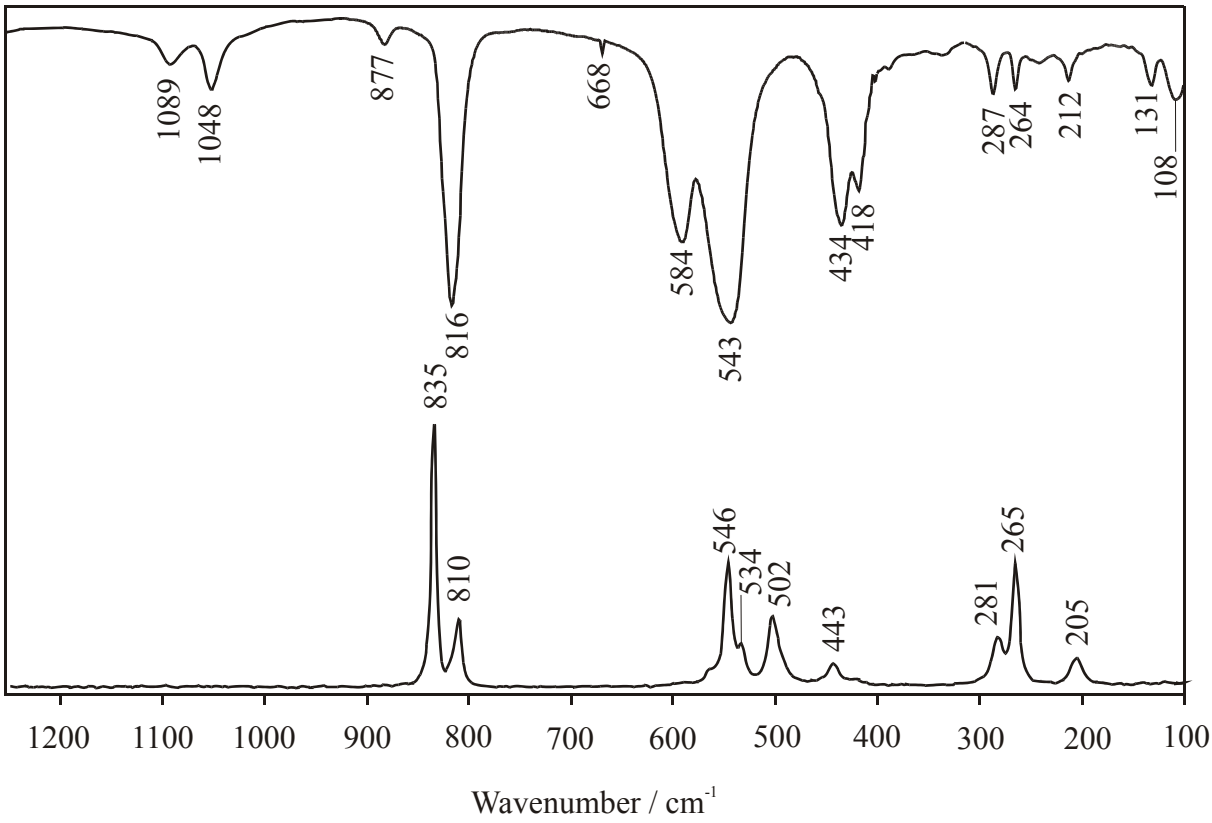

Figure 5.8: Infrared and Raman spectra of $Cs_3[Nb(O_2)_4]$.

The infrared and Raman spectra of Caesium Tetraperoxoniobate are taken also as the result of measurement at ambient temperature.

The Raman spectrum of $Cs_3[Nb(O_2)_4]$ contains nine bands, viz. at 205, 265, 281, 443, 502, 534, 546, 810, and 835 cm^{-1}.

Whereas, the middle infrared spectrum reveals up to nine bands, viz. at 418, 434, 543, 584, 668, 816, 877, 1048, and 1089 cm^{-1}, the far infrared spectrum contains five bands, viz. at 108, 131, 212, 264, and 287 cm^{-1} (see fig. 5.8).

The stretching vibrations of the tetraperoxo groups (O_2^{2-}) in the compounds of Tetraperoxoniobate – of Ammonium, Potassium and Caesium are found at 835 – 840 cm^{-1} (Raman) and at 810 – 816 cm^{-1} (IR). Whereas, the stretching vibrations of the peroxo groups

in the compound $Rb_3[Nb(O_2)_4]$ are found at 838 cm^{-1} (Raman) and at 814 cm^{-1} (IR) [18]. As it can be seen from the results, the stretching vibration values of the peroxo groups in the compounds $Rb_3[Nb(O_2)_4]$, $Cs_3[Nb(O_2)_4]$ and $(NH_4)_3[Nb(O_2)_4]$ are nearly the same (~814 cm^{-1} in IR and ~839 cm^{-1} in Raman).

5.4. IR and Raman spectra of tetraperoxotantalates $A_3[Ta(O_2)_4]$

The infrared and Raman spectra of the Tetraperoxotantalates of Ammonium, Potassium, Rubidium and Caesium are presented in the fig. 5.9, 5.10, 5.11 and 5.12, respectively.

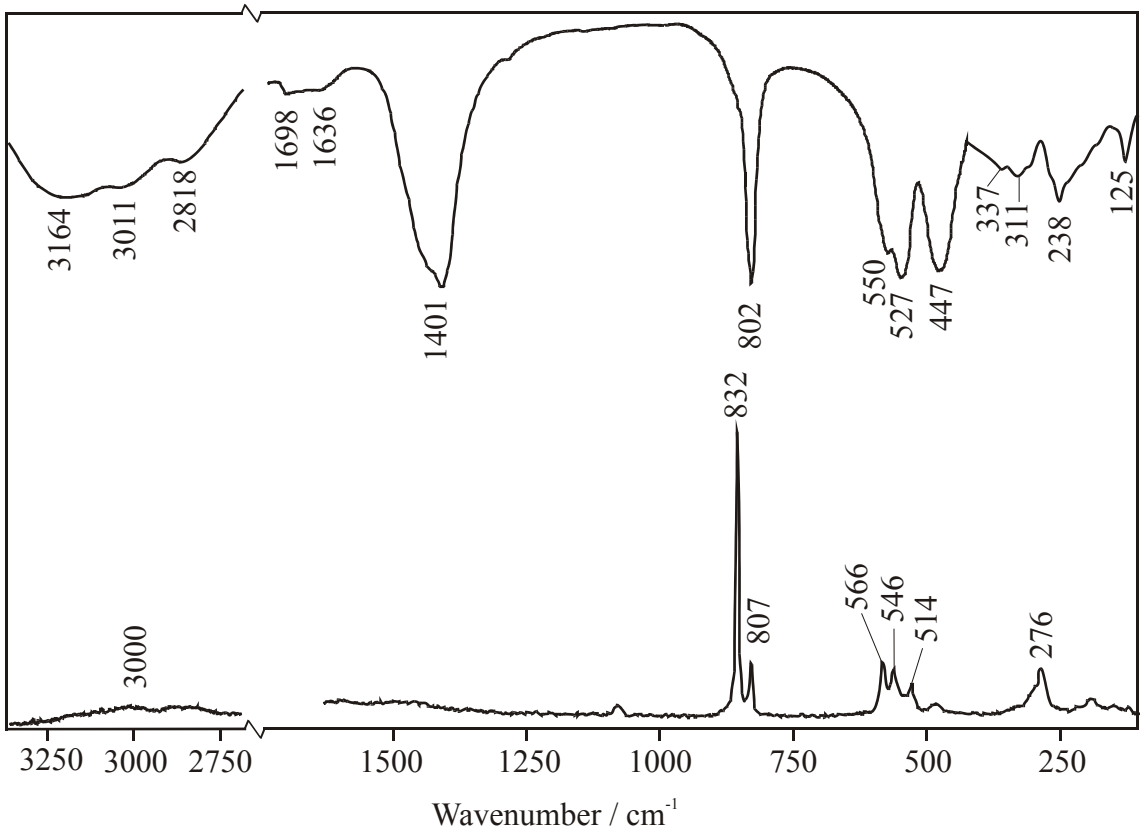

Figure 5.9: Infrared and Raman spectra of $(NH_4)_3[Ta(O_2)_4]$.

The measurements of infrared and Raman spectra of Ammonium Tetraperoxotantalate are done at liquid nitrogen temperature (~120 K). The spectral region of bands, appearing in this compound is located at 100 ~ 3500 cm^{-1}.

The Raman spectrum of $(NH_4)_3[Ta(O_2)_4]$ reveal up to seven bands, viz. at 276, 514, 546, 566, 807, 832, and ~3000 cm^{-1}.

Whereas, the middle infrared spectrum of that compound contains 10 bands, viz. at 447, 527, 550, 802, 1401, ~1636, 1698, ~2818, ~3011, and ~3164 cm^{-1}, the far infrared spectrum shows us four bands, viz. at 125, 238, 311, and 337 cm^{-1} (see fig. 5.9).

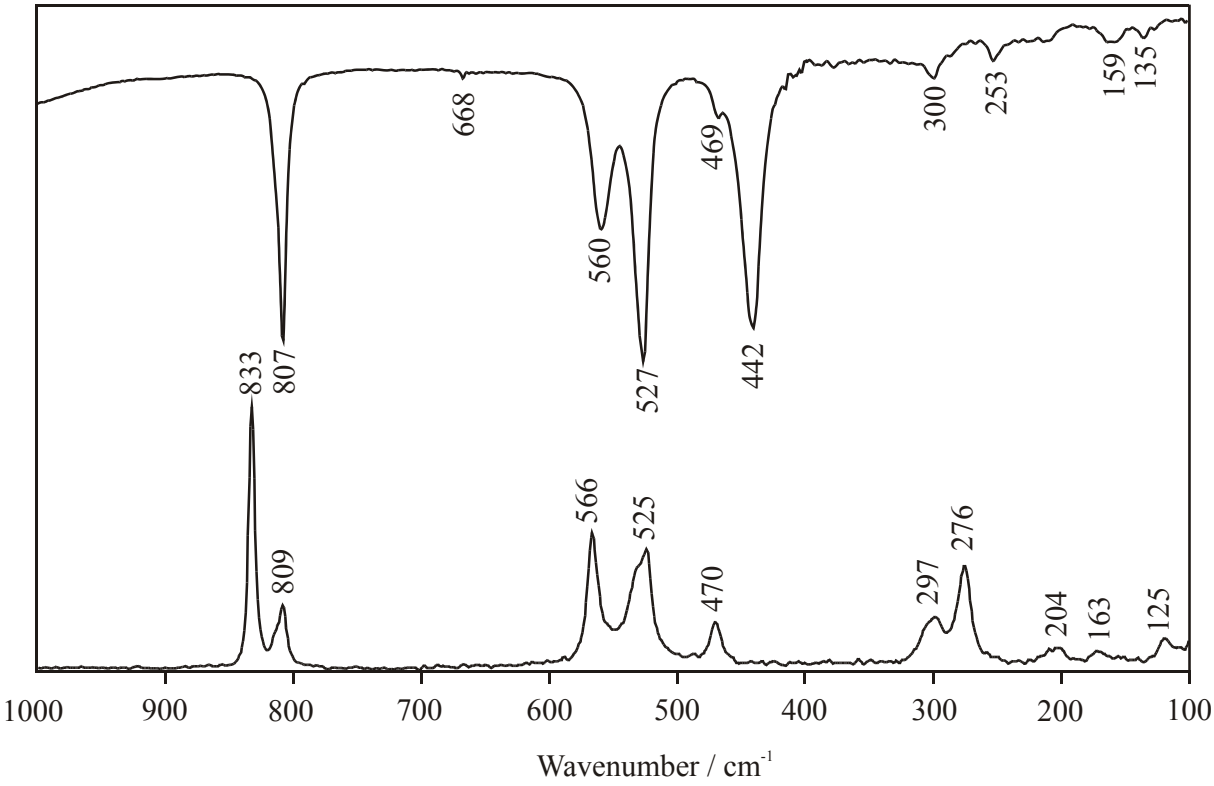

Figure 5.10: Infrared and Raman spectra of $K_3[Ta(O_2)_4]$.

The measurement of the infrared and Raman spectra of Tetraperoxotantalate of Potassium, Rubidium and Caesium are done at ambient temperature. The spectral region, where the bands are located is at 100 – 1000 cm^{-1}.

As it is shown in fig. 5.10, the Raman spectrum of $K_3[Ta(O_2)_4]$ reveals up to 10 bands, viz. at 125, 163, 204, 276, 297, 470, 525, 566, 809, and 833 cm^{-1}.

Due to the measurement in both regions of middle and far infrared, we find spectra with six bands (MIR) viz. at 442, 469, 527, 560, 668, and 807 cm^{-1}; and four bands (FIR) viz. at 135, 159, 253, and 300 cm^{-1}, respectively.

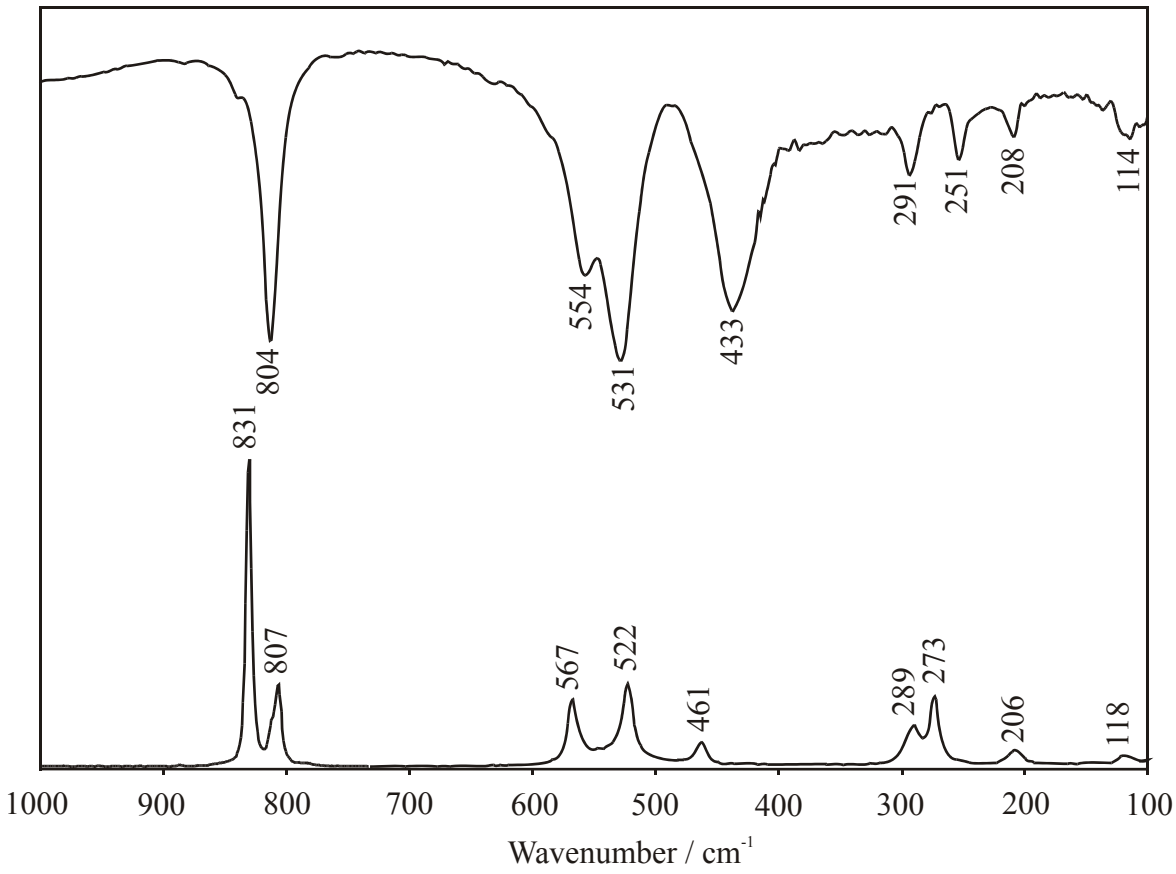

Figure 5.11: Infrared and Raman spectra of $Rb_3[Ta(O_2)_4]$.

The infrared and Raman spectra, measured at ambient temperature on powdered samples, gives us bands located at 100 – 1000 cm^{-1} spectral region.

The Raman spectrum of Rubidium Tetraperoxotantalate reveals up to nine bands, viz. at 118, 206, 273, 289, 461, 522, 567, 807, and 831 cm^{-1}.

The middle infrared spectrum of this peroxo compound shows us four bands, viz. at 433, 531, 554, and 804 cm^{-1}, while the far infrared spectrum contains other four bands, viz. at 114, 208, 251, and 291 cm^{-1} (see fig. 5.11).

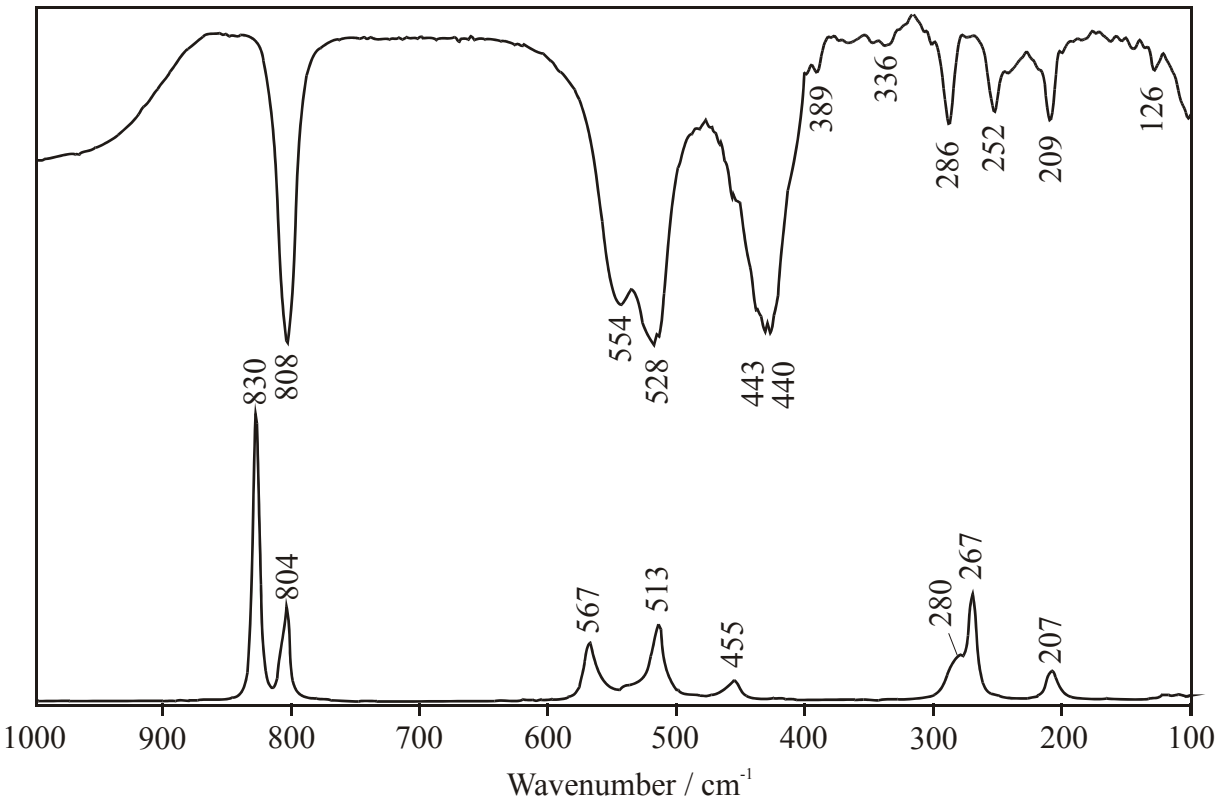

Figure 5.12: Infrared and Raman spectra of $Cs_3[Ta(O_2)_4]$.

The infrared and Raman spectra of Caesium Tetraperoxotantalate are also located in the spectral region 100 – 1000 cm^{-1}. The general appearance of the O – O stretching vibrations in the peroxo groups is at 830 cm^{-1} (Raman) and 808 cm^{-1} (IR).

The Raman spectrum of $Cs_3[Ta(O_2)_4]$ contains seven bands, viz. at 207, 267, 455, 513, 567, 804, and 830 cm^{-1}.

As the middle infrared spectrum shows five bands, viz. at 440, 443, 528, 554, and 808 cm^{-1}, the far infrared spectrum reveals up to six bands, viz. at 126, 209, 252, 286, 336, and 389 cm^{-1} (see fig. 5.12).

The stretching vibrations of the peroxo group for Tetraperoxotantalate of Ammonium, Potassium, Rubidium and Caesium appear at 830 – 833 cm^{-1} (Raman) and 802 – 808 cm^{-1} (IR).

5.5. Discussion and conclusions

The infrared and Raman spectra (recorded on powdered samples) for all the tetraperoxo compounds are discussed with respect to the internal vibrations of the peroxo – group and the dodecahedral $[B(O_2)_4]^{3-}$ ion (where B = Cr^{V+}, V^{V+}, Nb^{V+} or Ta^{V+}). In the structure of tetraperoxo compounds there are four equal O – O bonds and so there will be four O – O stretching vibrations. They can vibrate in phase and out – of – phase mode. Due to this analysis, it is possible to distinguish four different regions in the vibrational spectra of the tetraperoxo– chromates, vanadates, niobates and tantalates related to different groups of vibrations:

1. the stretching vibrations of the peroxo groups, expected in the region with $\tilde{\nu} > 800$ cm^{-1},
2. the B – O (B = Cr^{V+}, V^{V+}, Nb^{V+} or Ta^{V+}) stretching vibrations of the peroxo – chromate , vanadate, niobate or tantalate ion expected at $700\ cm^{-1} > \tilde{\nu} > 400\ cm^{-1}$,
3. the bending vibrations of the peroxo– chromate, vanadate, niobate or tantalate ion expected to be observed in the region with $400\ cm^{-1} > \tilde{\nu} > 200\ cm^{-1}$ and
4. the translational lattice vibrations and the librations of the $[Cr(O_2)_4]^{3-}$, $[V(O_2)_4]^{3-}$, $[Nb(O_2)_4]^{3-}$ and $[Ta(O_2)_4]^{3-}$ ion expected at $\tilde{\nu} < 200\ cm^{-1}$.

The factor group analysis for the $K_3[Cr(O_2)_4]$ – type results in the following distribution of the vibrational degrees of freedom over the species of point group D_{2d} [58]:

$$\Gamma = 4A_1 + 2A_2 + 3B_1 + 6B_2 + 9\ E$$

Of these, the 15 vibrations of species B_2 and E are both infrared and Raman active, seven vibrations of species A_1 and B_1 are only Raman active and the two vibrations of species A_2 are silent. So, in total we find 15 vibrations active in infrared and 22 vibrations active in Raman.

In a different approach, the vibrations can be classified as internal vibrations of the different molecular entities, i.e. the $[Cr(O_2)_4]^{3-}$ ion (site group symmetry D_{2d}) or the peroxogroups (see tab. 5.1). Three of the internal vibrations of the $[Cr(O_2)_4]^{3-}$ ion belonging to the species A_1, B_2 and E are related to the stretching vibrations of the peroxo groups, so the number of bending and Cr – O stretching vibrations of the $[Cr(O_2)_4]^{3-}$ ion is:

$$\Gamma = 3A_1 + A_2 + 2B_1 + 3B_2 + 4E$$

So, we have seven IR – active (B_2 + E) and 12 Raman – active vibrations ($A_1 + B_1 + B_2$ + E). One kind is also in silent (A_2).

At the same conclusion we came also for the other Tetraperoxoions of Vanadium, Niobium and Tantalum so, we are presenting the distribution of the vibrations only for the molecular entities $[Cr(O_2)_4]^{3-}$.

Table 5.1: Distribution of the internal, librational, and translational vibrations of the molecular entities $[Cr(O_2)_4]^{3-}$ and O − O over the species of point group D_{2d} and their activity.

	$[Cr(O_2)_4]^{3-}$			**O − O**			activity
	internal	librational	translational	internal	Librational	translational	
A_1	4			1	0	2	Ra
A_2	1	1			2	1	
B_1	2				2	1	Ra
B_2	4		1	1	0	1	Ra, IR
E	5	1	1	1	2	2	Ra, IR

In the case of the ammonium compounds: $(NH_4)_3[Cr(O_2)_4]$, $(NH_4)_3[V(O_2)_4]$, $(NH_4)_3[Nb(O_2)_4]$ and $(NH_4)_3[Ta(O_2)_4]$, in addition to the vibrations of the $K_3[Cr(O_2)_4]$ type the internal vibrations of the ammonium ions and their librational modes are observed in the spectra. While the stretching and bending vibrations of the ammonium ions will be found outside of the four spectral regions mentioned above, the librational modes may be found below 1000 cm^{-1}, i.e. in the same region as the internal vibrations of the peroxo – chromate, vanadate, niobate and tantalate ions. At 2500 – 3500 cm^{-1} spectral region are appearing the stretching

vibration of N – H in the ammonium groups. Also, below 100 cm^{-1} are appearing the translational vibrations of the ammonium groups. Concretely, the 221 cm^{-1} for $(NH_4)_3[Cr(O_2)_4]$ in IR, the 231 cm^{-1} for $(NH_4)_3[V(O_2)_4]$ in IR, 239 cm^{-1} for $(NH_4)_3[Nb(O_2)_4]$ in IR and 238 cm^{-1} for $(NH_4)_3[Ta(O_2)_4]$ in IR are found in the spectra which belongs to the translational vibration of the ammonium groups. On the other hand, the librational vibration of the ammonium groups in the ammonium tetraperoxo compounds are appearing at 952 cm^{-1} (IR) for $(NH_4)_3[Cr(O_2)_4]$, at 951 cm^{-1} (IR) for $(NH_4)_3[V(O_2)_4]$ and at 882 cm^{-1} (IR) for $(NH_4)_3[Nb(O_2)_4]$.

The assignment of the three possible stretching vibrations of the peroxo groups (see tab. 5.1) is straightforward. The strong lines in the Raman spectra at 916 – 919 cm^{-1} (for Tetraperoxochromates), 885 – 888 cm^{-1} (for Tetraperoxovanadates), 835 – 840 cm^{-1} (for Tetraperoxoniobates) and 830 – 833 cm^{-1} (for Tetraperoxotantalates) are due to the total symmetric vibration of all four peroxo groups of species A_1. The strong bands in the IR spectra at 881 – 883 cm^{-1} (for Tetraperoxochromates), 853 – 861 cm^{-1} (for Tetraperoxovanadates), 810 – 816 cm^{-1} (for Tetraperoxoniobates) and 802 – 808 cm^{-1} (for Tetraperoxotantalates) are assigned to the vibrations of species E which are also observed in the Raman spectra, although with slightly different wave numbers owing to the accuracy of the measurements. The third vibration of the peroxo groups of species B_2 is found at 848 cm^{-1} (for $(NH_4)_3[Cr(O_2)_4]$, $Rb_3[Cr(O_2)_4]$ and $(NH_4)_3[V(O_2)_4]$) in the Raman spectra but is not observed in the IR spectra, although it is both IR and Raman active. The additional lines observed in the Raman spectrum of $(NH_4)_3[Cr(O_2)_4]$ at 882 cm^{-1}, of $K_3[Cr(O_2)_4]$ at 879 cm^{-1} and of $Rb_3[Cr(O_2)_4]$ at 896, 877 and 868 cm^{-1}, are obviously due to overtone and combination vibrations. In $(NH_4)_3[Ta(O_2)_4]$ a strong broad absorption near 3000 cm^{-1} is caused due to the bonded N – H stretch in ammonium groups. The sharp strong absorption near 830 cm^{-1} (Raman) and near 800 cm^{-1} (IR) have been the most studied in the characterization of peroxo groups. The weak bands at 300 – 340 cm^{-1} are characteristic of deformation vibration (deforming the shape of the $[Ta(O_2)_4]^{3-}$ group by changing the O – Ta – O angle).

It is remarkable that for all the compounds in the same group (Tetraperoxochromates, Tetraperoxovanadates, Tetraperoxoniobates and Tetraperoxotantalates) under investigation the vibrations of the peroxo groups have nearly the same wavenumbers and are not so much affected by the different cations (see tab. 5.2):

Table 5.2: The values of the stretching vibrations of the peroxo groups in the structure of $A_3[B(O_2)_4]$ compounds.

Tetraperoxo compounds	IR $\tilde{\nu}_{O-O}$ [cm^{-1}]	Raman $\tilde{\nu}_{O-O}$ [cm^{-1}]
$K_3[Cr(O_2)_4]$	883	919
$Rb_3[Cr(O_2)_4]$	881	916
$(NH_4)_3[Cr(O_2)_4]$	882	917
$K_3[V(O_2)_4]$	861	888
$(NH_4)_3[V(O_2)_4]$	853	885
$K_3[Nb(O_2)_4]$	810	840
$Rb_3[Nb(O_2)_4]$	814	838
$Cs_3[Nb(O_2)_4]$	816	835
$(NH_4)_3[Nb(O_2)_4]$	814	839
$K_3[Ta(O_2)_4]$	807	833
$Rb_3[Ta(O_2)_4]$	804	831
$Cs_3[Ta(O_2)_4]$	808	830
$(NH_4)_3[Ta(O_2)_4]$	802	832

From this finding we conclude that the O – O distances in these Tetraperoxo compounds (inside the same group) are equal or at least very similar (see tab. 4.15). A comparison with the values obtained for the stretching vibrations of the peroxo groups in the corresponding Tetraperoxochromates, Tetraperoxovanadates, Tetraperoxoniobates and Tetraperoxotantalates shows that they change significantly with the central atom, although this is not involved in the vibrational mode, at least in the total symmetric vibration of species A_1 (see tab. 5.2). Therefore, this shift to lower wavenumbers with increasing mass of the central atom must be due to changes in the O – O stretching force constants, which become smaller with increasing mass of the central atom. i.e. we compare in the 100 – 1000 cm^{-1} spectral region the spectra of $K_3[Cr(O_2)_4]$, $K_3[V(O_2)_4]$, $K_3[Nb(O_2)_4]$ and $K_3[Ta(O_2)_4]$ in IR (see fig. 5.13) and Raman (see fig. 5.14).

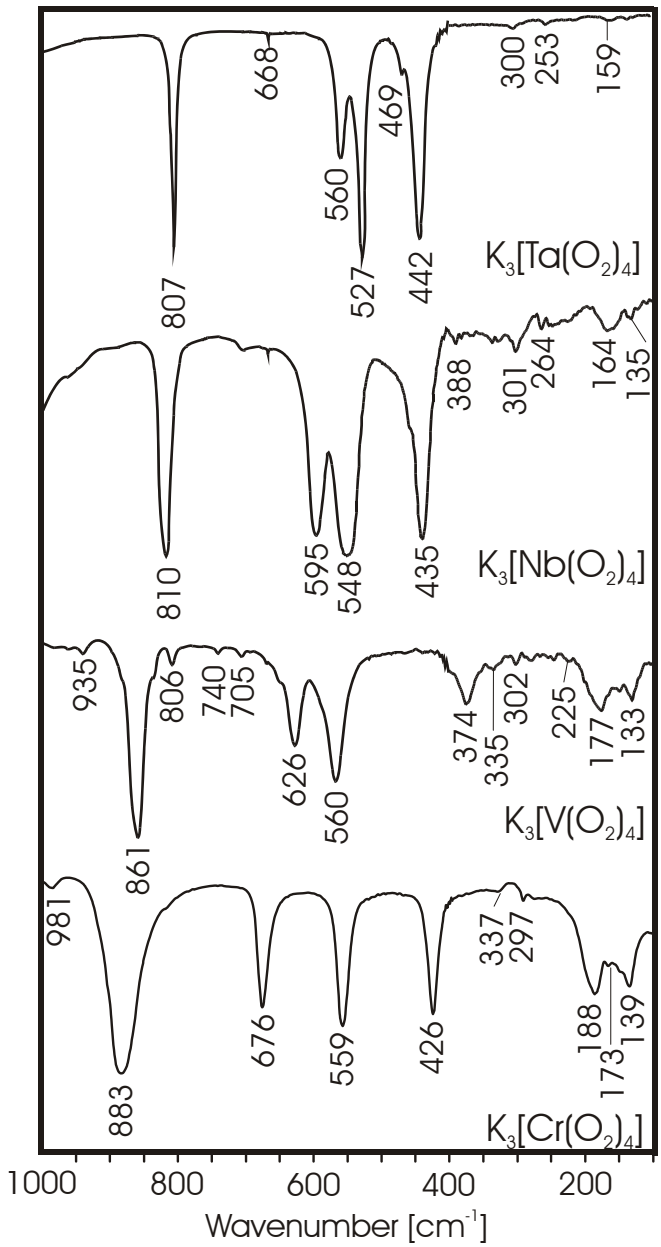

Figure 5.13: Infrared spectra of Tripotassium Tetraperoxo compounds of Chromium, Vanadium, Niobium and Tantalum.

The wavenumbers for the IR active O – O stretching vibrations are shifted to lower values with increasing mass of the central atom, as it can be seen in the infrared spectra from 883, 861, 810 to 807 cm^{-1} for $K_3[Cr(O_2)_4]$, $K_3[V(O_2)_4]$, $K_3[Nb(O_2)_4]$ and $K_3[Ta(O_2)_4]$, respectively (see fig. 5.13). This can be explained as the stretching vibration of the peroxo groups (of

species B_2) depends on the mass of the central atoms and on the force constants between oxygen atoms and the central metal atom. The mass of the central atom is increasing from Vanadium (50.9415 [59]), Chromium (51.9961 [59]), Niobium (92.90638 [59]) to Tantalum (180.9479 [59]), whereas, the force constants become smaller with increasing mass and the radius of the central atom. The radius of the five valent ion is decreasing from Nb^{V+} (69 pm [59]), Ta^{V+} (64 pm [59]), V^{V+} (59 pm [59]) to Cr^{V+}. The radius of Cr^{V+} is missing in literature (as Cr is in the unusual oxidation state of +V) but we know that it should be smaller than 56 pm which is the radius of the ion Cr^{IV+} [59]. At the same time, details of the bonding in the peroxometallate ion as known from the literature are playing an important role for the frequencies of the O – O stretching vibrations. According to Fischer *et al.* [14], the shift to lower wavenumbers is due to an overlap of the π* orbitals of the peroxo groups with empty dz^2 orbitals of the central metal atoms by which electron density is flowing from the antibonding orbitals of the peroxogroups to the central atom, thus strengthening the O – O bond and consequently enlarging the O – O stretching force constant.

As the result, we came into conclusion that such an overlap is better in the case of the central atoms with a smaller ionic radius, i.e. better for the chromium compounds than for vanadium, niobium or tantalum. The smaller the radius of the central atoms, the easier the flow of electron density from the antibonding orbitals of the peroxo groups to the empty dz^2 orbitals of the central atoms.

The same conclusion is coming also for the O – O distances in the peroxo group, which is becoming smaller with decreasing radius of the central atom (explained in chapter 4.6) while the stretching vibration of the peroxo ion is shifted to higher wavenumbers.

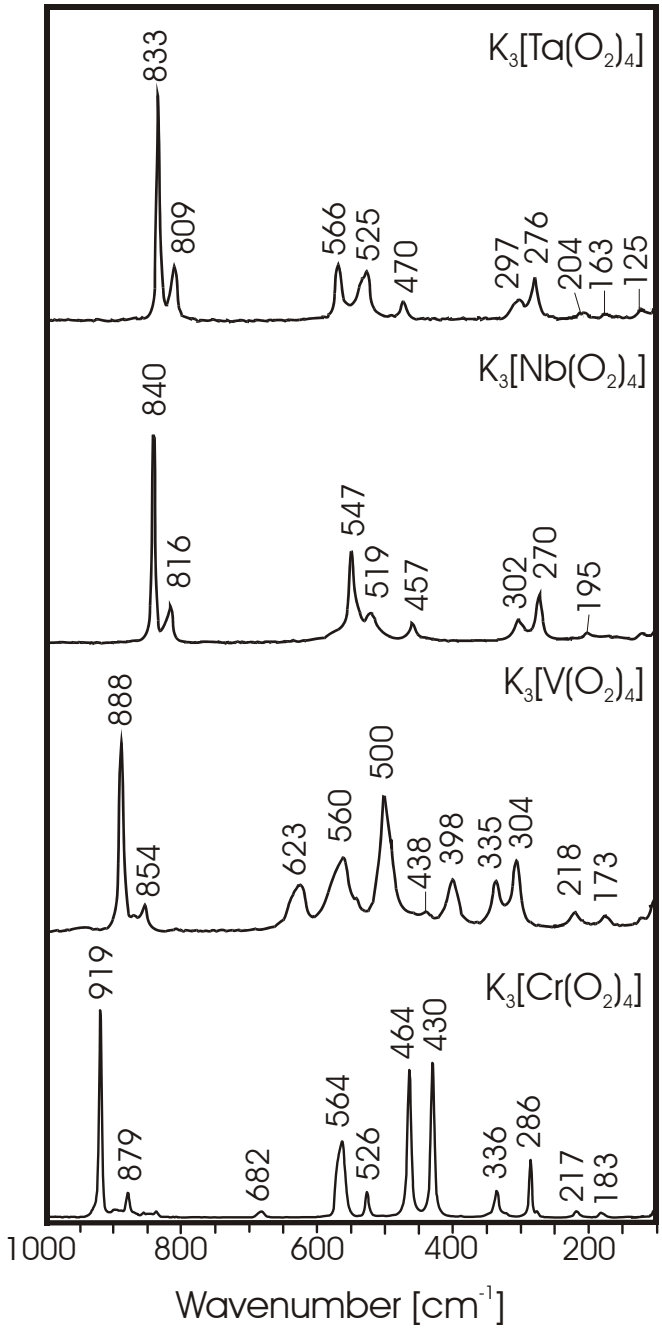

Figure 5.14: Raman spectra of Tripotassium Tetraperoxo compounds of Chromium, Vanadium, Niobium and Tantalum.

In the Raman spectra the wavenumbers of the O – O stretching vibrations are shifted from 919, 888, 840 to 833 cm^{-1} for $K_3[Cr(O_2)_4]$, $K_3[V(O_2)_4]$, $K_3[Nb(O_2)_4]$ and $K_3[Ta(O_2)_4]$, respectively (see fig. 5.14). In this case, the total symmetric stretching vibration of the peroxo

groups (of species A_1) depends only on the force constants and it does not depend on the mass of the central atoms as they do not participate in the vibration. The force constants between the peroxo groups and the central atom are rising with decreasing radius of the central atom. As it is mentioned in the case of the IR spectra, the radius of the ion is decreasing from Nb^{V+}, Ta^{V+}, V^{V+} to Cr^{V+}. But, the most important role plays the overlap of the antibonding π^* orbitals of the peroxo groups with empty dz^2 orbitals of the central metal atoms by which electron density is flowing from the antibonding orbitals of the peroxogroups to the central atom.

We came to the same conclusion as in the case of the IR spectra, that such an overlap is better in the case of the central atoms with a smaller ionic radius, i.e. better for the chromium compounds than for vanadium, niobium or tantalum. As the result, the values of the wavenumbers of the O – O stretching vibrations in the Raman spectra of Tetraperoxo – chromates , vanadates, niobates and tantalates are getting smaller, depending on the radius of the central atoms. Thus, the electron density of the peroxo groups in the Tetraperoxochromate flow easier from the antibonding orbitals to the empty dz^2 orbitals of the central atoms.

In the second region of the spectra from 700 to 400 cm^{-1}, we observe the B – O (B = Cr^{V+}, V^{V+}, Nb^{V+} or Ta^{V+}) stretching vibrations of the peroxo – chromate, vanadate, niobate or tantalate ion. This region may be analysed based on a description of the peroxo – chromate, vanadate, niobate or tantalate ion as a tetrahedral entity with rigid O_2 units on the corners of the tetrahedron. Owing to the site symmetry D_{2d} of the peroxo – chromate, vanadate, niobate and tantalate ion, the asymmetric stretching vibration of the tetrahedron splits into two components which occur in species B_2 and E which are both infrared and Raman active. The symmetrical stretching vibration on the other hand is still only Raman active in species A_1. Hence in a first approach we expect three vibrations to occur in this region: two in both the Raman and IR spectra and one in the Raman spectra only. An assignment based on this assumption is given for Tetraperoxochromates in tab. 5.3, for Tetraperoxovanadates in tab. 5.4, for Tetraperoxoniobates in tab. 5.5 and for Tetraperoxotantalate in tab. 5.6.

Table 5.3: Assignment of Cr – O stretching (ν) and O(2) – Cr – O(2) bending (δ) vibrations based on the assumption of a tetrahedral peroxochromate ion with rigid O(2) units on the corners of the tetrahedron.

	$(NH_4)_3[Cr(O_2)_4]$		$K_3[Cr(O_2)_4]$		$Rb_3[Cr(O_2)_4]$	
mode	IR	Raman	IR	Raman	IR	Raman
ν_s		474		464		450
ν_{as}	670		676	682	676	676
ν_{as}	555	559	559	564	555	553
δ_s (A_1)		533		526		519
δ_s (B_1)		n.o.		n.o.		348
δ_{as}				336	318	317
δ_{as}		302	297	286		282

Table 5.4: Assignment of V – O stretching (ν) and O(2) – V – O(2) bending (δ) vibrations based on the assumption of a tetrahedral peroxovanadate ion with rigid O(2) units on the corners of the tetrahedron.

	$(NH_4)_3[V(O_2)_4]$		$K_3[V(O_2)_4]$	
Mode	IR	Raman	IR	Raman
ν_s		496		500
ν_{as}	626		626	
ν_{as}	564	551	560	623
δ_s (A_1)		531		560
δ_s (B_1)		n.o.		n.o.
δ_{as}				335
δ_{as}		310	302	304

Table 5.5: Assignment of Nb – O stretching (ν) and O(2) – Nb – O(2) bending (δ) vibrations based on the assumption of a tetrahedral peroxoniobate ion with rigid O(2) units on the corners of the tetrahedron.

	$(NH_4)_3[Nb(O_2)_4]$		$K_3[Nb(O_2)_4]$		$Cs_3[Nb(O_2)_4]$	
mode	IR	Raman	IR	Raman	IR	Raman
ν_s		455		457		502
ν_{as}	586		595		584	
ν_{as}	543	545	548	547	543	546
δ_s (A_1)		535		519		534
δ_s (B_1)		n.o.		n.o.		n.o.
δ_{as}				302	287	281
δ_{as}		271	301	270		265

Table 5.6: Assignment of Ta – O stretching (ν) and O(2) – Ta – O(2) bending (δ) vibrations based on the assumption of a tetrahedral peroxotantalate ion with rigid O(2) units on the corners of the tetrahedron.

	$(NH_4)_3[Ta(O_2)_4]$		$K_3[Ta(O_2)_4]$		$Rb_3[Ta(O_2)_4]$		$Cs_3[Ta(O_2)_4]$	
mode	IR	Raman	IR	Raman	IR	Raman	IR	Raman
ν_s		514		470		461		455
ν_{as}	550		560		554	n.o.	554	n.o.
ν_{as}	527	566	527	566	531	567	528	567
δ_s (A_1)		546		525		522		513
δ_s (B_1)		n.o.		n.o.		n.o.		n.o.
δ_{as}				297	291	289	286	280
δ_{as}		276	253	276		273		267

The bending vibrations of the tetrahedral peroxo – chromate, vanadate, niobate or tantalate ion with rigid O(2) units split under site group symmetry into two components in species A_1 and B_1 for the symmetrical bending vibration and in species B_2 and E for the asymmetrical bending vibration. We therefore expect two absorption maxima due to bending vibrations in the IR spectra and four lines in the Raman spectra (species A_1 and B_1 are only Raman active, whereas species B_2 and E are both IR and Raman active). The total symmetric bending vibration of species A_1 (ν_s) we assign to Raman lines with relatively high wavenumbers (see tabs. 5.3 – 5.6) because during this vibration the O – O distances of the non – bonded oxygen atoms, which are 255.6 pm in the equilibrium structure of the $K_3[Cr(O_2)_4]$ [14], become even shorter. Hence there will be strong repulsive forces and thus high wavenumbers.

Similar for the other tetraperoxo compounds, we mention the distance between the non – bonded oxygen in $Rb_3[Ta(O_2)_4]$ (O – O) which is 266.7 pm in the equilibrium state [this work] which, is becoming even shorter during the vibration. Thus, we see high values of wavenumber for the vibration of species A_1.

In the other component of the symmetrical bending vibration belonging to species B_1, on the other hand, the distance between the other non – bonded oxygen atoms in the structure of $K_3[Cr(O_2)_4]$ or $Rb_3[Ta(O_2)_4]$, which have a much longer equilibrium distance of 276.8 pm for $K_3[Cr(O_2)_4]$ [14] and of 291.1 pm for $Rb_3[Ta(O_2)_4]$ [this work], is changed during the vibration. Therefore, we expect weaker restoring forces and hence lower wavenumbers for this vibration.

An assignment of the translational and librational lattice modes of the Tetraperoxo – chromate, vanadate, niobate or tantalate ions is not possible, as the spectra are not well resolved in the low – wavenumber region.

6. Summary

This thesis is devoted to the synthesis, structure determination, and vibrational spectroscopic investigation of several tetraperoxo complexes of transition elements.

The group of the tetraperoxo compounds of Cr^{V+}, V^{V+}, Nb^{V+} and Ta^{V+} with different cations such as $(NH_4)^+$, K^+, Rb^+ or Cs^+ were studied. The compounds of this group with the general formula $A_3[B(O_2)_4]$: $(NH_4)_3[Cr(O_2)_4]$, $K_3[Cr(O_2)_4]$, $Rb_3[Cr(O_2)_4]$, $(NH_4)_3[V(O_2)_4]$, $K_3[V(O_2)_4]$, $(NH_4)_3[Nb(O_2)_4]$, $K_3[Nb(O_2)_4]$, $Cs_3[Nb(O_2)_4]$, $(NH_4)_3[Ta(O_2)_4]$, $K_3[Ta(O_2)_4]$, $Rb_3[Ta(O_2)_4]$ and $Cs_3[Ta(O_2)_4]$ have been investigated in this work and found by X-ray analysis to crystallise isotypic with the Potassium Tetraperoxochromate type structure tetragonal in the space group $I\bar{4}2m$ (No. 121) with $Z = 2$. Lattice constants for the different compounds are refined and are given for the first time in the case of $(NH_4)_3[Cr(O_2)_4]$, $K_3[V(O_2)_4]$ and $(NH_4)_3[V(O_2)_4]$.

The crystal structure of Rubidium Tetraperoxotantalate has been solved on single crystal data and is reported for the first time and shown to be also isotypic to the $K_3[Cr(O_2)_4]$ – type.

The tetraperoxometallate ion $[B(O_2)_4]^{3-}$ where $B = Cr^{V+}$, V^{V+}, Nb^{V+} or Ta^{V+}, is of the form of a distorted dodecahedron built up from four peroxo groups. In all tetraperoxo compounds the distances between the centre atom (transition metal) and the two oxygen atoms of a peroxo group are not equal, one being slightly longer than the other.

As can be seen from a comparison of the structures based on single crystal data the oxygen – oxygen distance of the peroxo group depends both on the central metal ion and on the cations. The O – O bond length increases with increasing ionic radius of the central atom from chromium to niobium and tantalum, at the same time it is increasing with increasing ionic radius of the cation increasing from potassium, rubidium, caesium to ammonium.

The infrared– and Raman spectra are recorded for all the tetraperoxo compounds and are discussed with respect to the internal vibrations of the peroxo – group and the dodecahedral ion $[B(O_2)_4]^{3-}$ ($B = Cr^{V+}$, V^{V+}, Nb^{V+} or Ta^{V+}) (see chapter 5) on the basis of a factor group and site group analysis. The distribution of the internal, librational, and translational vibrations of the molecular entities $[B(O_2)_4]^{3-}$ and O – O over the species of point group D_{2d} and their activity is presented.

The stretching vibrations of the O_2^{2-} groups in the Raman spectra are found at 916 – 919 cm^{-1} for Tetraperoxochromates, at 885 – 888 cm^{-1} for Tetraperoxovanadates, at 835 – 840 cm^{-1} for Tetraperoxoniobates and at 830 – 833 cm^{-1} for Tetraperoxotantalates, i.e. they are relatively stable if the central atom does not change. The same can be found from the IR spectra where the stretching vibrations of the O_2^{2-} groups are found at 881 – 883 cm^{-1} for Tetraperoxochromates, at 853 – 861 cm^{-1} for Tetraperoxovanadates, at 810 – 816 cm^{-1} for Tetraperoxoniobates and at 802 – 808 cm^{-1} for Tetraperoxotantalates.

A comparison with the values obtained from the stretching vibrations of the peroxo groups in the corresponding Tetraperoxochromates, Tetraperoxovanadates, Tetraperoxoniobates and Tetraperoxotantalates shows that they change significantly with the central atom. The shift of the stretching vibrations of the peroxo group to lower wavenumbers with increasing mass of the central atom is explained by the change of the force constants in the O – O stretching, which become smaller with increasing mass of the central atom. This is due to an overlap of the π^* orbitals of the peroxo groups with empty dz^2 orbitals of the central metal atoms by which electron density is flowing from the antibonding orbitals of the peroxo groups to the central atom. Such an overlap is better in those cases where the central atom has a smaller ionic radius, i.e. this overlap is better for the chromium than for vanadium, niobium or tantalum tetraperoxo compounds.

7. References

[1]. Z. –W. Yu, P. –A. Jansson, B. I. Posner, U. Smith, and J. W. Eriksson
Peroxovanadate and insulin action in adipocytes from NIDDM patients. Evidence against a primary defect in tyrosine phosphorylation,
Diabetologia **40** (1997) 1197-1203.

[2]. M. Salvi, A. Toninello, M. Schweizer, S. D. Friess and C. Richter
Peroxovanadate inhibits Ca2+ release from mitochondria,
CMLS, Cell. Mol. Life Sci. **59** (2002) 1190-1197.

[3]. I.A. Wilson,
X-ray Analysis of Potassium Perchromate K_3CrO_8 and Isomorphous Compounds,
Arkiv för Kemi, Mineralogi och Geologi **15B** (1942) 1-8.

[4]. R. Stomberg and C. Brosset,
The Crystal Structure of Potassium Perchromate,
Acta Chem. Scand. **14** (1960) 441-452.

[5]. P. Schwendt and M. Sivák
Composition and Structure of Vanadium(V) Peroxo Complexes,
5th North American Chemical Congress (1998) 117-125.

[6]. J. W. Peters, J. N. Pitts, Jr., I. Rosenthal and H. Fuhr
A New and Unique Chemical Source of Singlet Molecular Oxygen. Potassium Perchromate,
J. Am. Chem. Soc. **94** (1972) 4348-4350.

[7]. J. H. Wang
Synthetic Biochemical Models,
Accounts Chem. Res. **3** (1970) 90-97.

[8]. E.H. Riesenfeld, H.E. Wohlers and W.A. Kutsch,
Höhere Oxydationsproducte des Chroms,
Chem. Ber.(1905) 1885-1898.

[9]. K. Gleu,
Red Permolybdate,
Z. Anorg. Allg. Chem. **204** (1932) 67-80.

[10]. J.E. Fergusson, C.J. Wilkins and J.F. Young,
The Constitution of Peroxy-compounds of the Vanadium and the Chromium Group,
J. Chem. Soc. (1962) 2136-2141.

[11]. W.P. Griffith,
Studies on Transition-metal Peroxy-complexes. Part III. Peroxy-complexes of Groups IVA, VA, and VIA,
J. Chem. Soc. (1964) 5248-5252.

[12]. J. Beltrán Martinez and B. Rodriguez Rioz,
Contribucion al estudio de los peroxivanadatos,
Anales R. Soc. Esp. de Fis. Quim. **14 B** (1952) 388-393.

[13]. M. Bonchio, V. Conte, F. Di Furia, G. Modena and S. Moro,
Correlation between One-Electron Reduction and Oxygen-Oxygen Bond Strength in d0 Transition Metal Peroxo Complexes,
Inorg. Chem. **32** (1993) 5797-5799.

[14]. J. Fischer, A. Veillard et R. Weiss,
Nature de la liaison dans l`ion tétraperoxochromate $CrO_8 3-$: une étude des structures cristalline et électronique,
Theoret. Chim. Acta **24** (1972) 317-333.

[15]. R. Stomberg,
Least-Squares Refinement of the Crystal Structure of Potassium Peroxochromate,
Acta Chem. Scand. **17** (1963) 1563-1566.

[16]. J. D. Swalen and James A. Ibers,
Chemical Bonding in the Perchromate Ion,
J. Chem. Phys. **37** (1962) 17-20.

[17]. R.M. Wood, K.A. Abboud, R.C. Palenik and G.J. Palenik,
Bond Valence Sums in Coordination Chemistry. Calculation of the Oxidation State of Chromium in Complexes Containing Only Cr – O Bonds and a Redetermination of the Crystal Structure of Potassium Tetra (peroxo) chromate (V),
Inorg. Chem. **39** (2000) 2065-2068.

[18]. H. Haeuseler, M. Wagener, H. Müller,
Darstellung, Kristallstruktur und Schwingungsspektren von Rubidiumperoxoniobat (Rb_3NbO_8),
Z. Naturforsch. **52b** (1997) 1082-1086.

[19]. G. Wehrum und R. Hoppe,
Zur Konstitution von Alkaliperoxotantalaten(V): Über den Aufbau von $K_3[Ta(O_2)_4]$,
Z. Anorg. Allg. Chem. **619** (1993) 1315-1320.

[20]. N. S. Dalal, J. M. Millar, M. S. Jagadeesh and M. S. Seehra,
Paramagnetic resonance, magnetic susceptibility and antiferromagnetic exchange in a Cr +5 paramagnet : Potassium perchromate (K_3CrO_8),
J. Chem. Phys. **74** (1981) 1916-1923.

[21]. B. Cage, W. Geyer, K. A. Abbound and N. S. Dalal,
Hydrated Cr(V) Peroxychromates $M_3CrO_8.XH_2O$ (M = Li, Na, Cs): Model 3d1 Systems Exhibiting Linear Chain Behavior and Antiferromagnetic Interaction,
Am. Chem. Soc. **13** (2001) 871-879.

[22]. B. Cage, K. Singh, S. Friedberg, S. Shimizu, J. S. Moodera, W. N. Lawless and N. S. Dalal
Alkali-metal peroxychromates: Cr(V)-based antiferromagnets with low-dimensional spin exchange and high specific heats,
Solid State Commun. **113** (2000) 93-97.

[23]. B. Cage and N.S. Dalal,
Unhydrated Cr(V) Peroxychromates M_3CrO_8 (M = Na, K, Rb): Low- Dimensional Antiferromagnets Exhibiting Large Specific Heats at mK to 5 K Temperatures,
Chem. Mater. **13** (2001) 880-890.

[24]. J.E. Guerchais et R. Rohmer,
Un nouveau sel d´ammonium : le perorthoniobate $(NH_4)_3NbO_8$; étude cristallographique et infrarouge,
Compt. Rend. **259** (1964) 1135-1137.

[25]. K.I. Selezneva and L.A. Nisel´son,
Preparation and Properties of Ammonium Orthoperoxoniobate and Orthoperoxotantalate,
Russ. J. Inorg. Chem. **13** (1968) 45-47.

[26]. R.N. Shchelokov, E.N. Traggeim, M.B. Varfolomeev, M.A. Michnik, S.V. Morozova,
X-ray Diffraction Study of Alkali Metal and Ammonium Tetraperoxoniobates,
Russ. J. Inorg. Chem. **17** (1972) 1273-1274.

[27]. G. V. Jere, L. Surendra and M. K. Gupta
Solid state decomposition studies on tetraperoxo species of transitional metals. Kinetics of the isothermal decomposition of $K_3Nb(O_2)_4$ and $K_3Ta(O_2)_4$,
Thermochim. Acta **63** (1983) 229-236.

[28]. J. K. Ghosh and G. V. Jere
Kinetics of solid state decomposition of K3[Nb(O2)4] and K3[Ta(O2)4]: a thermogravimetric study,
Thermochim. Acta **136** (1988) 73-80.

[29]. I. Svensson and R. Stomberg,
Studies on Peroxovanadates I. The crystal Structure of Ammonium μ-Oxo-bis (oxo-diperoxovanadate (V)), $(NH_4)_4[O(VO(O_2)_2)_2]$,
Acta Chem. Scand. **25** (1971) 898-910.

[30]. T. –J. Won, C. L. Barnes, E. O. Schlemper, and R. C. Thompson
Two Crystal Structures Featuring the Tetraperoxovanadate(V) Anion and a Brief Reinvestigation of Peroxovanadate Equilibria in Neutral and Basic Solutions,
Inorg. Chem. **34** (1995) 4499-4503.

[31]. W.P. Griffith and T.D. Wickins,
Studies on Transition-metal Peroxy-complexes. Part VI. Vibrational Spectra and Structure,
J. Chem. Soc. A (1968) 397-400.

[32]. P. Gili, A. Mederos, P.A. Lorenzo-Luis, E.M. de la Rosa, A. Muñoz,
On the interaction of compounds of chromium(VI) with hydrogen peroxide. A study of chromium(VI) and (V) peroxides in the acid-basic pH range,
Inorg. Chim. Acta **331** (2002) 16-24.

[33]. H. H. Eysel and S. Thym
Raman Spectra of Peroxides
Z. Anorg. Allg. Chem. **411** (1975) 97-102.

[34]. B. R. McGarvey
ESR and Optical Spectrum of Potassium Perchromate,
J. Chem. Phys. **37** (1962) 2001-2004.

[35]. M. H. Dickman and M. P. Pope
Peroxo and Superoxo Complexes of Chromium, Molybdenium and Tungsten,
Chem. Rev. **94** (1994) 569-584.

[36]. M. Roch, J. Weber, and A. F. Williams
Electronic Structure and Spectroscopic Properties of Chromium(V), Molybdenum(VI), and Niobium(V) Tetraperoxides,
Inorg. Chem. **23** (1984) 4571-4580.

[37]. T. R. Cundari, M. C. Zerner, and R. S. Drago
Electronic Causes of Dissymmetry in Side-On-Bonded Dioxygen Complexes,
Inorg. Chem. **27** (1988) 4239-4241.

[38]. J. W. Peters, P. J. Bekowies, A. M. Winer, and J. N. Pitts, Jr
An Investigation of Potassium Perchromate as a Source of Singlet Oxygen,
J. Am. Chem. Soc. **97** (1975) 3299-3306.

[39]. S. B. Brown, P. Jones, K. Prudhoe
A Double Isotope (18O) Kinetic Study of Peroxide Group Exchange between the Tetraperoxochromate Ion and Hydrogen Peroxide in Basic Solution,
Inorg. Chim. Acta **34** (1979) 9-12.

[40]. D. Quane and B. Bartlett
Optical Spectra of Potassium Tetraperoxychromate(V) and the Violet Diperoxychromate(VI) Ion,
J. Chem. Phys. **53** (1970) 4404.

[41]. A. C. Adams, J. R. Crook, F. Bockhoff, and E. L. King
The Preparation and Properties of Peroxychromium(III) Species,
J. Am. Chem. Soc. **90** (1968) 5761-5768.

[42]. V. V. Sviridov, A. I. Lesnikovich, S.V. Levchik, K. K. Kovalenko, and V. G. Guslev
Thermolysis of Potassium Tetraperoxochromate(V). I. Isothermal conditions,
Thermochim. Acta **77** (1984) 341-356.

[43]. A. I. Lesnikovich, S. V. Levchik, and V. G. Guslev
Thermolysis of Potassium Tetraperoxochromate(V). II. Linear heating,
Thermochim. Acta **77** (1984) 357-365.

[44]. A. I. Lesnikovich, S. V. Levchik, K. K. Kovalenko, and V. G. Guslev
Thermolysis of Potassium Tetraperoxochromate(V). III. Self-propagation regime,
Thermochim. Acta **81** (1984) 245-260.

[45]. A. I. Lesnikovich, S. V. Levchik, and K. K. Kovalenko
Thermolysis of Potassium Tetraperoxochromate(V). IV. Effect of additives on ordinary and self-propagating decomposition,
Thermochim. Acta **102** (1986) 293-302.

[46]. Visual WinXPOW, Version 1.6
STOE Powder Diffraction Software,
STOE&CIE GmbH, Darmstadt (1999).

[47]. G.M. Sheldrik
SHELX – 97, Programm zur Kristallstrukturverfeinerung,
Universität Göttingen (1997).

[48]. Klaus Brandenburg
Diamond Version 2.0B,
Crystal Impact GbR (1998) .

[49]. OPUS/IR Version 2.2,
Spektroskopiesoftware OPUS,
Bruker Analytische Messtechnik GmbH, (1991).

[50]. K. A. Hofmann und H. Hiendlmaier
Zur Kenntnis der Perchromate,
Z. Chem. (1905) 3059-3066.

[51]. R.N. Shchelokov, E.N. Traggeim, and M.A. Michnik,
Preparation of Various Tetraperoxoniobates(V),
Russ. J. Inorg. Chem. **16** (1971) 211-213.

[52]. C. W. Balke and E. F. Smith,
Observations on columbium,
J. Am. Chem. Soc. **30** (1908) 1637-1668.

[53]. B. Cage, A. Weekley, L. C. Brunel, and N. S. Dalal
K_3CrO_8 in K_3NbO_8 as a Proposed Standard for g-Factor, Spin Concentration, and Field Calibration in High-Field EPR Spectroscopy,
Anal. Chem. **71** (1999) 1951-1957.

[54]. V. A. Titova and I. G. Slatinskaya
Potassium and sodium peroxyorthoniobates,
Z. Neorg. Khim. **14(12)** (1969) 3283-3285.

[55]. G. A. Bogdanov, G. K. Yurchenko and O. V. Popov,
Potassium, rubidium and caesium peroxotantalates,
Z. Neorg. Khim. **27** (1982) 2143-2144.

[56]. L. Vaska
Dioxygen – Metal Complexes: Toward a Unified View,
Acc. Chem. Res. **9** (1976) 175-183.

[57]. V.A. Titova and I.G. Slatinskaya,
Preparation and properties of ammonium peroxo-orthoniobate,
Russ. J. Inorg. Chem. **12** (1967) 767-769.

[58]. H. Haeuseler and G. Haxhillazi
Vibrational spectra of the peroxochromates $(NH_4)_3[Cr(O_2)_4]$, $K_3[Cr(O_2)_4]$ and $Rb_3[Cr(O_2)_4]$,
J. Raman Spectrosc. **34** (2003) 339-344.

[59]. John Emsley
Die Elemente,
Walter de Gruyter **.** Berlin **.** New York 1994.

Publications

- Ammoniumperoxochromat, –niobat und –tantalat

  G. Haxhillazi, H. Haeuseler; Siegen**;** Poster A 26;

  11. Vortragstagung 24. - 26. September 2002 in Dresden

  Vortragstagung der GDCh-Fachgruppe Festkörperchemie und Materialforschung

- Vibrational spectra of the peroxochromates $(NH_4)_3[Cr(O_2)_4]$, $K_3[Cr(O_2)_4]$ and $Rb_3[Cr(O_2)_4]$,

  H.Haeuseler and G. Haxhillazi,

  J. Raman Spectrosc. 2003; **34**: 339-344.